Geotechnical Engineering

Project Day 2021

Organised by the
SRI LANKAN GEOTECHNICAL SOCIETY

SLGS

Content

1. **Prediction Cost effective road base with crushed stone and waste tyre: An Investigation** 1

   B.B. Ashab, M.M.F. Banu and A. Anburuvel

   Department of Civil Engineering, University of Jaffna, Sri Lanka

2. **Effect of the depth and location of a shear key on the behaviour and stability of cantilever type retaining walls** 61

   A. Gowshikan and L.I.N. de Silva

   Department of Civil Engineering, University of Moratuwa, Sri Lanka

3. **Development of an alternative approach for bored and cast in-situ pile design using PDA test results** 12

   A.A.S. Kaushalya and U.P. Nawagamuwa

   Department of Civil Engineering, University of Moratuwa, Sri Lanka

4. **A study on axial performance of helical piles on residual soils** 18

   C.N. Liyanage and L.I.N. de Silva

   Department of Civil Engineering, University of Moratuwa, Sri Lanka

5. **Use Of the Concept of Capillary Barriers to Optimize the Support Systems of Deep Vertical Excavations in Unsaturated Soils** 24

   R. Prasanna and S.A.S. Kulathilaka

   Department of Civil Engineering, University of Moratuwa, Sri Lanka

6. **Improvement of compressibility characteristics of waste material by dynamic compaction** 30

   R.I.A Rathnayaka and S.A.S. Kulathilaka

   Department of Civil Engineering, University of Moratuwa, Sri Lanka

7. **Stability analysis of Colombo Katunayake expressway (CKE) embankment using fly ash stabilized soil as embankment material** 36
K. Mathumidah, S. Lavanyan and M. C. M. Nasvi
Department of Civil Engineering, University of Peradeniya, Sri Lanka

8. **Prediction of Geotechnical Properties of Stabilized Soil Using Fly Ash Based Stabilizer Systems** 40
K.M.D. Nimesha, N.A.N.M. Nissanka and M. C. M. Nasvi
Department of Civil Engineering, University of Peradeniya, Sri Lanka

9. **Pavement Degradation Model for Road Infrastructure in Sri Lanka** 46
M.M.N.T. Meghasooriya, K.M.N.M. Jayarathna, and S.K. Navaratnarajah
Department of Civil Engineering, University of Peradeniya, Sri Lanka

10. **Engineering Behavior of Gravel Compaction Piles (GCP) under Drained Condition** 52
I.G.C.D. Dhanasekara and N.H. Priyankara
Department of Civil and Environmental Engineering, University of Ruhuna, Sri Lanka

11. **Variation of Shear Strength Characteristics of Sri Lankan Residual Soils** 56
D.M.S.W. Dissanayake and N.H. Priyankara
Department of Civil and Environmental Engineering, University of Ruhuna, Sri Lanka

12. **Shear Strength Characteristics of Municipal Solid Waste in Meethotamulla Dump Site** 62
M.A.G.P. Perera and N.H. Priyankara
Department of Civil and Environmental Engineering, University of Ruhuna, Sri Lanka

13. **Moderately Loaded Structures Supported on Soil-Cement Columns** 68
A.Yoganathan and N.H. Priyankara
Department of Civil and Environmental Engineering, University of Ruhuna, Sri Lanka

14. Strength Mobilization in Quarry Dust Mixed Sri Lankan Dredged Clays in Early Curing 74

S.H.L.T. Priyankara and W.M.N.R. Weerakoon

Department of Civil Engineering, University of Sri Jayewardenepura, Sri Lanka

15. Investigation of the shear strength characteristics of materials by experimental and numerical analysis 79

A.R.M.C.P.B. Amunugama, D.G.L.S. Kulasekara

Department of Civil Engineering, South Eastern University of Sri Lanka

16. Prediction of post-construction settlement of road embankment 84

G.A.N Jayaratne and H.S. Thilakasiri

Department of Civil Engineering, Sri Lanka Institute of Information Technology, Sri Lanka

Message from the President - SLGS

From its inception, Sri Lankan Geotechnical Society has provided a forum for disseminating new knowledge in the field of geotechnical engineering and promoting research. The Project Day competition was commenced in year 2000 with the objective of encouraging the undergraduates conducting projects in the field of Geotechnical Engineering to do good research, publish and make effective presentations. This year we have made number of changes in the format of papers and presentations. The evaluation process was also revised. A detailed marking rubric was formulated to minimize any biasness in the evaluation.

Participants are expected to present their findings in a four to six paged paper and make a 5 minute oral presentation. The best paper and the second paper will receive cash awards and certificates. The competition was held annually uninterrupted to date.

Many winners in the past years have proceeded to do higher studies and established good carriers in the field of Geotechnical Engineering as both academics and practicing engineers.

There are sixteen papers on a wide variety of topics this year. Participation of students from new Engineering faculties at Sri Jayawardenapura, Jaffna and South Eastern University is very encouraging. I thank all the authors for their interest and commitment and hope they will continue with the habit of presenting their research in written form. It is only when one starts to write his findings he would realize the gaps in his work or knowledge and would be able to rectify them.

Currently there are many ongoing projects with wide applications in Geotechnical Engineering. We believe that many research ideas would generate in this background.

This time there were two independent panels and each panel was requested to evaluate eight papers. I wish to convey my sincere gratitude to the panel of evaluators; Professor U G A Puswewala, Dr Jayantha Amaratunge, Dr Prasanna Ratnaweea, Mr Kirthi Senananyaka , Mr K L S Sahabandu and Dr. J. S. M. Fowze.

Prof. Athula Kulathilaka
President – SLGS

Cost effective road base with crushed stone and waste tyre: An Investigation

B.B. Ashab, M.M.F. Banu and A. Anburuvel
Department of Civil Engineering, University of Jaffna, Sri Lanka

ABSTRACT: In road base construction, substituting conventional mineral aggregates partially with waste tyre is envisaged in reducing natural aggregate consumption and providing a sustainable way to dispose waste tyres. This study explored the feasibility of it by assessing compaction characteristics and cost. The experiments conducted on crushed stone with waste tyre of 2%, 5% and 8% by weight found that, increase in waste tyre content of the mix adversely affects its compaction characteristics. 2% waste tyre replacement resulted in 68% CBR and a drastic drop was observed for further increase in waste tyre content. Cost analysis revealed that there was a reduction of 10% of the conventional construction cost for 2% waste tyre substitution. Considering strength and cost contexts, this study recommends crushed stone partially substituted with 2% shredded waste tyre by weight for road bases of low traffic volume roads in Sri Lanka.

KEY WORDS: road base, crushed stone, waste tyre, compaction, pavement

1 INTRODUCTION

Road has been the primary mode of transportation in Sri Lanka. Presently, the country has a well-connected road network, which comprises of 15% national highways and 85% low volume provincial or local roads as per the statistics of Road Development Authority (2021). Constructing low volume roads with inexpensive waste materials with adequate structural reliability could extensively contribute to economic thrift.

Several studies explored the feasibility of adopting waste materials by mixing them with conventional road construction materials and using them for the construction of different pavement elements. The study of Huang et al. (2007) showed that, secondary materials like waste glass, scraped tires, steel slags and plastics could be used in road construction. Another study by Anupam et al. (2013) assessed the utilization of agricultural and industrial waste materials, viz. Fly Ash (FA), Rice Husk Ash (RHA), Bagasse Ash (BA) and Rice Straw Ash (RSA) as a soil admixture, to improve engineering properties of soil that made it suitable for bottom layers of a road. Researchers envisaged of introducing waste tyre into conventional road construction materials to exploit possible advantages. Poulikakos et al. (2017) showed that introduction of crumb rubber properly into the pavement layers reduced layer thickness by half. Sheikh et al. (2013) recommended preloading of mixtures to prevent high settlements due to resilient nature of rubber.

To the best of authors' knowledge, in Sri Lanka, studies that utilize waste materials for road construction are very limited. Nawagamuwa et al. (2008) investigated about soil stabilization by RHA in Jaffna peninsula. In another study, Sathik and Udakara (2019) explored about using crumb rubber tyres for aggregate replacement. Yasanthi et al. (2016) examined about using PET fiber as part of the filler, as an additive, and as aggregate with asphalt mix.

Vehicle usage in Sri Lanka has dramatically increased during the last decade. Almost 8 million vehicles have been registered until 2019 according to Ministry of transport (2020). Large vehicle population tends to generate significant amount of waste tyre after usage. Disposing generated waste tyre raises concerns financially and environmentally.

Construction of road pavement consists of several stages. Among them extraction and transport of mineral aggregates contribute to significant increase in the prices of road construction. Asphalt mixture in a pavement consists of more than 90% of aggregates by weight (Huang et al., 2007). Therefore, substituting mineral aggregates partially or fully with waste materials could help to prevent extraction of excessive natural resources and dispose waste materials in an unconventional way.

Application of waste tyre in the context of road construction raises two major concerns; defining standards for testing of the new technology and regulations related to environment and adaptability by industries for large-scale applications (Heitzman, 1992). High compressibility of pavements would not be recommended when carrying loads. Based on standard laboratory tests, a degree of feasibility in terms of structural stability and costs can be further extended or tuned to suit the industrial applications.

This paper discusses about an experimental study conducted to assess the compaction characteristics of crushed stone partially substituted with shredded waste tyre, and financial feasibility of deploying it for road base construction in Sri Lanka.

2 MATERIALS AND METHODS

2.1 *Experimental study*

2.1.1 *Preparation of crushed stone*

Crushed stone used in this study was mined from a rock exposure, situated in Medawachiya, North-central part of Sri Lanka. To conduct experiments, crushed stone with nominal maximum size of 20 mm was taken. Grain size distribution is summarized in Table 1, which was in line with Overseas Road Note 31 (ORN31, 1993) that governs design of road bases in tropical and sub-tropical countries. Crushed stones of different sizes were blended together in required proportions to prepare the final crushed stone mix as shown in Fig. 1.

2.1.2 *Preparation of shredded waste tyre*

Considering the availability in local shops, motor cycle waste tyre was chosen to partially substitute crushed stone. Initially, surface impurities on waste tyre were cleaned by water, and then air-dried for 1 day. Afterwards, steel belt reinforcement in the tyre was removed using an angle grinder. Then, tyre was fed into shredder machine to get shredded particles as shown in Fig. 2a. Size of shredded tyre particles were ranging between 0.6 and 6.3 mm. Fig. 2b shows particle size distribution of shredded waste tyre.

Table 1. Grading of crushed stone and respective grading limits according to the standard

Sieve (mm)	Cumulative % passing		
	Crushed stone	Upper limit*	Lower limit*
28	100	-	100
20	92	100	90
10	64	75	60
05	45	60	40
0.425	15	27	13
0.075	05	12	05

*ORN 31/SLS

Fig. 1. Crushed stone mix

a. Shredded waste tyre

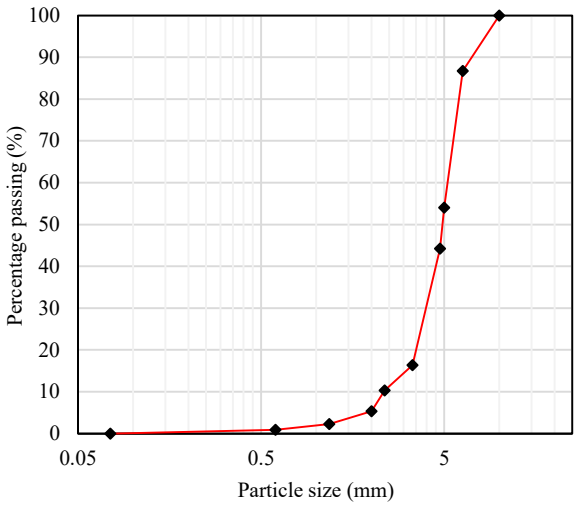

b. Particle size distribution curve

Fig. 2. Appearance and size distribution of shredded waste tyre

2.1.3 *Preparation of crushed stone – waste tyre mix*

According to literature, higher degree of waste tyre replacement is not preferred in the crushed stone-waste tyre matrix, as it will highly reduce the strength of pavement structure. Study of Gamalath et.al (2016) showed that compressive strength of concrete paving blocks reduced drastically with the increase in rubber content in the mix. Therefore, the usage was restricted to non-traffic applications. Waste tyre replacement in this study was limited to 0 – 8% by weight of the total crushed stone mix. Accordingly, mixtures of different compositions of crushed stone and shredded waste tyre were prepared as shown in Table 2 to study the influence of shredded waste tyre composition in the mix.

Table 2. Crushed stone and shredded waste tyre mix proportions

Mixture	Shredded waste tyre (%)	Crushed stone (%)
Mix – 0%	0	100
Mix – 2%	2	98
Mix – 5%	5	95
Mix – 8%	8	92

2.1.4 *Properties of crushed stone and waste tyre*

Physical properties of crushed stone and waste tyre were determined according to British Standard laboratory tests (1989, 1995, and 2012), and are shown in Table 3. The determined properties of them found to be in compliance with the standard specifications of materials used for road bases, which indicates that both crushed stone and waste tyre have no specific influence on compaction characteristics of mixture.

Table 3. Properties of crushed stone and waste tyre

Material	Parameter	Value
Crushed stone	Compacted density (Mg/m^3)	1.899
	Uncompacted density (Mg/m^3)	1.720
	Apparent specific gravity	2.85
	Flakiness index (%)	23.5
	Water absorption (%)	0.52
	Plasticity	Non
Waste tyre	Compacted density (Mg/m^3)	0.533
	Uncompacted density (Mg/m^3)	0.454

To examine the compaction characteristics, modified Proctor compaction test (1990) was carried out on crushed stone only (Mix - 0%). Compaction test results revealed that crushed stone reached its Maximum Dry Density (MDD) of 2.347 Mg/m^3 at Optimum Moisture Content (OMC) of 6.2% as illustrated in Fig. 3. With the obtained OMC, subsequent compaction and California Bearing Ratio (CBR) (1990) tests were carried out for crushed stone and waste tyre mixes.

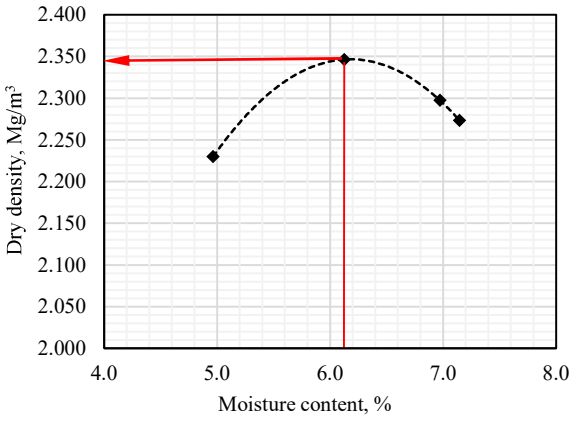

Fig. 3 Dry density/moisture content relationship of crushed stone

2.2 *Cost estimation*

2.2.1 *Road base configuration*

The cost estimation was performed for 1 km long road section of lower volume road. As per Road Development Authority (1999) regulations, the width of a typical low volume road is 5.5 m.

Representative CBR values of the subgrade in construction site ranged between 15 and 20. For the particular range of CBR values, ORN 31 (1993) recommends subgrade strength class to be S5. Considering the road base construction for the low traffic volume, traffic class T3 was selected for the analysis. Fig. 5 illustrates the minimum layer thickness required for the selected category of granular road base/ surface dressing as recommended in ORN 31 (1993).

For the recommended dimensions of 175 mm x 5.5 m x 1 km, total compacted volume of road base was calculated as 962.50 cu.m, which consisted of alternative compositions of crushed stone and shredded waste tyre.

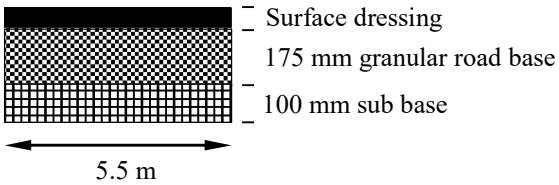

Fig. 5 Sectional details of granular road base type pavement

2.2.2 *Cost involved in crushed stone – waste tyre mix construction*

The cost estimation was done according to Highway Schedule Rates (HSR, 2019), Sri Lanka. While calculating cost of aggregates, extraction and crushing cost, loading and unloading cost, transport cost, and laying cost at the construction site were considered. For the estimation of transportation costs, a quarry was considered at 150 km from the road construction site in the Northern province of Sri Lanka.

In the preparation of shredded waste tyre, major costs incurred were cost of waste tyre, transport cost for collection and supply of waste tyre to the site, cost for shredding, electricity cost, and labour costs according to the present industrial rates. End-of-life tyres were obtained free of charge in local automobile shops for the experiment.

3 RESULTS AND DISCUSSION

3.1 *Compaction characteristics*

In order to initiate the tests for compaction characteristics, the particle size distributions of crushed stone – shredded before and after compaction for different waste tyre substitutions were done to ensure that mixture of crushed stone and waste tyre is in the range recommended by ORN 31 (1993). Fig. 6 illustrates that all mixtures are well within the limits.

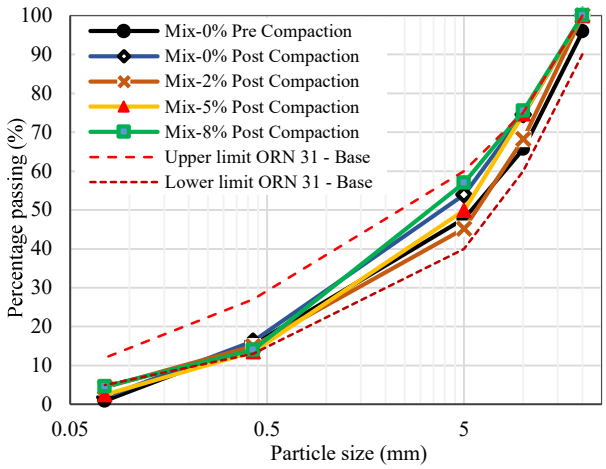

Fig. 6 Particle size distribution of crushed stone before and after compaction

PSD analysis was carried out due to the uncertainty of compaction effect can change the sizes of crushed stone particles. Fortunately, no any significant changes were observed. This phenomenon can be explained as cushion effect provided by the finer particles in the crushed stone mixture. In the crushed stone matrix, 45% of the particles were finer than 5 mm that it served as a cushion to absorb compaction energy and thus protect coarse particles from being subjected to compaction forces. Therefore, it is obvious that the presence of shredded waste tyre particles of sizes ranging from 3.35 to 6.30 mm in the mix did not provide any significant cushion effect to coarse particles on top of fine crushed stone particles.

From the modified compaction tests, MDD were obtained for various waste tyre percentages and crushed stones mixture. Fig. 7 illustrates the test results, that satisfied minimum of required MDD recommended for upper sub-base in Sri Lankan standard (2009) of 1.750 Mg/m^3.

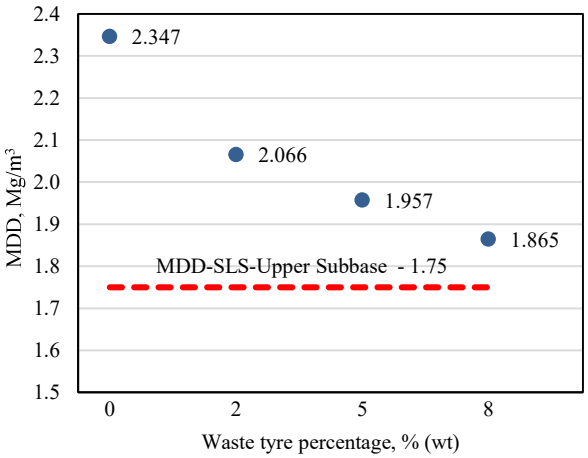

Fig. 7 Maximum dry density variation with partial waste tyre replacement

When increasing the percentage of waste tyre content, the MDD reduces significantly. Cause of this phenomenon explained as compaction effort applied on crushed stone and waste tyre mix was partially absorbed by waste tyre, and with its elastic behaviour, that portion of energy got dissipated instead of contributing to dense packing. Considering the minimum requirement for MDD, mix with 8% waste tyre content marginally becomes eligible.

Unlike MDD, CBR values showed extreme reduction even for the replacement of 2% is shown in Fig. 8. Recommended value for soaked CBR by ORN 31 (1993) was 80%. This reduction is due to the softening effect of waste tyre in the mix. To investigate the influence of waste tyre granules in CBR penetration, rebound of CBR mix after penetration was measured. As Fig. 9 illustrates, a considerable rebound after penetration was observed. Since the crushed stone chosen in the study is of maximum nominal size 20 mm and of dense grading, the effect of waste tyre was dominant. This effect needs further study by changing crushed stone grading and size of waste tyre in order to precisely define the application of waste tyre in road bases.

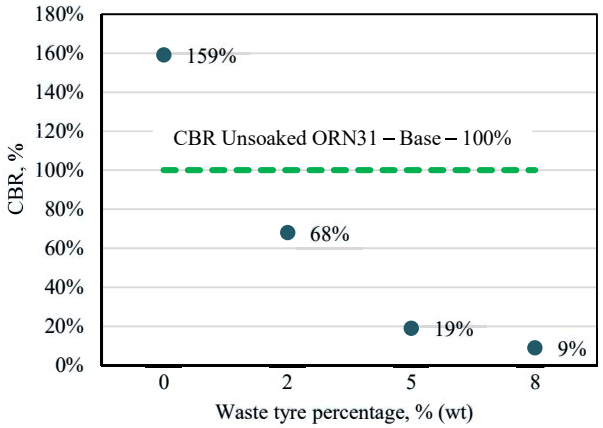

Fig. 8 CBR variation with partial rubber replacement

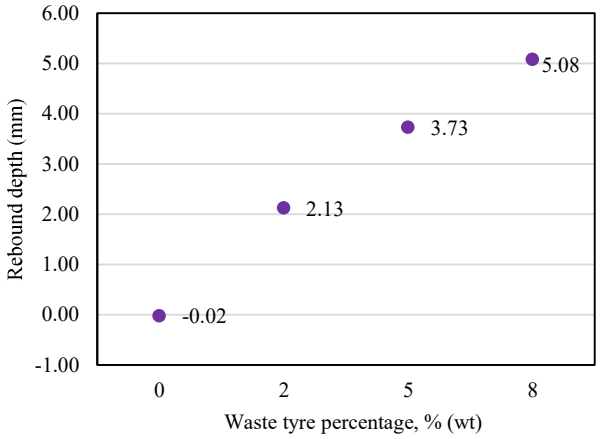

Fig. 9 Rebound depth variation after CBR test, with partial rubber replacement

3.2 *Cost feasibility*

The estimated cost of crushed stone and shredded waste tyre mix of 0% and 2% for the given road base is tabulated in Table 4. The savings of Mix-2% shown in the table clearly indicate the financial advantage of 1.14 million SLR by substituting shredded waste tyre into crush stone mix.

Table 4. The total cost involved in preparing crushed stone and shredded waste tyre mix for the road base

Description of item	Crush stone – shredded waste tyre mix	
	Mix-0%	Mix-2%
Required crushed stone (includes 5% wastage, Cu.m)	1,379	1,190
Required shredded waste tyre (includes 5% wastage, Cu.m)	-	76
Cost of crushed stone (in million, SLR)	11.791	10.167
Cost of shredded waste tyre (in million, SLR)	-	0.482
Total cost of mixture (in million, SLR)	11.791	10.649
Savings (in million, SLR)	-	1.142
Percentage savings (%)	-	9.68%

4 CONCLUSION AND RECOMMENDATIONS

The following salient conclusions can be drawn based on the outcome of this study,

- With the increase of shredded waste tyre substitution, while MDD remained above the limit, compaction resistance decreased drastically. However, the substitution up to 2% by weight was possible while retaining the required compaction characteristics as per the standards.
- The cost reduction for the mixes substituted with shredded waste tyre from 0 to 2% by weight was significant, 1.14 million SLR can be saved per km.
- Shredded waste tyre of 0.6 to 6.3 mm size particles could be used to replace conventional dense graded crushed stone up to 2% by weight for the construction of lower volume road base in Sri Lanka.

ACKNOWLEDGMENTS

The authors would like to convey their sincere gratitude to the department of civil Engineering, University of Jaffna for providing laboratory facilities.

REFERENCES

A guide to structural design of road under Sri Lankan condition, (1999), Road Development Authority, Sri Lanka.

Anupam, A.K., Kumar, P. and Ransinchung, G.D., (2013), Use of various agricultural and industrial waste materials in road construction, Procedia-Social and Behavioural Sciences, 104:264-73.

Gamalath, H.G.P., Weerasinghe, T.G.P.L. and Nanayakkara, S.M.A., (2016), Use of waste rubber gran-ules for the production of concrete paving blocks, The 7th International Conference on Sustainable Built Environment, Kandy, Sri Lanka.

Heitzman, M., (1992), Design and Construction of Asphalt Paving Materials with Crumb Rubber Modifier, Transportation Research Record No. 1339, Transportation Research Board, Washington, DC.

Highway Schedule of Rates - Northern Province, Sri Lanka, (2019), Ministry of Highways & Road Development and Petroleum Resources Development, Sri Lanka.

Huang, Y, Bird, R.N. and Heidrich, O., (2007), A review of the use of recycled solid waste materials in asphalt pavements, Resources, Conservation and Recycling, 52:58-73.

Huang, Y., Bird, R.N. and Heidrich, O., (2007), A review of the use of recycled solid waste materials in asphalt pavements, Resources, Conservation and Recycling, 52:58-73.

Methods of test for - Soils for civil engineering purposes - Part 4, in Compaction-related tests, BS 1377-4 (1990), United Kingdom: British Standards Institution.

National Highways (Class A, B & E Roads), (2021), Road Development Authority, Sri Lanka.

Nawagamuwa, U.P., Shabry, A.G.S., Ainkaran, K., Prasad, D.L.S. and Madushanka, H.K.P., (2018), Use of Industrial Byproducts to Improve Unsuitable Soils for Road Construction in Sri Lanka, Proceedings of GeoShanghai International Conference 2018, Transportation Geotechnics and Pavement Engineering, Singapore, pp. 299-308.

Overseas Road Note 31, (1993), T. R. L. Overseas Centre, United Kingdom.

Poulikakos, L.D., Papadaskalopoulou, C., Hofko, B., Gschösser, F., Falchetto, A.C., Bueno, M et al., (2017), Harvesting the unexplored potential of European waste materials for road construction, Resources, Conservation and Recycling, 116:32 – 44.

Sathik, H.L.S. and Udakara, D.D.S., (2019), Soil Stabilization using waste materials in Sri Lanka, International Journal of Trend in Scientific Research and Development, 3:4:500-2.

SCA/5, Standard Specifications for Construction and Maintenance of roads and bridges, (2009), Sri Lanka: Institute for Construction Training and Development (ICTAD).

Sheikh, M. N., Mashiri, M. S., Vinod, J. S. and Tsang, H.H., (2013), Shear and Compressibility Behavior of Sand-Tyre Crumb Mixtures, Journal of Materials in Civil Engineering, 25:1366-74.

Testing aggregates - Part 105 Flakiness index, BS 812-105.1: (1989), United Kingdom: British Standards Institution.

Testing aggregates Part 2, BS 812: Part 2 (1995), United Kingdom: British Standards Institution.

Tests for geometrical properties of aggregates Determination of particle size distribution. Sieving method, BS EN 933-1 (2012), United Kingdom: British Standards Institution.

Vehicle population, (2020), Ministry of Transport, Sri Lanka. < https://www.transport.gov.lk/web/ >, (Oct. 5, 2021)

Yasanthi, R.G.N., Mahesh, G.A.C., Rengarasu, T.M. and Bandara, W.M.K.R.T.W., (2016), Investigation of suitability of waste materials as aggregates in asphalt concrete: Undergraduate Research Symposium, Faculty of Engineering, University of Ruhuna, Galle, Sri Lanka.

Effect of the depth and location of a shear key on the behaviour and stability of cantilever type retaining walls

A. Gowshikan and L.I.N. de Silva
Department of Civil Engineering, University of Moratuwa, Moratuwa

ABSTRACT**:** Retaining walls are categorized into several types, out of which cantilever retaining walls are the commonly used retaining wall type. Shear keys are the structures incorporated in the cantilever retaining walls to increase their resistance to sliding, thus, increasing the Factor of Safety against sliding. In the current study, the optimal location and depth of the shear key are investigated to yield maximum use from it. Both the theoretical approach based on limit equilibrium and numerical modelling have been adopted in the analysis. Graphical representations of the variation of Factor of Safety (FOS) against sliding and overturning with varying depth and location of the shear key are presented. Finite Element Analysis was carried out to validate the results obtained from the theoretical approach. It was observed that the use of a shear key enhances the stability of the retaining wall against sliding. The optimum location of shear key is at the heel of the wall base. It was also found that the increasing depth of shear key reduces the stability of the retaining wall against overturning.

KEY WORDS: Shear key, Finite Element Analysis, FOS, Stability, Limit equilibrium

1 INTRODUCTION

Retaining walls are the structures that support the soil laterally and help them restrain at a slope which is not occurring naturally. Gravity retaining walls are the walls with a base that can take significant vertical load. Cantilevered retaining walls are the most common type of gravity retaining walls used widely.

The stability of these walls should be ensured for its long-term use without any anticipated failures. A retaining wall can fail due to four main failure mechanisms: sliding, overturning, bearing capacity failure and deep-seated failure. Cantilever type retaining walls are prone to sliding failure due to its thin section.

Shear key is a structural element which is frequently used in the footing of the retaining walls to increase the wall's sliding resistance. In a retaining wall, resistance to sliding is provided by the friction between the bottom of the base slab and the soil surface. Hence the friction depends on the weight of the wall and weight of the backfill above the base slab. An additional resistance must be generated, if this friction force does not provide the required safety against sliding. By the use of shear key, development of passive earth pressure due to the soil in front of the shear key will generate an additional resistance against sliding. The depth and the location of shear key would influence the stability of the cantilever type retaining walls.

This study was carried out with the intention of studying on how the dimensions and location of shear key can have an effect on the stability of retaining walls against potential failure mechanisms.

Cantilevered walls are economical up to wall height of 7 m (Sarita, S. & Sakshi G., 2012). There are many different types of cantilevered retaining walls, with the common feature being a footing that supports the vertical wall stem. Typical cantilevered walls are inverted T-shaped, L-shaped, or reverse L-shaped. Reverse L-shaped cantilever wall was selected for the analysis.

Nisha Sarath et al. (2011) conducted a study to investigate the role of shear keys in cantilever retaining wall. They have concluded that, by using shear key, development of passive earth pressure due to the soil in front of the shear key will generate additional resistance against sliding. The depth and location of shear key would influence the stability of the cantilever type retaining walls. It is also affected by several other characteristics such as soil type, slope angle, height and width of the wall and ground water table etc.

Study by John S. Horvath, (1991) concludes that only at higher loads, the heel key exhibit slightly superior behaviour both at translation and rotation. The basic flat bottom case outperformed the toe key alternatives at higher loads.

Study by Anthony T.C. Goh, (1993) investigates the behaviour of concrete cantilever retaining walls

to determine if current analytical procedures provide realistic estimates of earth pressure distribution under working load conditions by using finite element method. Study by Anthony T.C. Goh, (1993), concluded that finite element method allows for more realistic consideration of the soil-structure interaction, the construction sequence involved and other complex initial conditions, in comparison to other conventional design methods.

Study by Salahudeen A.B. and Ketkukah T.S. (2019) concludes that the effect of shear key position is insignificant for Factor of Safety against sliding. But for safety factor against overturning, shear key position is a considerable issue.

In this study, limit equilibrium analysis is carried out to identify on how the following parameters will influence the stability of cantilever type retaining walls.

1. Depth of shear key
2. Location of shear key

In addition, Numerical modelling will also be carried out to investigate the deformation characteristics and to evaluate the assumed point of rotation of the wall.

2 LIMIT EQUILIBRIUM ANALYSIS

Limit equilibrium analysis was carried out to obtain FOS against sliding failure, FOS against overturning failure and maximum bearing pressures at the base of the retaining wall by changing the location and depth of the shear key and other governing parameters such as height of the wall and length of the wall base. Strength properties of soil are kept constant by referring to the shear strength properties of commonly used backfill materials in Sri Lanka.

Table 1 shows the design soil parameters considered for the analysis. Design soil parameters are calculated using BS 8002:1994. BS 8002 recommends a factor called mobilization factor (*M*) to convert peak shear strength to shear strength mobbed in working conditions. *M* is taken as 1.2 in this analysis.

For the analysis, two different scenarios are considered based on the distribution of lateral loads due to active soil condition (Fig. 1 and Fig. 2)

Scenario 1 – Active earth pressure is extending up to the depth of the shear key.

Scenario 2 – Active earth pressure is not extending beyond the base of the retaining wall.

Table 1. Design soil parameters

Design Soil parameters	Value
Design backfill soil cohesion c_{des}	4.17 kPa
Design angle of shearing resistance φ_{des}	26°
Design angle of base friction $\delta_{b\,(des)}$	20°
Design founding soil cohesion $c_{b\,(des)}$	4.17 kPa
Design wall base adhesion $c_{a\,(des)}$	3.13 kPa

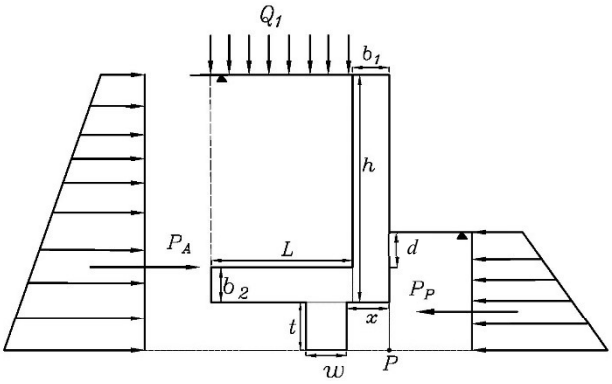

Fig. 1 Pressure diagram for Scenario 1

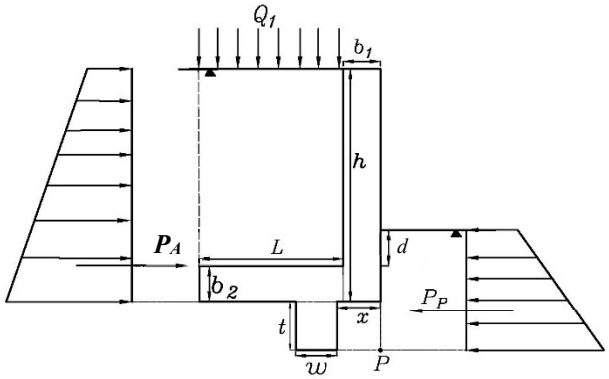

Fig. 2 Pressure diagram for Scenario 2

In this analysis, Rankine's method is used for active and passive earth pressure computation.

2.1 *Stability against sliding*

Factor of Safety for sliding is the ratio between the forces resisting the sliding and forces inducing sliding.

$$FOS = \frac{\text{Sliding resistance}}{\text{Force inducing sliding}} \quad (1)$$

Sliding resistance (R) is given by,

$$R = \sigma_v \tan\delta_b + C_b + P_p \quad (2)$$

Where,

$$\sigma_v = (w_s + w_1 + w_2 + w_k + Q_1 L) \quad (3)$$

Where $\mathbf{w_s}$ is weight of the backfill soil above the base, $\mathbf{w_1}$ is the weight of the wall stem, $\mathbf{w_2}$ is the weight of the wall base, $\mathbf{w_k}$ is the weight of the shear key, $\mathbf{Q_1}$ is the Surcharge and **L** is the length of the base.

For cantilever retaining wall without a shear key, the sliding failure plane will be under the base of the wall, hence,

$$\delta_b = \delta_{b\,(des)} = \frac{2}{3} \times \varphi' \quad (4)$$

$$C_b = c_{a\,(des)} \times (L + b_1) \quad (5)$$

Huntington W.C. (1961) suggests when a shear key is used, sliding occurs on a horizontal plane through the soil at the bottom of the shear key. The different failure planes are shown in Fig. 3.

Therefore, when a shear key is used,

$$\delta_b = \varphi_{des} \quad (6)$$

$$C_b = c_{b\,(des)} (L + b_1 - b) + c_{a\,(des)} b \quad (7)$$

Where, $\boldsymbol{b_1}$ is the stem thickness and $\boldsymbol{b}$ is the key width.

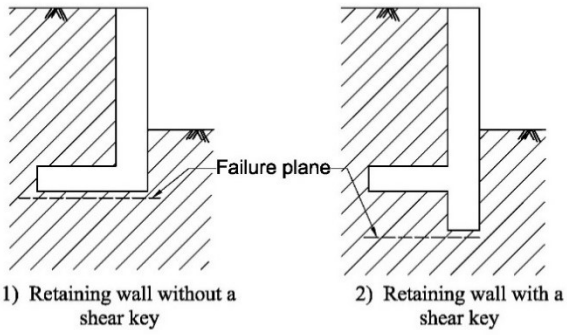

Fig. 3 Sliding failure plane

P_p is the lateral load due to passive pressure. Force inducing sliding is the lateral load due to active pressure (P_A).

2.2 *Stability against overturning*

Factor of Safety against overturning is the ratio between the restraining moments and disturbing moments.

$$FOS = \frac{\text{Resisting Moment } (M_r)}{\text{Disturbing Moment } (M_o)} \quad (8)$$

Moments are taken about the Point of rotation (P) (see Fig. 1 and Fig. 2). Resisting Moment (M_r) is caused by the weight of the backfill soil, Surcharge load, weight of the stem, base and shear key and load due to lateral passive pressure multiplied by their respective lever arms about P. Disturbing Moment (M_o) is caused by the load due to lateral active pressure multiplied by its lever arm about P.

An excel spreadsheet was prepared to obtain analysis the effect of shear key on the stability of cantilever retaining wall using limit equilibrium approach. Different spreadsheets were prepared for the Two scenarios and FOS against sliding, overturning, and bearing pressure variations at the base of the footing were computed for different depths and locations of shear key. i.e., other than ***x*** and ***t*** (see Fig. 1 and Fig. 2), other parameters are kept constant during the analysis.

Graphical representations for the variation of FOS against sliding and overturning with the change in depth and location of shear key and change in maximum and minimum bearing pressures at the base of the retaining wall are obtained to arrive at a conclusion for the study.

3 FINITE ELEMENT ANALYSIS

Finite Element Analysis was carried out using PLAXIS 2D to fulfil the following objectives:

1. To verify the assumed point of rotation in limit equilibrium approach is appropriate
2. To evaluate the effect of depth and location of shear key on the deformation of stem of the wall
3. To compare the maximum and minimum bearing pressures calculated through limit equilibrium approach with those values obtained from the numerical modelling

Fig. 4 shows the deformed mesh of the model. Plate elements are used to model the retaining wall and shear key. Modelling was done with shear key located at the heel of the wall base and five models were created considering 5 depths of shear key and no shear key situation is also modelled. Table 2 shows the material properties used for both founding soil and backfill.

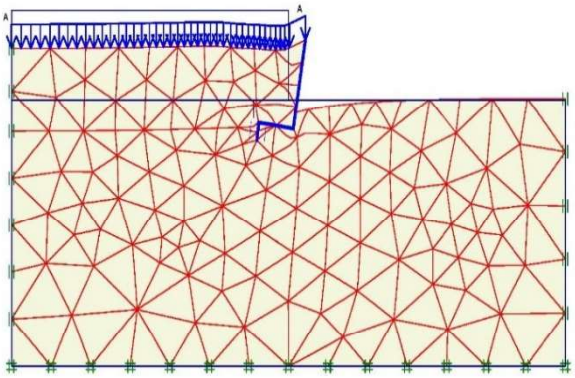

Fig. 4 Deformed mesh for the model

Table 2. Material properties of soil used in PLAXIS 2D

Parameter	***Name***	***Value***
General		
Material model	Model	Mohr-Coulomb
Type of material behaviour	Type	Drained
dry unit weight	γ_{unsat}	17 kN/m^3
Saturated unit weight	γ_{sat}	20 kN/m^3
Parameters		
Young's modulus	E'	1.3 x 10^4 kN/m^2
Poisson's ratio	ν'	0.3
Cohesion	c'	5.0 kN/m^2
Friction angle	φ'	26.0°
Dilatancy angle	ψ	0.0°

Elastic modulus of concrete = 30,000 x 103 kPa and Poisson's ratio of 0.20 is used for concrete.

Dimensions used for the retaining wall and other parameters used in the model are shown in Table 3.

Table 3: Dimensions of wall and other parameters

Parameter	***Value***
Thickness of stem	0.3 m
Thickness of base	0.3 m
Width of shear key	0.6 m
Height of the stem	5.0 m
Length of the base	2.5 m
Surcharge on retaining side	10 kN/m^2
Unit weight of concrete	24 kN/m^3

From the Finite Element analysis, values for the horizontal deformation at the top of the stem for each case, maximum bearing pressures immediately below the base of the retaining wall were obtained and compared to arrive at conclusions related to the study.

4 RESULTS AND DISCUSSION

From the limit equilibrium analysis using spreadsheet, charts are obtained showing the variation of FOS against sliding varying with the depth of shear key, FOS against overturning varying with the depth and location of shear key and maximum bearing pressure variation with the depth and location of shear key.

Following charts show the results obtained from the current study.

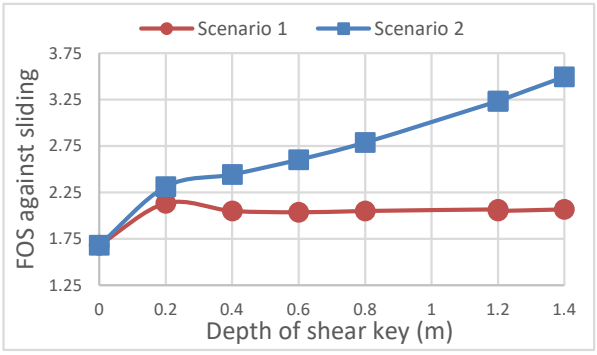

Fig. 5 FOS against sliding vs depth of shear key

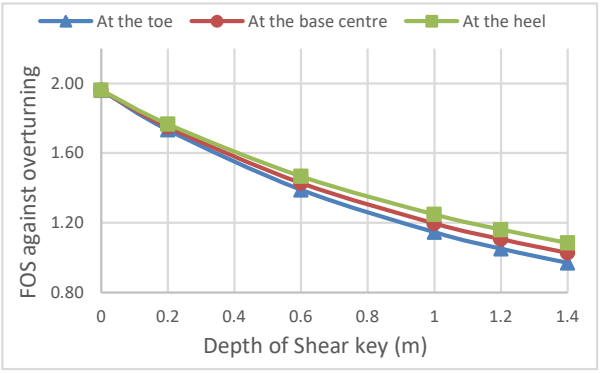

Fig. 6 FOS against Overturning vs Depth of shear key – Scenario 1

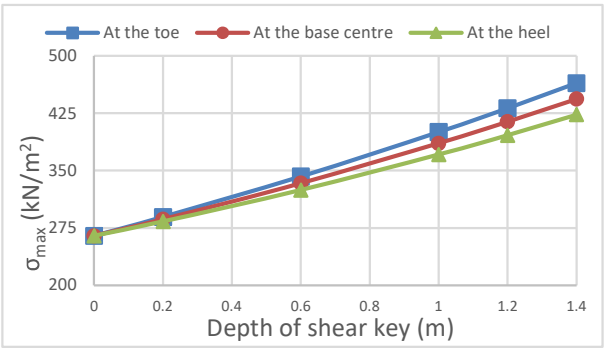

Fig. 7 Variation of σ_{max} with the depth of shear key – Scenario 1

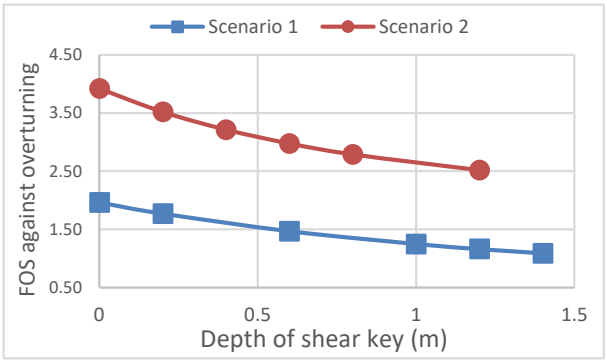

Fig. 8 Comparison of FOS against overturning at heel

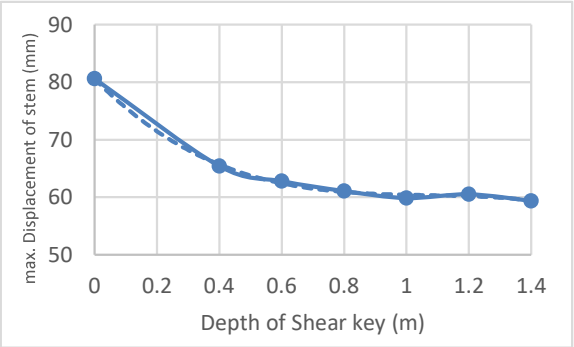

Fig. 9 Displacement at the top of the stem vs depth of the shear key at heel

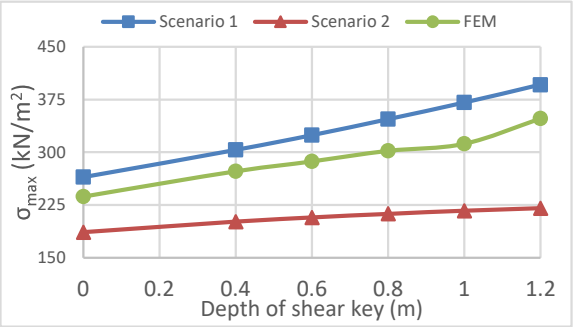

Fig. 10 Maximum bearing pressure vs depth of the shear key at heel

From Fig. 5, it can be observed a steady increase in the FOS with the increase in the depth of key in Scenario 2 whereas, FOS is slightly increasing with the increase in depth of the key in Scenario 1. This is due to the increase in active pressure with the depth of key in Scenario 1 whereas in Scenario 2, increase in depth of the shear key has no effect on the active pressure in Scenario 2.

Eq. (7) is not depending on x (See Fig. 1 and Fig. 2), thus changing the location of shear key will not have any effect on the stability against sliding, i.e., FOS against sliding will only depend on the depth of the shear key.

Effect of depth and location of shear key on the FOS against overturning is evaluated and presented in Fig. 6. It was observed that the stability against overturning decreases with the increase in depth of shear key in Scenario 1. It was also observed that the shear key at heel exhibits superior behaviour than the other locations of shear key. Same kind of variation is obtained from the analysis for Scenario 2 as well.

From Fig. 7, with the increase in depth of shear key, the maximum bearing pressure at the base of the wall is also increases in Scenario 1. Bearing pressure is comparatively lesser when the shear key is at the heel. Same kind of variation is obtained from the analysis for Scenario 2 as well.

Comparison of FOS against overturning varying with the depth of shear key at the heel of the base for both scenarios in shown in Fig. 8. There is a significant variation in FOS against overturning, where values are higher in Scenario 2 compared to Scenario 1. This is because, the increase in active pressure with the depth of key in Scenario 1 causes increase in overturning moment. In Scenario 2, its active pressure does not increase with the depth of shear key and overturning moment will not change despite of increasing depth of shear key.

Variation shown in Fig. 9 is obtained from the results of Finite Element analysis. Horizontal displacement is decreasing with the increasing shear key depth, thus showing that the stability is increasing with the increasing depth of shear key.

From Fig. 10, maximum bearing pressure calculated in Scenario 1 is in greater agreement with the results from the Finite Element Analysis than Scenario 2. Analysis in Scenario 2 underestimates the bearing pressure and thus it may lead to bearing failure of the structure if it is used in designing the retaining wall. But it is worthy to note that, in 2015 IBC (International Building Code), clause 1807.2.1 states that when a key is provided extending below the wall base to engage passive pressure and enhance sliding stability, lateral soil pressures on both sides of the key shall be considered in sliding analysis. But this provision was removed in the 2018 IBC. This supports the analysis criteria used in Scenario 2.

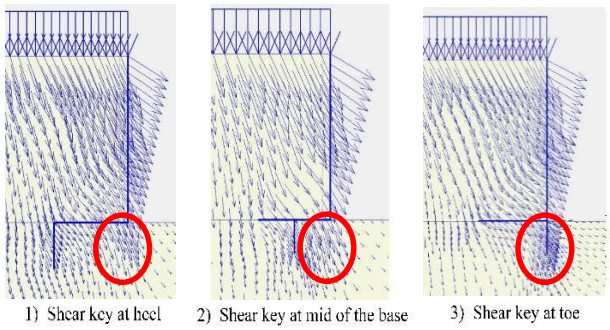

Fig. 11 Total increments obtained for different locations of shear key

When calculating the moments, most of the studies considered the point of rotation as the toe point of the base and neglected the passive pressure component below the toe point (which will otherwise produce an overturning moment). The three diagrams in Fig. 11 shows the total incremental displacements obtained during the analysis using PLAXIS 2D.

In the area highlighted by the red circle, change in the direction of displacement is visible.

Displacements are becoming nearly vertical i.e., angle of displacements with the horizontal is increasing. As there is a change in the direction of displacement, point of rotation is likely to be lied in the highlighted region. Therefore, the assumed point of rotation for limit equilibrium analysis in both the scenarios is reasonable.

5 CONCLUSION

From the limit equilibrium analysis and Finite Element modelling, it was observed that use of shear key has a significant effect on the stability and behaviour of cantilever retaining walls. Following conclusions can be arrived from the above study:

1. Location of shear key has no effect on the stability against sliding. Installing shear key at the toe, centre of the base and at the heel yielded same results of FOS against sliding for a particular depth of key.
2. Increase in depth of shear key will cause an increase in FOS against sliding.
3. Increase in depth of shear key will decrease the stability of the wall against overturning. Therefore, choice of optimum depth of shear key is important to satisfy the recommended FOS for both sliding and overturning.
4. Positioning the shear key at the heel of the footing is the best practice to enhance the safety against overturning failure of the wall.
5. When evaluating the stability of retaining wall with a shear key against overturning, Point of Rotation should be taken as the point located under the toe of the wall at a depth of the shear key.

ACKNOWLEDGEMENT

Continuous support throughout the research by Department of Civil Engineering, University of Moratuwa and specially L.I.N. De Silva is greatly appreciated

REFERENCES

Bentler, Joseph G., Labuz, Joseph F. (2006). Performance of a Cantilever Retaining Wall. *Journal of Geotechnical and Geoenvironmental Engineering,* ASCE, 132(8), pp. 1062-1070.

Horvath, John S. (1991). Effect of Footing Shape on behaviour of Cantilever retaining wall. *Journal of Geotechnical Engineering,* 117(6), pp. 973-978.

Huntington, W. C. (1961). *Earth Pressures and Retaining Walls*. Wiley, New York.

Goh, Anthony T.C. (1993). Behaviour of Cantilever Retaining Walls. *Journal of Geotechnical Engineering,* 119 (11), pp. 1751-1770.

Institution, B. S. & British Standards Institution. (1994). *Code of Practice for Earth Retaining Structures*. British Standards Institution.

International Code Council. (2017). *2018 International Building Code (International Code Council Series)*. International Building Council.

Lahande, R. Snehal (2016). Analytical study of cantilever retaining wall including effect of soil structure interaction, *International Journal of Advanced Research in Engineering and Technology (IJARET),* 3(4), pp. 1579-1585.

Rohaya Alias, Siti Jahara Matlan, Anuar Kasa. (2020). Finite Element Performance with Different Mesh Size of Retaining Walls. *International Journal of Advanced Research in Engineering and Technology (IJARET),* 11(3), pp. 381-389.

Salahudeen, A.B., Ketkukah, T.S. (2019). Effect of Earth Pressures and Shear Key on the Structural Stability of Gravitiy Retaining Wall Supporting Anisotropic Soil. *Nigerian Research Journal of Engineering and Environmental Sciences,* 4(2), pp. 961-971

Sarath, Nisha., Shivashankar R., Ravishankar, A.U. (2011). Role of Shear keys in Cantilever Retaining Wall. *Proceedings of Indian Geotechnical conference,* K-056, pp. 627-630.

Development of an alternative approach for bored and cast in-situ pile design using PDA test results

A.A.S. Kaushalya and U.P. Nawagamuwa
Department of Civil Engineering, University of Moratuwa, Sri Lanka

ABSTRACT: Bored and cast in-situ pile designs are mostly carried out using ICTAD guideline in Sri Lanka. End bearing and skin resistance of the rock are only considered in most of the pile designs. In this study, applicability of estimation of carrying capacity of pile considering the soil layers which have higher SPT "N" values was verified. Furthermore, the estimated capacity considering the proposed method was compared with the actual pile capacity which had been obtained from PDA test. As per the analysis, the estimation of the pile carrying capacity considering all the layers which have SPT "N" values more than or equal to 15 is better predicted than the estimation of carrying capacity of the pile only considering the skin resistance of rock and end bearing of the pile. It has to be further noted that, accurate soil parameters and properties should be the key in accurate estimations.

KEY WORDS: Bored and Cast in-situ Piles; Carrying Capacity of Piles; Pile Designing Methods; High Strain Dynamic Load Test

1 INTRODUCTION

Foundation is the element of any structure that transmits loads to underlying soil or rock. There are two types of foundations: shallow and deep foundation. This study was focused on deep foundations which takes support from deeper soils or bedrock. Based on the method of construction, deep foundations are classified as precast piles (Steel, Timber, Reinforcement concrete, Prestressed concrete) and bored cast-in-situ piles. In this research, bored and cast in-situ piles were considered.

A structurally intact pile can fail due to, shear failure of soil surrounding the pile or excessive settlement of the pile. Therefore, the task of the foundation designer is to find an economical pile to carry the working load with a sufficient safety margin against shear failure of soil while keeping the resultant settlement within the allowable limits. In designing a single pile, it is customary to estimate the maximum load that can be applied to a pile without causing shear failure. This load is referred to as the ultimate load of the pile.

There are two methods available to estimate the ultimate carrying capacity of piles based on Allowable Stress Design method (ASD) including Static methods and Dynamic method. There are three methods of estimating the ultimate carrying based on Static method (Bowles, 1996),

- Using strength parameters of soil and/or rock.
- Using empirical corrections based on in-situ test results such as Standard Penetration Test (SPT), Cone Penetration Test (CPT), etc.
- Using static pile load tests

Development of empirical correlations is based on in-situ test results such as SPT, CPT, etc. (ICTAD/DEV/15, 2011). Designing of piles according to ICTAD guidelines is the most popular and acceptable method in Sri Lanka. There are technical concerns of pile designing according to ICTAD/DEV/15. One of the issues is using less accurate field testing results such as SPT, CPT, and RQD values for pile designing. When gathering the field test results, errors can occur due to bad machine conditions as well as site conditions. Another issue of pile designing according to the ICTAD/DEV/15, does not consider the variety of soil properties and soil behaviour with time and environmental conditions. Also, there are many limitations used in the above procedure (Thilakasiri, 2009).

Furthermore, other methods of pile designing which are used in the construction industry can be identified as Ultimate pile capacity from Poulos and Davis, (1980), Ultimate point bearing capacity from Bowels (1996), Pile designing according to Euro code 7 guidelines, etc. The capacity values calculated according to the above methods on same soil conditions differ from each other. Therefore, selecting the correct capacity value for design is not an easy task. It is observed that most of the design values which are estimated using the above design methods are overestimated or underestimated values when comparing with the actual test results(Thilakasiri, 2009).

However, the actual results of test piles can be misguided by less reliable observations due to bad practices in installing the test piles. The general guidelines about pile designing and constructing proposed by the Institution of Civil Engineers (1978) suggest that at least one preliminary test pile be installed for each major zones of the site, or at least one pile for each hundred working piles, on a site. Also, EN 1997 - 1 (2004) suggests that; if one load testing of test pile is carried out, the test pile must be located where the weakest ground condition is observed and if load tests are carried out on two or more test piles, the test locations should be representative of the site.

When considering the pile designing is done according to the ICTAD guidelines, an allowable carrying capacity value can be directly estimated for the pile by using ICTAD guidelines. However, the Euro code 7 guideline recommends the design value for carrying capacity of the pile using partial factors.

Furthermore, the pile designing is mostly carried out only considering the skin and toe resistance in the bedrock of the pile in Sri Lanka. Because of this phenomenon, soil layers which have high SPT "N" values are not considered in pile designing. In this research, a comparative study is conducted using of the above mentioned soil layers in designing piles together with the following objectives.

It is required to evaluate which design procedure is more effective when the estimation of the pile capacity considering all the layers which have SPT "N" values more than or equal to 15 or the pile capacity only considering the skin and toe resistance in the bedrock. Comparison of compare the estimated allowable carrying capacity values according to the ICTAD and Euro code 7 guidelines with the actual allowable carrying capacity values which have taken from the PDA test results is also considered as a primary objective in this study.

2 METHODOLOGY

2.1 *Data Collection*

Required data and information for the research were gathered from the Construction of Pile Foundation of Manning Market Relocation Project (MMRP) from Pettah to Peliyagoda. First, approval for the data collection was taken from Central Engineering Consultancy Bureau (CECB). Then site investigation report with 13 borehole logs and 37 PDA test reports were collected for this study. The piles with a diameter of 600mm, 750mm, 900mm, 1000mm, and 1200mm were designed for the MMRP and pile layouts are provided separately.

Pile founding rock level, at this site, is adopted as the rock level at which a core recovery (CR) of more than 80% and a rock quality designation (RQD) of more than 45% were obtained. This concept correlates to an allowable bearing capacity of 6 N/mm^2(ICTAD/DEV/15, 2011). Rock socketing length for piles is used as 1.5 times pile diameter. Concreting was carried out with grade 30 concrete by using ordinary Portland cement or sulphate resistance cement. Pile loading test details were included in Table 1,

Table 1. Working load and testing load of the piles

Pile Diameter (mm)	Working Load (KN)	Maximum Test Load (KN)
600	2120	3180
750	3310	4965

Then, the piles with PDA reports were categorized to the borehole zones for estimation of capacity and comparison.

2.2 *Obtaining the corrected SPT "N" values and soil parameters for borehole details*

First, the corrected SPT "N" values were calculated for each borehole. After that, the friction angles of granular soil layers and undrained cohesion of cohesive soil layers were obtained for each borehole respectively and calculations were carried out according to (Bowles, 1996).

2.3 *Estimating of allowable carrying capacity values according to ICTAD guidelines*

According to ICTAD guidelines (ICTAD/DEV/15 ,2011), the pile carrying capacity was estimated under two design criteria for each borehole location. They are as follows,

- **Criteria 01**: Estimation of pile capacity considering all the layers which have SPT "N" values more than or equal to 15
- **Criteria 02**: Estimation of pile capacity only considering the skin and toe resistance in bedrock

All piles were designed as end bearing rock socketed piles. Allowable carrying capacity was obtained by using Equation (1) (ICTAD/DEV/15, 2011),

$$P_{allowable} = \frac{q_u A_b}{F_b} + \frac{f_u A_s}{F_s} \quad (1)$$

Where,

p_u- Ultimate carrying capacity of pile

q_u- Ultimate end resistance per unit area of base

f_u - Ultimate skin friction resistance per unit surface area of the shaft

A_b, A_s- Area of the base, and surface area of the shaft respectively

$P_{allowable}$- allowable carrying capacity of a single pile; and F_b is the safety factor with respect to end bearing & F_s is the safety factor with respect to skin friction

Assumptions made for the capacity estimation are the unconfined compressive strength of Fresh to slightly weathered rock is 30 MPa. (For allowable bearing capacity 6 N/mm^2 and 45% RQD) and if bentonite is used in drilling process, the allowable skin friction should be taken as 25% of the ultimate skin friction obtained from the above estimated value.

Then, negative skin friction of the piles was estimated for each borehole location. When estimating the negative skin friction, few assumptions were made including Filling height after pile construction is 0.5m and the filling material is embankment type 2 material with 15.9 kN/m^3 dry unit weight; and the water table is at the ground level.

After that, the adequacy of the design was checked using working load, self-weight of the pile, and negative skin friction.

2.4 *Estimation of design carrying capacity values according to Euro code 7*

In this above method, the design capacity values were estimated under both criteria according to all three approaches of Euro code 7 and partial factors were used for calculation as per the Euro code 7 (EN 1997-1). Previously made assumptions were followed in this estimation as well. Finally, the adequacy of a design was checked with the degree of utilization calculated using summation of action forces.

2.5 *Comparison of two design criteria*

In this section, criteria that is more effective when comparing the estimation of the pile capacity was evaluated by considering all the layers which have SPT "N" values more than or equal to 15 or the pile capacity only considering the skin and toe resistance in the bedrock. The above comparison was proceeded according to both the ICTAD and EC7 guidelines. It was represented as a percentage of the difference between the capacity values of two criteria.

2.6 *Comparison between the estimated and actual allowable capacities*

In this stage, the estimated allowable carrying capacity values according to the ICTAD and Euro code 7 guidelines were compared with the actual allowable carrying capacity values which were taken from the PDA test results. More suitable design criteria based on the above comparison was used for the capacity estimation.

An allowable carrying capacity value of the piles can be directly estimated by using ICTAD guidelines. However, Euro code 7 provides a design capacity value. Therefore, the design capacity value should be converted into an allowable capacity value. Dias and Sivakumar (2012) have mentioned that service loads can be approximately obtained from the ultimate load by dividing the latter by 1.4 in reinforced concrete structures. As per the above reference, 1.4 partial factor was used to convert the design value into allowable capacity value in Euro code 7.

Generally, when estimating the capacity value in Euro code 7, the toe resistance and skin resistance of rock were calculated as allowable resistance values meanwhile the skin resistance of soil was calculated as design resistance value. Therefore, the above mentioned 1.4 partial factor was used only for the estimation of allowable skin resistance of the soil. Above 1.4 partial factor was only introduced for Approach 01(combination 01), Approach 02 and Approach 03 of Euro code 7.

Then, the actual allowable capacity values were obtained from PDA test. In the test report, load-settlement curve of the pile is usually provided in CAPWAP result section. The actual allowable capacity of the piles was obtained for 12mm settlement of top of the pile by using above mentioned graph. The observation had been made only for the piles which have mobilized settlement more than 12mm. Finally, the estimated allowable capacities were compared with the actual values. The above comparison was represented graphically and numerically (in percentage) with the level of overestimation or underestimation.

3 ANALYSIS AND DISCUSSION

3.1 *Comparison of estimated allowable capacities according to ICTAD and design capacities according to EC7 guidelines using two criteria*

Summary of analyzed data of comparison 1 is in the Table 2

Table 2. Summary of the comparison

Borehole	Pile Dia. (mm)	Percentage of difference between allowable or design capacities of Criteria 01 and 02 (%)				
		ICTAD	EC7			
			App1 Com1	App1 Com2	App2	App3
BH04-01	600	20.3	49.1	37.8	44.6	42.5
	750	16.3	39.3	30.2	35.7	34.0
BH05-01	600	11.2	32.8	25.2	29.8	28.5
	750	8.9	26.2	20.2	23.8	22.8
BH07-01	600	33.2	74.2	57.1	62.2	65.1
	750	26.6	59.4	45.7	54.0	52.1
BH03-02	600	8.1	20.3	15.6	18.5	17.6
	750	6.5	16.3	12.5	14.8	14.1
BH04-02	600	65.2	149.2	114.8	135.6	129.1
	750	52.2	119.4	91.8	108.5	111.4

When considering the acceptability of the design, more suitable designing criteria is the estimation of allowable or design capacity considering all the layers which have SPT "N" values more than or equal to 15. Percentages difference between allowable and design capacities of criteria 1 and 2 have varied from borehole location to borehole location. When estimating the allowable and design capacities based on criteria 02, the skin resistance of rock shaft and toe resistance were only taken into consideration. Quality of the bed rock was assumed as the same one for the entire project area. Because of this phenomena, the allowable and design capacities estimated for criteria 02 were similar for all borehole locations. The reason for the variation of capacities of criteria 01 can be identified as the arrangement of soil layers and their properties. When considering all designing approaches, the pile designs have relatively low percentages at BH05-01 and BH03-02 locations. The reason behind that is the availability of only thinner dense sand or completely weathered rock layer with SPT "N" value more than or equal to 15 in the above mentioned locations. Therefore, these locations have relatively lower capacity values estimated for criteria 02. However, the higher percentages were obtained for BH07-01 and BH04-02 locations. The reason for the above variation is the availability of highly weathered rock, completely weathered rock and moderately weathered rock layers with lower RQD (<40) at the above locations. These layers provide higher contribution for the skin resistance of the pile and they helped to increase the value of total skin resistance. If the pile is to be designed without considering the above layers in the same situation, the design will not be an economical one. According to the above comparison, the more suitable designing criteria is the estimation of allowable or design capacities considering all the layers which have SPT "N" value more than or equal to 15.

3.2 *Comparison of estimated allowable capacities according to ICTAD and EC7 guidelines with actual allowable capacities observed from PDA test results*

The second comparison was carried out considering criteria 01 which is selected as more suitable designing criteria from the above comparison. Figures 1 and 2 provide details of comparisons for different pile diameters.

The comparison indicates that there can be underestimations or overestimations of the allowable capacity values when compared to the actual values. The percentage of under estimation or over estimation than the actual allowable capacity can be stated as following Table 3.

Table 3. Percentage for overestimation or underestimation based on actual allowable capacity

BH	Pile Dia. (mm)	Percentage for overestimation or underestimation based on actual allowable capacity			
		ICTAD	Euro code 7		
			App01-com 01	App02	App03
BH 4-1	600	23.82	14.51	16.53	23.71
	750	20.88	12.87	14.61	21.82
BH 5-1	600				
	750	32.01	25.90	26.96	32.90
BH 7-1	600				
	750	10.14	-1.08	1.65	9.95
BH 3-2	600	34.07	30.18	30.98	36.55
	750	28.60	25.17	25.88	31.79
BH 4-2	600				
	750	-9.30	-33.06	-27.50	-15.39

Highlighted values (minus values) were values for overestimation.

When comparing estimated allowable capacities with actual values, most of the estimations capacities revealed as underestimations.

According to the above results, estimation of skin resistance of bedrock and toe resistance were similar for all the capacity estimations. So, the difference between the estimated capacities occurred due to variation of the skin resistance of soil layers from borehole to borehole. When calculating the skin resistance values for soil layers according to the ICTAD guidelines, the field SPT "N" values are used. Also, the soil properties which are obtained from corrected SPT "N" values are used to estimate capacity according to Euro code 7. So, the reason for the under estimation can be identified as the low accuracy of the soil parameters which are included in the investigation report. Also, the assumptions made for the calculations may cause the above problem.

In addition to that, when comparing the estimated allowable capacities with actual values, an over estimation can be identified in BH04-02 for both ICTAD and Euro code 7 guidelines. BH04-02 comprises of highly weathered rock and the moderately weathered rock layers with 0 RQD value. These layers were taken into the calculation of the skin resistance provided by soil. So, the 75 SPT "N" value was assumed for highly weathered rock layer and 100 was assumed for moderately weathered rock layer. Those assumed values can be the reason for the above mentioned over estimation. These assumptions were made due to the lack of proper values of soil properties in the investigation stage.

It can be concluded that, if all layers which have SPT "N" values more than or equal to 15 are considered for the estimation of capacities, soil properties should be more accurate.

4 CONCLUSION

Estimation of the pile carrying capacity considering all the layers which have SPT "N" values more than or equal to 15 (when estimating the skin resistance of the pile) is better than the estimation of carrying capacity of the pile only considering the skin resistance of rock and end bearing of the pile.

Results from the comparisons of the actual and estimated allowable capacities which were conducted in accordance with the selected criteria as in above, it can be concluded that it is possible to obtain overestimations or underestimations that will rely on the assumptions made about the properties of soil and rock layers.

Further, the accurate soil parameters and properties should be maintained in estimations. Furthermore, the geotechnical investigation of the site should be more accurate.

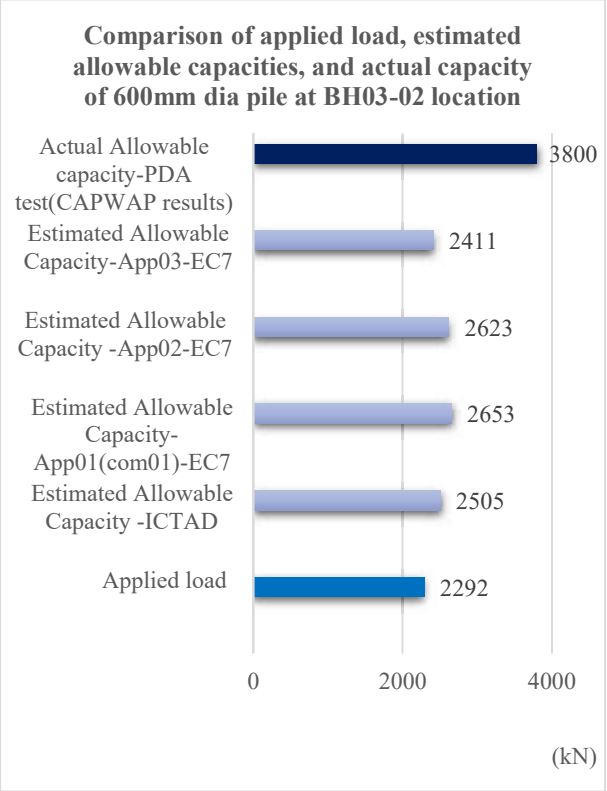

Figure 1. Comparison for 600mm dia. Pile at BH03-02 location

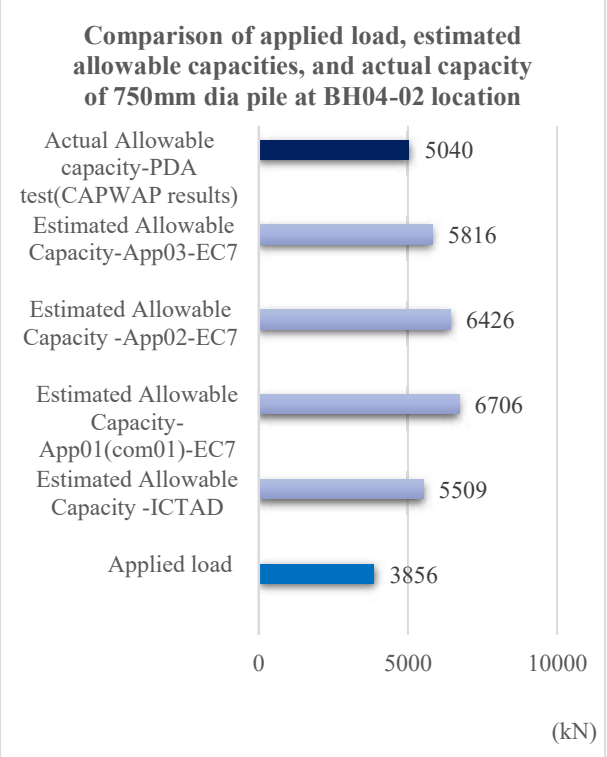

Figure 2. Comparison for 750mm dia. Pile at BH04-02 location

REFERENCES

Bowles, (1996), "Foundation Analysis and Design", McGraw-Hill http://10.1.1.57:8888/dspace/handle/hau/4588

Dias P., & Sivakumar K., (2012), "Graded Example in Reinforced Concrete Design to Euro code 2" (3rd ed.), Society of Structural Engineering - Sri Lanka

EN 1997 - 1, (2004), Euro code 7: Geotechnical design part , https://www.ngm2016.com/uploads/2/1/7/9/21790806/eurocode_7_-_geotechnical_designen.1997.1.2004.pdf

ICTAD/DEV/15, (2011), "Specification for Bored and Cast In-situ Reinforced Concrete Piles" (second edition,. Institute for Construction Training and Development, Ministry of Housing, Construction and Public Utilities, Colombo, Sri Lanka

Institution of Civil Engineers, (1978), "Piling: Model procedures and specifications", London: The Institution

Poulos H. G., and Davis E. H., (1980), "Pile foundation analysis and design", New York; Toronto: J Wiley

Thilakasiri H. S., (2009), "Construction & Testing of Piles" (First Edition), Sarasavi Publishers

A study on axial performance of helical piles on residual soils

C.N. Liyanage and L.I.N. de Silva
Department of Civil Engineering, University of Moratuwa, Sri Lanka

ABSTRACT: Denser/harder soil layers often found under very shallow depths in Sri Lanka. In such circumstances, helical piles offer an economical alternative to traditional foundation types such as pad footings, rafts or piles while providing required support to the structure. This paper presents an analysis on the axial performance of helical piles in Sri Lankan soils through in-situ static load tests, theoretical studies, numerical modelling, and empirical relationships. Based on results, suitability of using empirical factors (K_t) given in literature to determine axial pile capacities or to find installation torque needed in achieving design loads is checked. In this study, 19 static load tests were conducted and suitable values for K_t will be suggested under Sri Lankan subsoil conditions if values given in literature does not provide accurate estimations.

KEY WORDS: Helical piles; Axial performance; Capacity correlations; Numerical modelling

1 INTRODUCTION

Helical piles, also known as screw piles, were used initially for supporting small tensile forces specially to counter loose soil conditions. Helical piles allow for better connection with the ground mainly due to helices attached to the steel shaft made of high strength steel. With improvement of interest in research related to helical piles, larger, higher capacity helical piles are currently being used in many applications to support much larger axial and lateral loads. With wide range of load carrying capacities being available, fast installations, low disturbances, elegant simplicity, and their ability to be loaded immediately after installations make them an appealing alternative to traditional foundation types.

With increase in usage, certain risks could be developed due to lack of understanding between performance of helical piles and their capacity evaluations in design solutions. Installation torque has long been incorporated into helical pile design methodology where it is considered as a quality assurance and quality control parameter. Hoyt and Clemence (1989) proposed an empirical model that can be used to approximate helical pile capacity with installation torque. This became popular worldwide as designers were able to use this relationship for in situ verification of pile capacity and to determine average installation torque requires to install a pile. But because of the varying conditions from country to country it is always better to understand the suitability of using torque-to-capacity relationships in determining helical pile capacity by conducting a thorough analysis on axial performance with different methods suggested in literature so that finding could be used to further economize helical pile foundation applications.

2 AXIAL CARRYING CAPACITY OF HELICAL PILES

In this study axial performance of helical pile under compression and tension loads is determined through in situ tests, theoretical methods, numerical models, and empirical relationships.

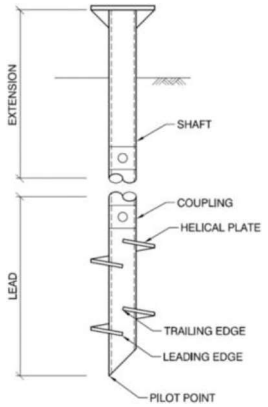

Fig. 1 Components of a helical pile

Balla (1961) categorized helical pile installation as either *'Deep'* or *'Shallow'* based on *H/D* ratio (where *'H'* is depth to topmost helix and *'D'* is top helix diameter; a pile installation is considered '*Deep'* when $H/D > 5$). All the piles associated in this study are classified as *'Deep'* piles. Narasimha Rao et al. (1989) shown through experimental studies when $S/D \leq 3$ (where *'S'* is spacing between two helices and *'D'* is lowest diameter of the two helices), piles undergo *'Cylindrical Shear Failure'* and otherwise *'Individual Plate Bearing'* would occur.

CHANCE helical piles manufactured by Hubbell Power System, Inc. (HPS) were used in this study and helices of these piles are spaced approximately

at three times the diameter of lower helix (*S/D ≈ 3)*. Although this is considered as the interval between two failure mechanisms, CHANCE Technical Design Manual suggest that this condition ensure bearing of individual helices do not affect each other. Therefore, *Individual Plate Bearing* method is used to calculate axial capacities of *'Deep'* piles. Following equations are used to determine bearing capacity of each plate and pile as a whole (P_u).

$$P_u = \sum_n q_{ult} A_n + \alpha H(\pi d) \quad (1)$$

$$q_{ult} = cN_c + q'N_q + 0.5\gamma D N_\gamma \quad (2)$$

Where $\boldsymbol{q_{ult}}$ is the ultimate bearing pressure of an individual plate derived from Terzaghi (1943), $\boldsymbol{A}$ is the helix area of the n^{th} helix, $\boldsymbol{\alpha}$ is the adhesion between soil & shaft, $\boldsymbol{H}$ is the shaft length above the top helix, d is the diameter of a circle circumscribed around the shaft, $\boldsymbol{c}$ is the cohesion of soil and $\boldsymbol{q'}$ is effective overburden pressure at n^{th} helix level. CHANCE (2018) suggest that width term of Eq. (2) can be neglected when helix diameter, D is less than 0.6m. For fine-grain soil, Skempton (1951) showed that N_c approaches a constant value of 9 for deep foundations and $N_q = 1$, $N_\gamma = 0$. Meyerhof (1976) suggested that for deep installations bearing capacity factor N_q can be found from,

$$N_q = 0.5(12\emptyset')^{\emptyset'/54} \quad (3)$$

Where $\boldsymbol{\phi'}$ is the effective friction angle.

A breakthrough on using empirical relationships to determine pile capacities based on installation torque came when Hoyt et al., (1989) conducted 91 tension load tests on helical piles at 24 different locations with various soil conditions ranging from fine grain to coarse grain and following empirical relationship was introduced,

$$P_u = K_t T \quad (4)$$

Where $\boldsymbol{K_t}$ is the torque-to-capacity ratio in $\boldsymbol{ft^{-1}(m^{-1})}$, $\boldsymbol{P_u}$ is pile capacity and $\boldsymbol{T}$ is effective/average torque over final three readings. $\boldsymbol{K_t}$ was determined based on effective shaft diameter (Table 1). HPS extracted those findings to approximate helical pile capacities or to determine average installation torque required to gain a given design capacity.

Table 1; Values for K_t by Hoyt et al., (1989)

Helical Pile Type	$K_t(m^{-1})[ft^{-1}]$
Square Shaft (Type SS*)	33[10]
Round Shaft (RS* 2875.203 & RS 2875.276)	30[9]
Round Shaft (RS 3500.300)	23[7]
Round Shaft (RS 4500.237 & RS 4500.337)	20[6]

*SS-Square Shaft, *RS-Round Shaft pile or extension

Perko (2009) conducted over 200 in situ load test under compression, tension and following relationships were suggested to determine K_t,

$$K_t = 1970 d_{eff}^{-1.01} \ (tension) \quad (5)$$

$$K_t = 1039 d_{eff}^{-0.84} \ (compression) \quad (6)$$

where $\boldsymbol{d_{eff}}$ is effective shaft diameter (in *mm*).

3 IN-SITU TESTING

Load tests were carried out in Katuwawala area in Kesbewa. Maximum depth of installation for a pile was 10.7m with minimum being 3.7m. ASTM 1143-07 and ASTM 3689-80 test methods were followed in determining axial capacities of helical pile under compression and tension respectively. A preload of 76.6kN was applied to stabilize the reaction frame and load was incremented by 10% of estimated pile capacity (theoretical capacity from CHANCE (2018) or from HeliCap; a cloud software by HPS) in 4-minute intervals before unloading in 4 equal decrements.

Installation torque for each pile installation was measured using a wireless torque indicator and readings were taken at every 0.3m interval. Effective torque was then obtained by averaging torque readings in final three 0.3m intervals to determine field torque-to-capacity factor K_t.

3.1 *Pile description*

Because of the denser soil layers at shallow depths in Sri Lanka, SS175/RS3500.300 combo piles (SS175 lead section and RS3500 extension) and SS175 helical piles manufactured by HPS were used in this study. In each configuration lead section (SS175) consists of three helices (helix diameters 200 mm, 250 mm, and 300 mm) welded to the pile shaft (either RS or SS). Each helix has a 75 mm pitch. *S/D* ratio is approximately 3 for these piles.

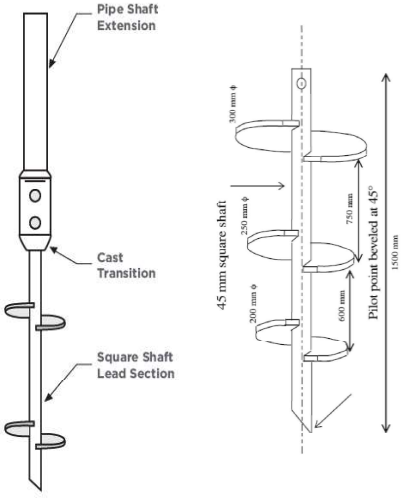

Fig. 2 SS/RS combo pile & SS175 lead section

3.2 *Site description*

Piles were installed in three sites and to understand subsoil condition, samples from boreholes were analyzed. Bedrock was found at 8.55m depth in site 01, at 15m in site 02 and 17.2m in site 03. Refer to Table 4-6 for soil profiles and properties in each site. (Site 02 and 03 were based on University of Western Ontario in London and relevant load test results were extracted from findings by Ben Livneh et al., (2008))

3.3 *Failure criterion and test results*

Given the unique geometry of helical piles, based on experimental studies, both CHANCE (2018) and Ben Livneh et al., (2008) expressed that, under tensile and compressive loads, ultimate load occur when the pile head displacement is equal to 8%-10% of the largest helix diameter plus the elastic movement of the shaft (*Diameter Method*).

$$\frac{PL}{AE} + 0.1D(or\ 0.08D)\ (mm) \quad (7)$$

Where ***P*** is axial load, ***L*** is length of shaft, ***A*** is cross section area of shaft, ***E*** is Young's modulus of shaft meterial and ***D*** is diameter of top most helix.

Table 2 and Table 3 represent results from compression and tension tests respectively.

Table 2. Compression test results

Pile ID (Site)	Soil Type	Pile Type	Pile Capacity (kN)	$K_t(m^{-1})$
KC (Site 1)	Clayey Sand	SS175/ RS350 0.300	413	45.46
P1 (Site 2)	Dense Silt	SS175	465	39.54
P2 (Site 2)	Dense Silt	SS175	496	42.98
P4 (Site 2)	Clayey Silt	SS175	356	35.78
P5 (Site 2)	Clayey Silt	SS175	327	37.46
P6 (Site 2)	Clayey Silt	SS175	328	38.14
P13(Site 3)	Sand	SS175	695	61.45
P14(Site 3)	Sand	SS175	660	62.09

Table 3. Tension test results

Pile ID (Site)	Soil Type	Pile Type	Pile Capacity (kN)	$K_t(m^{-1})$
KT (Site 1)	Clayey Sand	SS175/ RS350 0.300	291	28.62
P7 (Site 2)	Clayey Silt	SS175	226	25.36
P8 (Site 2)	Clayey Silt	SS175	260	26.53
P9 (Site 2)	Clayey Silt	SS175	181	27.63
P16(Site 2)	Clayey Silt	SS175	250	32.72
P20(Site 3)	Clayey Silt	SS175	295	29.21
P10(Site 2)	Clayey Silt	SS175	245	24.67
P17(Site 2)	Dense Silt	SS175	256	36.21
P15(Site 2)	Dense Silt	SS175	381	39.56
P12(Site 3)	Sand	SS175	379	30.69
P19(Site 3)	Sand	SS175	406	36.94

4 THEORETICAL PILE CAPACITIES

Every pile in this study were installed to a depth such that they would act as *'Deep'* piles (*H/D > 5*). Therefore, Eq. (1) & (2) under Section 2 were used to calculate ultimate axial capacity of piles. According to CHANCE (2018), experimental studies have found that SS piles does not necessarily develop any friction resistance along the shaft and even in round shaft helical piles, shaft resistance can be considered negligible when shaft diameter is less than 89mm.

'β method' was used to evaluate friction developed along the shafts. For all the piles involved in this study, mobilized skin friction resistance was negligible along the shaft.

5 NUMERICAL MODELLING

Each pile was modelled using Plaxis2D software and due to negligence of helix pitch, assumption that soil layers remain horizontal and modelling of square shafts as round shafts with an equivalent diameter, *'Axisymmetric'* model type was followed for quick results. To account for soil disturbances during installation, interface elements were introduced assuming 33% reduction in strength parameters around the pile. To avoid any boundary effect interference on pile response horizontal boundary was set at $2.5L_p$ from the edge of pile, vertical boundary at $3.5L_p$ below ground level (Mestat, 2017). As for boundary conditions, Lateral boundaries were pinned ($u_x = 0$) and for Vertical boundaries; top was set free and bottom was fixed ($u_x = u_y = 0$)

Table 4 to Table 6 shows the soil parameters used for finite element modelling (Ben Livneh, 2008). Line displacement was introduced at the pile head to ensure uniform displacement and it was incremented in 5mm intervals. Capacity at each displacement was recorded and then the method given under Section 3.3 was used to determine ultimate pile capacity under given loading condition.

Table 4. Soil properties for site 01

Soil Layer	Depth (m)	SPT N-value	γ * (kN/m^3)	γ_{sat} * (kN/m^3)	c′ or (c_u) * [kPa]	∅′ * (°)	E* (kN/m^2)
Very soft peaty clay (W.T. = 0m depth)	4.5	1	10	10	(10)	-	2000
Stiff sandy clay	6	11	15	16	(75)	-	10000
Very dense clayey sand	8.55	>50	20	21	10	38	35000

Table 5. Soil properties for site 02

Soil Layer	Depth (m)	SPT N-value	γ * (kN/m^3)	γ_{sat} * (kN/m^3)	c′ or (c_u) * [kPa]	∅′ * (°)	E* (kN/m^2)
Stiff sandy clayey silt	2.4	19	17.3	17.3	10	28	60000
Very stiff clayey silt (W.T.)	4.1	25	17.5	18.5	21	27	85000
Stiff clayey silt	5.8	11	16.5	18.5	9	23	100000
Very stiff sandy clayey silt	7.3	17	15	18	20	30	400000
Dense silt	>7.3	>30	17	19	19	34	65000

Table 6. Soil properties for site 03

Soil Layer	Depth (m)	SPT N-value	γ * (kN/m^3)	γ_{sat} * (kN/m^3)	c′ or (c_u) * [kPa]	∅′ * (°)	E* (kN/m^2)
Stiff sandy clayey silt	2.6	34	18.5	18.5	22	33	40000
Very stiff clayey silt (W.T.)	5.2	20	17	19	23	27	300000
Dense fine sand	>5.2	>32	18	20	6	38	100000

*γ is dry unit weight of soil. *γ_{sat} is saturated unit weight. *E is Young's modulus of soil. * $\mathbf{c'(c_u)}$ is effective cohesion (undrained cohesion) and * ∅′ is effective friction angle for each soil.

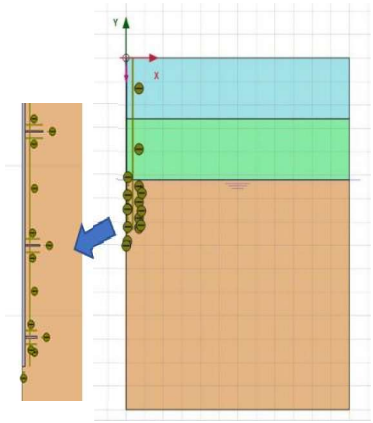

Fig. 3 A typical finite element model used for analysis

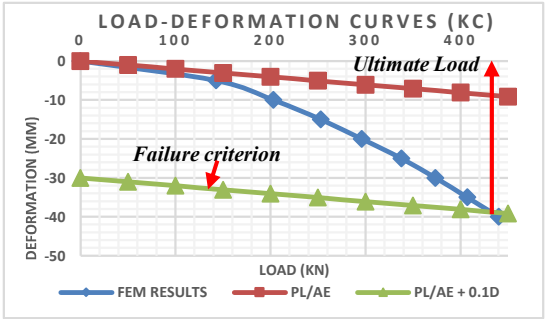

Fig. 4 Typical analysis results for a finite element model under compression

6 RESULTS FROM EMPIRICAL RELATIONSHIPS

For average installation torque observed in field tests, axial capacities were calculated using Eq. (4) under Section 2, considering torque-to-capacity ratios suggested by Perko (2009).

7 RESULTS AND FINDINGS

Ratio of axial capacities evaluated from empirical relationships, theoretical methods, and numerical models to in-situ capacity values from field tests are listed in Table 7 (in the order of A, B, C) to see which method is more consistent with actual axial capacity (in-situ value) of helical piles to establish torque-to-capacity factors based on soil types.

Table 7. Result comparison

Pile ID	Soil Type	Loading Type	A*	B*	C*
KC	Clayey Sand	Compression	60	91	96
KT	Clayey Sand	Tension	89	97	88
P1	Dense Silt	Compression	81	81	92
P2	Dense Silt	Compression	74	76	98
P4	Clayey Silt	Compression	89	26	57
P5	Clayey Silt	Compression	85	30	65
P6	Clayey Silt	Compression	84	30	64
P13	Sand	Compression	52	85	77
P14	Sand	Compression	52	92	82
P7	Clayey Silt	Tension	85	42	95
P8	Clayey Silt	Tension	88	64	79
P9	Clayey Silt	Tension	92	65	86
P16	Clayey Silt	Tension	92	66	84
P20	Clayey Silt	Tension	97	67	81
P10	Clayey Silt	Tension	82	68	73
P17	Dense Silt	Tension	83	69	65
P15	Dense Silt	Tension	76	70	99
P12	Sand	Tension	98	71	78
P19	Sand	Tension	81	72	77
		Median (%)	**84**	**69**	**81**

*A-Ratio of empirical value and in-situ value (%), *B-Ratio of theoretical value and in-situ value (%), *C-Ratio of FEM value and in-situ value (%)

Median for each method shows that empirical and numerical models generally offer a better approximation of actual pile capacities. Therefore, to predict typical values K_t, it is viable to use load capacities from empirical (from literature) and numerical models with static load test results compared to other methods. For the analysis, it is assumed that installation torque remains constant for each capacity evaluation method as it primarily depends on sub soil conditions. Hoyt et el., (1989) showed through experimental analysis that installation torque and helical pile axial capacity has a liner relationship with slope yielding torque-to-capacity factor, K_t (Eq. 4 under Section 2).

Based on pile capacities from in-situ tests, empirical relationships, and numerical models, following plots can be generated for a given pile configuration under different soil conditions. For each soil type, if capacity values from numerical models are on average within 20% of in-situ pile capacity (From Table 7; column 'C'), K_t values from numerical models are considered as a safety margin in evaluation of new K_t values suitable for Sri Lankan conditions.

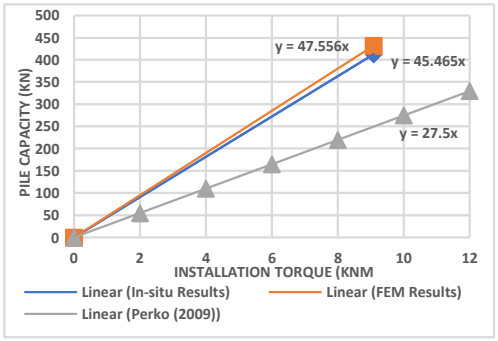

Fig. 5 Clayey sand under compression (SS/RS pile)

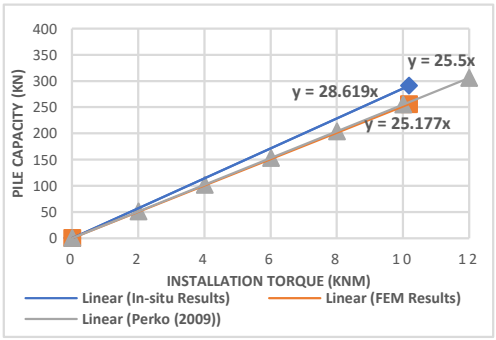

Fig. 6 Clayey sand under tension (SS/RS pile)

For Clayey Sands, under both loading types, pile capacities from in-situ tests and numerical models are within 20% of each other. Considering compressive loads (Fig. 5), K_t from in-situ tests and numerical models are higher compared to values suggested by Perko (2009) considering SS/RS combo piles. And numerical model results slightly overpredict the in-situ test values as well. Therefore, a suitable range to be used for K_t would be 27.5-45.5m^{-1} with an average of 36.5m^{-1}. Under tensile loads (Fig. 6), numerical model underpredict the in-situ capacities as well as empirical values. Therefore, a suitable range to be used for K_t would be 25.2-28.6 m^{-1} with an average of 26.9 m^{-1}.

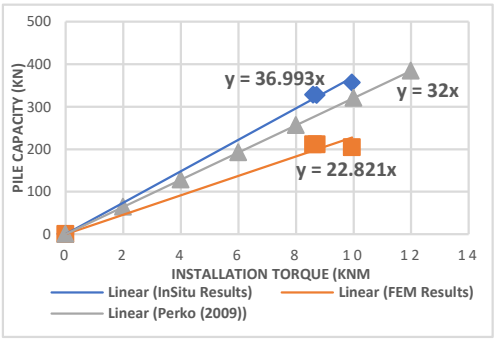

Fig.7 Clayey silt under compression (SS175 helical pile)

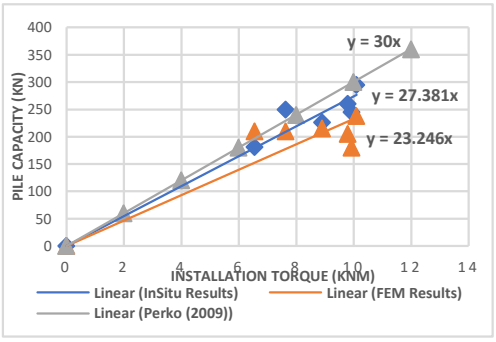

Fig.8 Clayey silt under tension (SS175 helical pile)

Considering compressive loads (Fig. 7), suitable range to be used for K_t would be 32-37 m^{-1} with an average of 34.5 m^{-1}. Under tensile loads, both capacities from filed tests and numerical models are lesser compared to empirical results. Therefore, suitable range to be used for K_t would be 23.25-27.4 m^{-1} with an average of 25.33 m^{-1}.

Similar methods were followed in suggesting suitable values for K_t for other soil conditions as well.

Table 8. Result comparison

Soil Type	Pile Type	Loading Type	Suggested value for K_t
Clayey Sand	SS175/ RS3500.300	C*	36.50
		T*	26.90
Dense Silt	SS175	C	36.62
		T	34.20
Clayey Silt	SS175	C	34.50
		T	25.33
Sand	SS175	C	46.90
		T	31.75

*C – Compression, *T – Tension

Other than that, based on displacement contours for each pile in the numerical model, it was observed that load transfer mechanism under either tension or compression, followed a tapered cylindrical surface between helices and bearing of lead helix in the direction of loading as shown by Fig. 9.

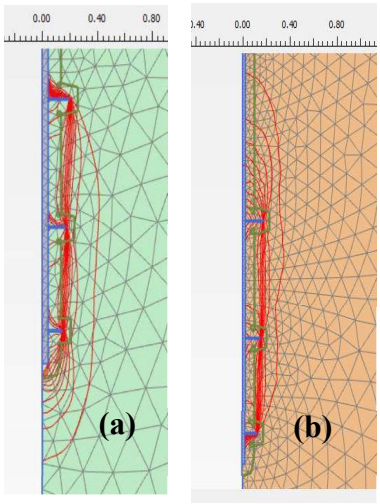

Fig. 9 Load transfer mechanism under (a) compression and (b) tension

Thus, for helical piles with $S/D \approx 3$, use of *'individual bearing method'* to approximate axial capacity of helical piles would yield conservative results.

8 CONCLUSIONS

This study was conducted with the intention of analyzing axial performance of helical piles and finding suitable values for torque-to-capacity correlation factors that can used in Sri Lanka for different soil conditions. Based on finding through various analyses, following conclusions can be yielded.

1. Considering field test results for SS175 piles, K_t could be found depending on sub-soil condition and direction of loading primarily. But both Hoyt and Clemence (1989) and Perko (2009) have shown experimentally that it also dependent upon pile configurations as well.

2. Values for K_t tend to be higher compared to values suggested in literature under compression and lower or around the limit under tension for different soil conditions

3. Under compressive loads, numerical models provide more consistent results and under compression and lower or around the limit under tension for different soil conditions.

4. Based on displacement contours in numerical model for each pile, load transfer mechanism for all test cases were found to be through bearing of lead helix in the direction of loading and a tapered cylindrical shear failure surface. Therefore, to improve accuracy of theoretical capacity approximations, methods suggested by Ben Livneh (2008) for compressive loads and Mitsch and Clemence (1985) for tensile loads may followed.

5. In the case of numerical modelling, discretizing continuous mediums such as soils involve inherent approximations and inaccuracies. In finite element models for this research, pitch of helices was considered zero and square shafts were modelled as circular shaft with an equivalent diameter. Installation effects cannot be modeled accurately as disturbed soil strength parameters were unknown. Based on the results (Table 7 under Section 7), except for Clayey Silts under compressive loads, numerical models provide results that are within 25% on average in comparison with in-situ pile capacities. Therefore, 2D finite element modelling can still be recommended to approximate helical pile capacities.

ACKNOWLEDGEMENT

Continuous support throughout the research by Department of Civil Engineering, University of Moratuwa and specially Dr. L.I.N. de Silva are greatly appreciated. Cooperation of St. Theresa Industries and Hubbell Power Systems Inc. are also greatly appreciated.

REFERENCES

Ben Livneh, H. Hesham El Naggar. (2008). Axial testing and numerical modeling of square shaft helical piles under compressive and tensile loading. *Canadian Geotechnical Journal, 45*(8), pp. 1142-1155. doi:https://doi.org/10.1139/T08-044

CHANCE. (2018). *CHANCE Technical Design Manual Edition 4.* Hubbell Power Systems, Inc.

Hoyt, R., & Clemence, S. (1989). Uplift Capacity of Helical Anchors in Soil. *Soil Mechanics and Foundation Engineering*, (pp. 1019-1022). Rio de Janeiro, Brazil.

Lakhdar Salhi, Ouahcene Nait-Raba, Christop Roos. (2013). Numerical Modeling of Single Helical Pile Behavior under Compressive loading in Sand. *Electronic Journal of Geotechnical Engineering, 18*, 4319-4338.

Mestat, P. (1997). Maillage d'éléments finis pour les ouvrages de géotechnique: conseils et recommandations. *Bulletin des laboratoires des ponts et chaussées*.

Mitsch M.P., S. C. (1985). The Uplift Capacity of Helix Anchors and Sand. *Uplift Behavior of Anchor Foundations in Soil*, pp. 56-47.

Perko, H. A. (2009). *A Practical Guide to Design and Installation.* Wiley.

Skempton. (1951). The Bearing Capacity of Clays. *Proceedings of the Building Research Congress*, *1*, pp. 180-189.

Terzaghi, K. (1943). Theoretical Soil Mechanics. John Wiley & Sons, Inc. doi:10.1002/978047017276

Use Of the Concept of Capillary Barriers to Optimize the Support Systems of Deep Vertical Excavations in Unsaturated Soils

R. Prasanna and S.A.S. Kulathilaka
Department of Civil Engineering, University of Moratuwa, Sri Lanka

ABSTRACT: In deep excavations, it is necessary to guarantee stability against catastrophic failure and to ensure that the deformations in the surrounding are within acceptable limits. Excavations done about groundwater table can be supported with simple structures such as soldier pile walls. But the stability of the structure is affected by the infiltration of rainwater. If the infiltration of rainwater can be reduced the construction of deep vertical excavation can be optimized. A capillary barrier which consists of a fine layer lying on top of a coarse layer at the ground level can cutoff the infiltration into the lower layers. In this research study, attempts were made to establish the critical parameters though parametric studies. Numerical analyses were done on a laboratory size model 2 Dimensionally with GeoStudio, 2012 SEEP/W software. A model was made physically. The effectiveness of the capillary barrier in the case of a field excavation supported by a soldier pile wall was numerically evaluated through Midas GTS-NX 3D software.

KEY WORDS: capillary barrier; infiltration; porewater pressure; deep excavation

1 INTRODUCTION

Due to the scarcity of land, deep vertical excavations have become necessary for providing adequate parking spaces. If the excavations extend below the groundwater table expensive watertight retaining wall systems in the form of diaphragm walls and secant pile walls would be required. Vertical cuts made in unsaturated soils above groundwater table may be stable without any support system during the periods of dry weather. Alternatively, they may be supported with simpler retaining wall systems such as soldier pile walls. But during the rainy seasons the infiltration of rainwater into the unsaturated soil will reduce the matric suction and affect the stability of the cut adversely. Therefore, the supporting systems need to be strengthened which will make it expensive and time consuming. A properly designed capillary barrier system with; material of contrasting hydraulic properties, adequate layer thickness and sloping angle could cutoff the infiltration to the underlying layers significantly. This could economize the excavation supporting system. Hence, a study of capillary barrier concept is very important.

2 CAPILLARY BARRIER IN DEEP VERTICAL EXCAVATION

A capillary barrier is a cover system commonly consisting of a relatively fine soil layer placed over a relatively coarse soil layer. Capillary barriers are generally unsaturated and function in response to changes in negative pore-water pressures.A capillary barrier is effective if the combined effect of evaporation, transpiration and lateral diversion exceeds the infiltration from the precipitation (Rahardjo, Leong, & Tami, 2004). In the case of deep vertical excavations capillary barriers can be used on the top of the excavated sides and the top surface of the capillary barrier should be kept horizontal to allow the construction process without any hindrance as shown in Figure 1. The fine-coarse layer boundary should be made to an adequate slope. The capacity of the barrier will be enhanced with the increase of the slope angle. The length of the barrier will be restrained by the space available in the site. It is necessary to drain out the water at the edge of the capillary barrier. The thickness of the layers should also be optimized. In this research a parametric study was done on the critical dimensions and the performance of a capillary barrier was evaluated.

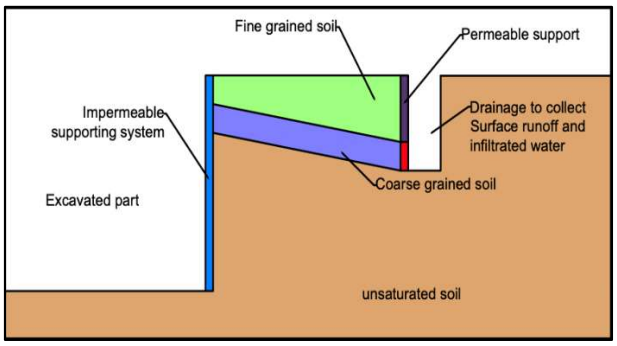

Fig 1: Proposed Capillary barrier in a deep vertical excavation

3 METHODOLOGY

In this research study a laboratory scale physical model of a capillary barrier was made with appropriate material. A lateritic gravelly soil was compacted to simulate the natural soil in the site. The capillary barrier was made with fine river sand as the fine layer and coarse fraction (coarser than 1.18mm) as the coarse layer. Arrangements were made to install tensiometers and moisture sensors at appropriate locations to assess the performance as shown in figure 2. Unfortunately, due to malfunctioning of the tensiometers the study could not be completed at the time of writing the paper.

As such, this paper presents a numerical analysis of rainwater infiltration to the model at two sections: one within the capillary barrier and another outside it. The results would be compared with the experimental values once obtained. GEOSLOPE SLOPE/W 2012 software was used in the study. Another analysis was done studying the effect of rainfall on the prop forces on a soldier pile wall done of an unsaturated soil with a deep groundwater table. Infiltration was studied with and without the capillary barrier. This study was done with MIDAS GTS NX software under 3 Dimensional conditions.

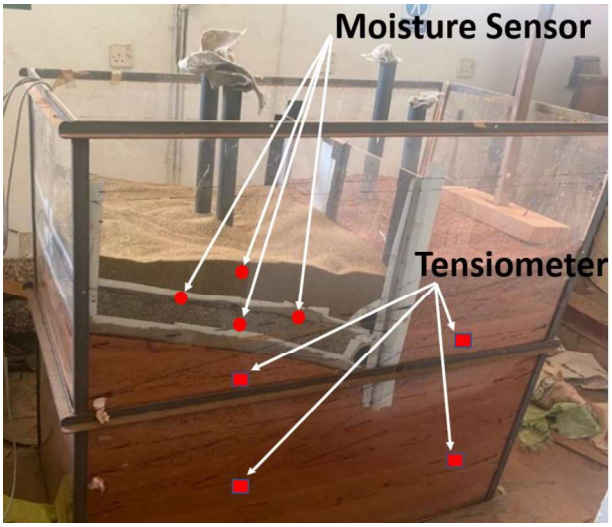

Fig 2:Laboratory infiltration model with instrument placements

4 PROPERTIES OF SOILS

Capillary barrier consists of fine-grained soil layer on top of a coarse-grained soil layer with proper contrast on their hydraulic conductivity. A typical set of curves are presented in Figure 3. At high matric suctions, the permeability of the coarse-grained layer is lower than that of fine-grained layer and the infiltrated rainwater can be retained under capillary action and moved away under the condition of lateral diversion if there is a sufficiently large inclination at the interface. There should be an adequate thickness of the fine layer. In this research locally available fine river sand and coarse fraction (greater than 1.18mm in size) of manufactured sand (crushed aggregates) will be used as fine and coarse layer, respectively. The hydraulic properties of these materials Soil Water Characteristic Curve (SWCC) and Permeability Function of these material were obtained in the previous studies done by (Havishanth, 2021), (Muthuhetige, 2020),(Dhananjaya, 2019), and (Nandasekara, 2020).

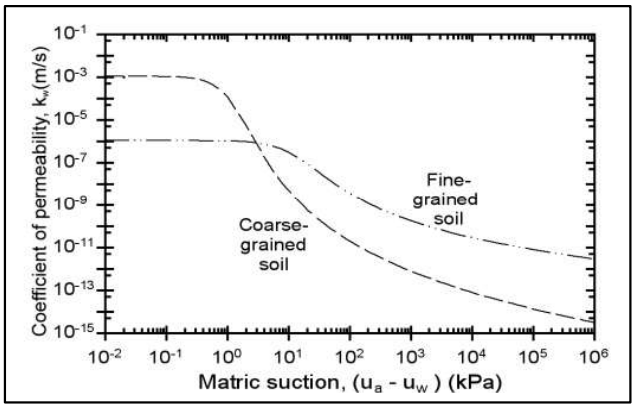

Fig 3: Permeability curves of capillary barrier materials

4.1 *Properties of fine river sand*

The basic properties of fine Sand are; specific gravity = 2.7, maximum dry density = 1673.8kg/m^3, optimum moisture content = 7%, Coefficient of uniformity, C_u = 2.44, Coefficient of curvature, C_c = 0.78, and Saturated hydraulic conductivity, k = 2.1×10^{-4}m/s. In this study, for the numerical analysis conducted with GEOSLOPE SEEP/W software, SWCC was idealized through Fredlund Xing parameters as shown in Table 1. The permeability at different matric suctions could be related to the saturated permeabilty through SWCC.

Table 1: Fredlund Xing best fit parameters – River sand

Material	θ_s	Best fit parameters		
		a(kPa)	m	n
River sand	0.35	25	0.21	17.23

4.2 *Properties of manufactured sand*

Manufactured sand used in this research was purchased from Tokyo super plant. Basic soil properties and SWCC of the manufactured sand (coarse fraction) were determined through laboratory

experiments to be; Coefficient of uniformity, C_u = 3, Coefficient of curvature, C_c = 0.9, Saturated hydraulic conductivity, k = 2.8×10^{-2}m/s. For the numerical analysis in this research SWCC was idealized through Fredlund Xing parameters shown as shown in Table 2.

Table 2: Fredlund Xing best fit parameters –M-sand

Material	Θ_s	Best fit parameters		
		a(kPa)	m	n
M-sand	0.22	0.9	0.38	3.83

4.3 *Properties of residual soil*

In Sri Lanka majority of these deep excavations are done in residual soils - the product of weathering of metamorphic parent rock. Table 3 presents the basic properties of the residual used in this research. Fredlund Xing best fit parameters were used in the establishment of SWCC of the residual soils in the numerical simulations. Table 4 presents the best fit parameters used in the study.

Table 3: Basic properties of residual soil

Specific Gravity	2.64
Maximum Dry density	1589kg/m^3
Optimum moisture content	21.8%
LL	46.2
PL	41.6
PI	4.6
Saturated hydraulic conductivity	1×10^{-5}m/s

Table 4: Fredlund Xing best fit parameters – Residual soil

Material	Θ_s	Best fit parameters		
		a(kPa)	m	n
Residual soil	0.55	13	4.8	0.97

5 NUMERICAL SEEPAGE ANALYSIS OF THE CAPILARY BARRIER COVER SYSTEM – LABORATORY INFILTRATION MODEL

This numerical analysis was done to demonstrate the effectiveness of capillary barrier in reducing the infiltration. Two cases of infiltration; under normal conditions and with the capillary barrier are analyzed. The capillary barrier in the physical model is of length 600mm. The thickness of fine layer is 200mm and coarse layer thickness is 100mm coarse layer thickness with a slope of 30% was selected. Site extent was selected as 600mm. Analysis was done for a duration of 20 hours with rainfall of intensity 10mm/hr. Figure 4 shows the geometry, boundary conditions and cross sections used.

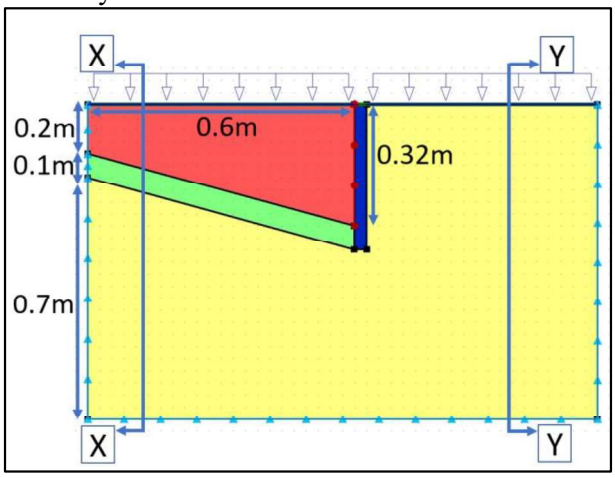

Fig 4: Model used for numerical analysis

5.1 *Results and discussions*

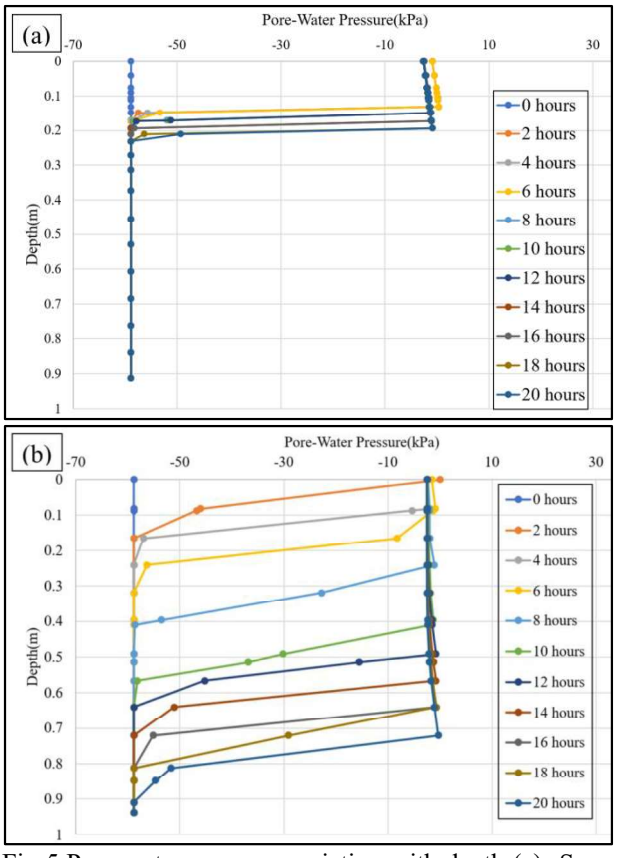

Fig 5:Pore water pressure variation with depth (a)- Section X-X, (b)- Section Y-Y

As shown in figure 5, the suction and pore water pressure variations were plotted with depth for cross-section X-X and Y-Y. Figure 5a shows that the capillary barrier cut the infiltration for more than 20 hours into the residual soil for a rainfall of intensity 10mm/hr. Figure 5b shows that the site extent without the capillary barrier got infiltration into the residual soil in greater depths in the same analysis

time. This shows the usefulness of the presence of the capillary barrier.

6 SEEPAGE MODELLING OF CAPILLARY BARRIER COVER SYSTEM – FIELD SIZE DEEP VERTICAL EXCAVATION

In this study of the actual case, 6m deep vertical excavation with a width of 20m was selected. Length of the capillary barrier was designed to extends up to 4.5m with the lined drain at the bottom part. The site extent limited to a length of 5m to simulate the worst scenarios in the actual cases. For the analysis of this study capillary with 100mm fine-grained soil layer and 100mm coarse grained soil layer with a slope of 20% was selected. Due to the symmetry of the model half of the model was analyzed to reduce the analyzing time and the geometry, boundary conditions and the cross-section names are shown in figure 6.

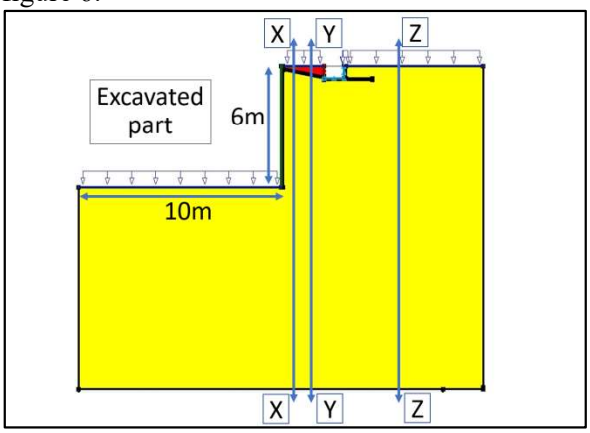

Fig 6: Boundary conditions and geometry of the model

For this analysis various factors like permeability of the drain material and variation in rainfall were used to simulate the condition that can be presence in an actual field. Cases considered for the analysis were,

1. Permeability of the drain material
    - Drain lined with impermeable material at bottom
    - Drain not lined with impermeable material at bottom

2. Variation in rainfall
    - 10mm/hour continuously for 2 days
    - 10mm/hour for 6 hours in 6 hours interval for 2 days

6.1 *Results and discussions*

Combination of each factor were analysed to simulate the actual field conditions and the results were compared to verify the performance of the selected capillary barrier system in cutting the infiltration in to the residual soil effectively. Results of capillary barrier with both layers 20% slope, with drain not lined at bottom with intensity of 10mm/hr continuous for 48 hours which is the worst combination of all factors are presented in figure 7.

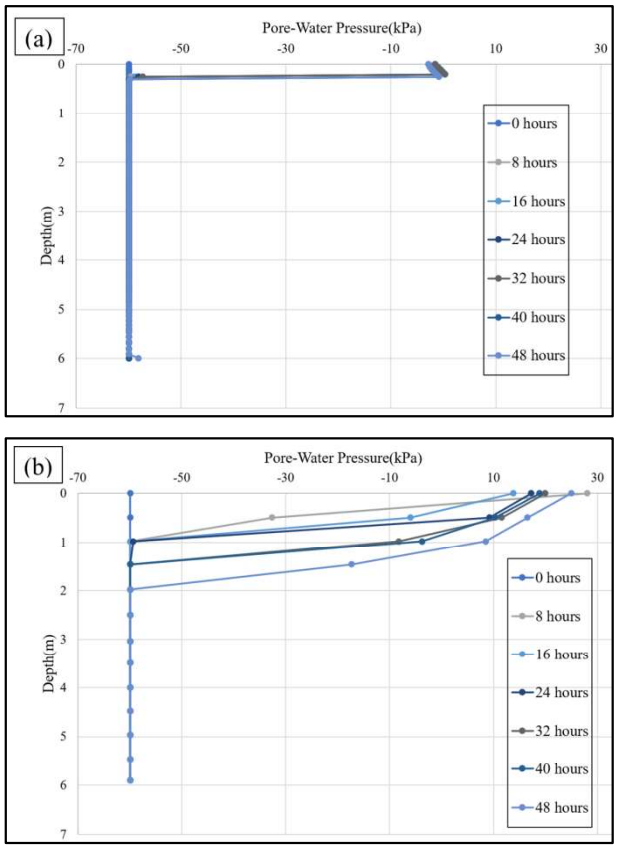

Fig 7: Pore water pressure variation with depth (a)- Section X-X, (b)- Section Z-Z

Figure 7c shows the rainwater infiltrated into residual soil up to depth of 1.5m and figure 7a shows that infiltration happened in the section Z-Z was eliminated with the help of capillary barrier. Results of the worst combination is presented in figure 7, similarly for every combination the selected capillary barrier system performed effectively well and cut the infiltration into the residual soil. From these analyses capillary barrier system with both fine and coarse layers of 100mm and slope 20% can cut the infiltration in to the residual soil for 2days, and it leads to the prevention of loss of matric suction of the deep vertical excavated sides and there by maintaining a high shear strength and there by

ensure safety of the excavated sides with economical support systems.

7 SEEPAGE AND STABILITY ANALYSIS OF CAPILLARY BARRIER COVER SYSTEM – FIELD SIZE VERTICAL EXCAVATION

The analyses done under section 7 discussed about the seepage conditions for an actual vertical deep excavation of 6m deep and 20 m wide. More than that it is important to analyze the conditions relating to the stresses involved due to the pore water pressure variations. In the sense of optimizing the support of deep vertical excavation analyses should be done regarding the reduction of forces on the supports of the excavated sides due to the use of capillary barrier.

Fig 8: Actual excavation with soldier pile wall

Due to limitations in 2-D numerical analysis in attaining numerical convergence with capillary barrier cover in stress- seepage analysis, the further studies were performed on 3-D model using MIDAS GTS NX software. Figure 9 shows the geometry, boundary conditions and prop levels used for the analysis.

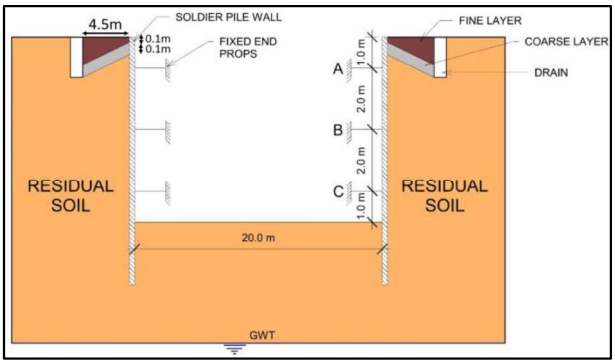

Fig 9: Geometry, boundary conditions and prop levels of the model

For the Stress-Seepage analysis three types of cases were considered to compare the results with each other so that the effectiveness of the capillary barrier can be studied. The cases considered were,

1. Excavation without capillary barrier in the absence of rainfall
2. Excavation without capillary barrier in the presence of rainfall
3. Excavation with capillary barrier in the presence of rainfall

Analysis was done for a rainfall of 10mm/hr continuously with lateral prop spacing of 1m.

7.1 *Results and discussion*

According to the analysis done under the cases considered under section 8 forces acting on the props at 3 levels due to the rainfall of intensity 10mm/h were obtained. Graphs were drawn for the props A, B, C as shown in figure 9 separately. Figure 10 presents the prop force variations for case 1 which do not include any effect of rainfall but to give an idea about the initial forces acting on the props. Prop forces in A, B, C at the end of the excavation process is respectively 16.6kN, 19.0kN, and 18.5kN.

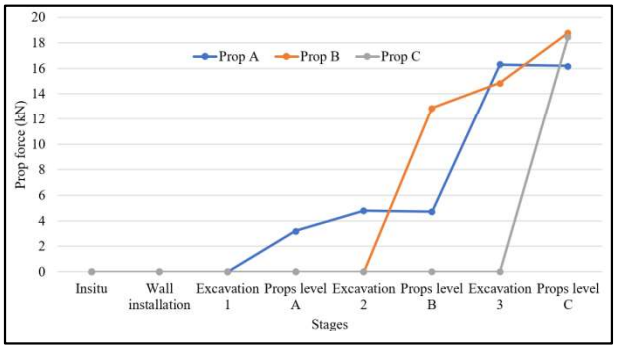

Fig 10:Variation of prop forces with stage (case 1)

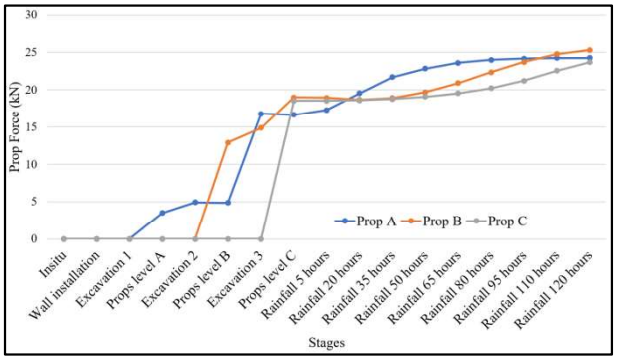

Fig 11:Variation of prop forces with stage (case 2)

Figure 11 presents the results of case 2 which shows the increase in the prop forces in each A, B, C levels for a period of 5 days due to the infiltration of rainwater.

From the analysis, increase in prop forces in prop levels A, B, C are respectively 8.3kN, 6.3kN, and 5.2kN for a rainfall of 10mm/hr continuously for 5 days. The effect of rainfall in the

prop forces decrease with the depth and this is due to the infiltration of the rainfall affects the top-level props because the infiltration into the residual soil is limited to about a depth of 4.5 m according to the analysis.

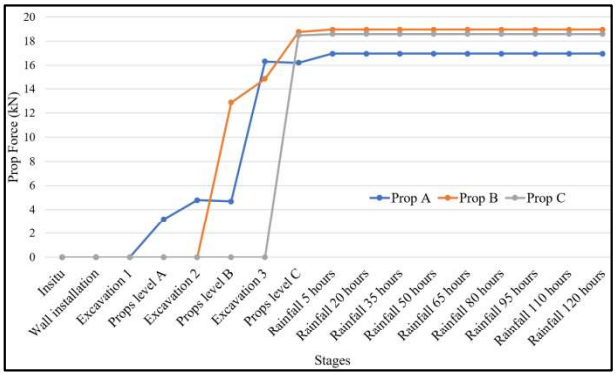

Fig 12: Variation of prop forces with stages (case 3)

From the results of the analysis of case 3, increase in prop forces in prop levels A, B, C are respectively 0.75kN, 0.18kN, and 0.11kN for a rainfall of 10mm/hr continuously for 5 days. This comparison shows the effectiveness of capillary barrier in optimising the supporting systems of deep vertical excavation.

Table 5: Increase in prop force

Prop level	Increase in prop force without capillary barrier		Increase in prop force with capillary barrier	
	(kN)	(%)	(kN)	(%)
A	8.3	50	0.75	4.63
B	6.3	33.16	0.18	0.96
C	5.2	28.12	0.11	0.6

Table 5 provides the increase in prop forces at the end of analysis period of 5 days. Results of these analyses show the effectiveness of the capillary in reducing the prop forces during rainy seasons by comparing case 2 and case 3.

7.2 *Comparison of manual and FEM results*

Table 6: Comparison of results

Prop level	Analysis without capillary barrier		Analysis with capillary barrier	
	Prop load Manual (kN)	Prop load FEM (kN)	Prop load Manual (kN)	Prop load FEM (kN)
A	45	24.8	20.26	16.95
B	72	25.3	32.4	18.95
C	72	23.7	32.4	18.59

Comparison of the manual calculation and numerical results show comparatively wide scatter of results for strut loads. Empirical methods being much conservative gave higher values compared to the numerical analysis.

8 CONCLUSION

Using appropriately selected materials, capillary barriers were found to be effective in minimizing the infiltration of rainwater into unsaturated vertical excavated slopes. By minimizing the infiltration, it maintains high matric suction and shear strength of the deep vertical slopes. Therefore, capillary barriers have high potential for application in optimizing the support systems of deep vertical excavation. Seepage conditions and their related stress conditions were studied in detail and their applicability in Sri Lankan residual soil with local available materials like river sand and manufactured sand were studied. This research study provides an initiative to use the capillary barrier concept in deep vertical excavations in Sri Lanka because it is a proven solution in economizing the support systems.

9 REFERENCES

Dhananjaya, K. K. (2019). Establishment of Soil Water Characteristic Curves for Sri Lankan Residual Soils. *University of Moratuwa (UG research)*.

Havishanth, E. (2021). Possibility of using capillary barriers for landslide risk reduction. *University of Moratuwa (Msc research)*.

Muthuhetige, W. (2020). Establishment of Soil Water Characteristic Curves for Sri Lankan Soils. *University of Moratuwa (UG research)*.

Nandasekara, T. (2020). Use of the concept of capillary barriers to optimize support of deep vertical excavation in unsaturated soils. *University of Moratuwa (UG research)*.

Rahardjo, H., Leong, E., & Tami, D. (2004). Capillary Barrier for slope stabilization.

Improvement of compressibility characteristics of waste material by dynamic compaction

R.I.A Rathnayaka and S.A.S. Kulathilaka
Department of Civil Engineering, University of Moratuwa, Sri Lanka

ABSTRACT: Open dumping is the most prevalent method of waste disposal in Sri Lanka. These sites, which are currently used as waste dump yards in urban areas, will have to be rehabilitated to be converted to be used as parks, roads or for other different construction projects. Establishing the strength and stiffness characteristics of these waste materials at different levels of degradation and how these characteristics can be enhanced to suit the proposed developments is a major challenge. This paper presents a study of the effectiveness of dynamic compaction as a technique of enhancing the compressibility characteristics of waste dumps. MSW was subjected to dynamic compaction in a laboratory test setup, and the compressibility characteristics were assessed by conducting the consolidation tests on compacted MSW. The effectiveness of the process is compared with that of preloading. Dynamic compaction has improved the compressibility characteristics of MSW but less effective than preloading.

KEY WORDS: MSW; Preloading; Dynamic compaction; Compressibility; Consolidation

1 INTRODUCTION

1.1 *Background*

Municipal solid waste (MSW) is solid waste resulting from, or incidental to, municipal, community, commercial, institutional, and recreational activities, but not including industrial hazardous or 'special wastes. According to the Environmental Foundation Limited (EFL)(2021), Sri Lanka generates about 7000MT of solid waste per day with the Western Province accounting for nearly 60% of waste generation. Each person generates an average of 0.4-1kg of waste per day.

Open dumping is the most common method of disposal of municipal solid waste (MSW) in Sri Lanka due to low cost and less processing involved.

Rapid development in urban areas in the past decades has created a high demand for lands. The lands, which were use as open dumping yards in the past, can be consider as valuable sources that can fulfill this demand to some extent. Therefore, the sites, which are currently used as waste dumping yards, will have to be rehabilitated to be converted to be used as parks, roads, or many other construction projects.

These waste materials would be in different levels of degradation. Enhancement of strength and stiffness characteristics to suit the proposed development is a major challenge. This study was done to assess the effectiveness of dynamic compaction as a viable and economical technique of enhancing the compressibility characteristics of waste dumps.

1.2 *Background knowledge*

According to Naveen et al (2018), determination of the geotechnical properties of waste is challenging because of the heterogeneity of the material. Durmusoglu et al. (2006) reported that, although principles of the general soil mechanics are usually applied because of high deformability and microbial decomposition of waste, the process is quite problematic.

The mechanisms of settlement that govern the solid waste material are numerous and complex. Bowders et al (2001) reported that there are many reasons behind this behaviour of waste such as extreme heterogeneity of the wastes, their own particle deformability, the large voids present in the initial waste fill, and their biodegradability. Settlements of MSW are not as well understood as those for soils and are more difficult to estimate.

According to Watts and Charles (1990) and Manassero et al. (1996), the settlement behaviour of MSW is often classified as occurring in several distinct phases.

Primary consolidation of solid waste occurs due to the self-weight of the waste or application of surcharges such as fill over the time. Bajarngard et al (1990) and Stulgis et al. (1995) reported that previous data on waste settlements have indicated that primary compression of waste fills complete in 10 to 90 days after dumping.

Primary compression is then followed by the secondary compression. Secondary compression occurs due to biodegradation process in waste fill, and it can take years for this settlement to complete depending upon varies phases of waste that it con-

sists of. Wall and Zeiss (1995) reported that the biodegradation components of long term (secondary) compression or bio consolidation is due to a process by which solid organic particles in the waste are solubilized and converted to methane and carbon dioxide.

1.2.1 *Dynamic compaction*

Late French engineer Louis Menard invented dynamic compaction in 1969. Dynamic compaction (DC) is a ground improvement technique by transmitting high-energy impacts to the ground. A conventional crane may be used to repeatedly raise and drop a tamper from a predetermined height in a grid to achieve a target maximum depth of improvement.

According to Van Impe and Bouazza (1996), use of dynamic compaction for the densification of MSW can be considered as a challenging task due to many reasons such as:

- Moisture condition of waste fills mainly depend on rain and cannot be expected to have optimum conditions for compaction.
- Secondary compression of solid waste occurs due to biodegradation, and it can take up to 20-25 years after the dumping for it to complete.
- The composition of solid waste varied significantly and a uniform composition (such as in a soil) cannot be expected.

The effect of the dynamic compaction depends on the saturated and unsaturated conditions of the waste fill. Usually, a waste fill is designed to be above the phreatic line and can be considered as unsaturated. If the fill is unsaturated, the dynamic energy will directly transfer to the waste material and compaction will occur in a quick manner.

2 METHODOLOGY

2.1 *Overview*

The following steps were followed in order to achieve the objectives of the study.

I. A detailed literature review was carried regarding compressibility characteristics of waste material and methods of improvement.
II. MSW samples were collected and prepared in order to carry out the testing according to the standards.
III. A dynamic compaction apparatus was fabricated to simulate the field conditions.
IV. Waste samples were compacted using the dynamic compaction apparatus and compacted waste sample was extruded using a cutter. Some samples were left uncompacted.
V. MSW samples in both compacted as well as in un-compacted state subjected to loading in a Rowe Cell of diameter 150 mm and height 50 mm.
VI. Results were analyzed to establish the compressibility characteristics, namely coefficient of volume compressibility (m_v), compressibility index (C_c), coefficient of consolidation (C_v) and coefficient of secondary compression ($C\alpha$).
VII. Results were compared to assess the effect of dynamic compaction on compressibility characteristics of MSW.

2.2 *Collection and preparation of MSW samples*

Municipal solid waste used in this study was collected from Meethotamulla landfill site that had been used for waste dumping for more than 20 years.

There are some limitations on the maximum particle size, which can be used for specimen preparation. Typically, the largest particle size should be 1/6 of the specimen diameter. As the Rowe cell diameter is 150 mm, largest particle size should be about 25mm. Hence, fragments greater than 25mm of MSW either were discarded or, where possible, were broken/cut to make them fit inside the cell.

2.3 *Determination of basic parameters of MSW*

Density of the MSW sample before and after the compaction were measured using the water replacement method in the prepared test pit.

In order to determine the specific gravity, laboratory specific gravity tests were conducted using a pycnometer with a volume of 1000ml and generally followed the procedure used for soil testing as per the ASTM D854.

In order to determine the moisture content air-dried method was adopted for specimens obtained from tested samples.

The basic parameters of MSW are presented in table 01.

Table 1. Basic Parameters of MSW

Test Set	Sample Condition	Bulk Unit weight (kg/m^3)	Specific Gravity	Moisture Content (%)
1	Compacted	873.45	1.41	21.4
2	Non-compacted	493.41		20.2

The density values observed in this study can be considered as low for MSW compared to the values reported in the literature. This is most likely due to the difference in the composition of MSW used in this study.

2.4 *Determination of waste composition*

Waste classification framework proposed by Dixon and Langer (2006) is used in this study based on the relevancy to nature of MSW in Sri Lanka. Composition of MSW is presented in table 2.

Table 2. Composition of MSW sample

Material Type	%
Soil like	36.2
Paper/ Cardboard	0.00
Flexible plastics/ Rigid plastics	24.5
Rubber	0.00
Metals	0.00
Glass, Minerals	14
Wood, Textiles	20.3
Miscellaneous	5
Total	100

As fragments greater than 25mm of MSW specimen used in this study were broken/cut to make them fit inside the cell, subdivision of component in each material group based on shape related properties was not carried out in this study.

2.5 *Aspects of dynamic compaction apparatus*

To simulate the field dynamic compaction in the laboratory, a dynamic compaction mechanism was prepared. A hume pipe of a diameter of 4 ft and a height of 4 ft was installed on the ground. Soil was placed inside to a height of 300mm in two layers and compacted.

A hole of plan dimensions 400 mm x 400 mm and depth of 200mm was made within the compacted soil in the Hume pipe to fill/compact the waste samples. Fig. 1 and fig. 2 presents the arrangement for the dynamic compaction.

Dynamic compaction through free falling of the weight was achieved using an electromagnet and a pulley mechanism (Fig 3). A weight of 31.8 kg was dropped from a height of 1 m on the waste. The weight was dropped 20 times on the same location in order to achieve the compaction. Weight was lifted to the top again by a rope. In a field operation the weight would be dropped appropriate number of times in a grid pattern covering the area to be improved. Several cycles of dropping will be done by increasing the weight and height in later stages.

According to Van Impe and Bouazza (1996) depth of improvement of MSW by dynamic compaction is given by;

$$D = n\sqrt{WH} \quad (1)$$

Here D is the depth of influence (m), W is the weight of the pounder (tons), H is the drop height (m) and n is a coefficient that accounts for soil type, type of pounder, etc.

Zekkos et al. (2013) has suggested an n value of 0.4±0.05 for MSW regardless of the age. Using this value, the achieved depth of improvement is 84 mm. As a sample thickness about 50mm was to be used inside the Rowe cell, this depth of improvement was adequate.

After the dynamic compaction, samples were extruded using a cutter with a diameter of 150 mm.

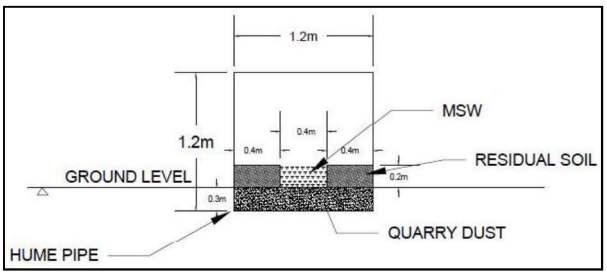

Fig.1 Cross section of the dynamic compaction arrangement

Fig.2 Arrangement for dynamic compaction

2.6 *Testing of MSW samples*

Rowe Cell of diameter 150 mm was used for performing compressibility tests. Head (1997) stated that vertical single drainage with equal strain test method is the test closely related to traditional Oedometer tests and settlement reading can be directly related to volume change measurement in the drainage line. Hence, vertical single drainage with equal strain test method is selected for the testing.

Two MSW samples were tested using the Rowe cell (Fig. 4) One sample was from the MSW subjected dynamic compaction and the second sample was from the non-compacted MSW.

For the two samples, two different loading sequences were implemented. Compacted MSW sample was subjected to only loading and unloading increments. The non-compacted MSW sample was subjected to loading, unloading and reloading increments. Reloading increments in the non-compacted sample would represent the behaviour of the MSW subjected to preloading. Compacted sample was not taken through reloading increments.

Fig. 3 Free falling of the weight and lifting up by rope

Fig.4 Sample loaded in the Rowe cell

3 RESULTS AND DISCUSSION

3.1 *Variation of compression index (c_c) and recompression index (c_r)*

Void ratio was evaluated with the average specific gravity obtained and plots were done to compute compressibility indices. Fig.5 presents the e vs. log (σ) curves for compacted and non-compacted samples.

The indices computed using e vs. log (σ) graph are presented in Table 3.

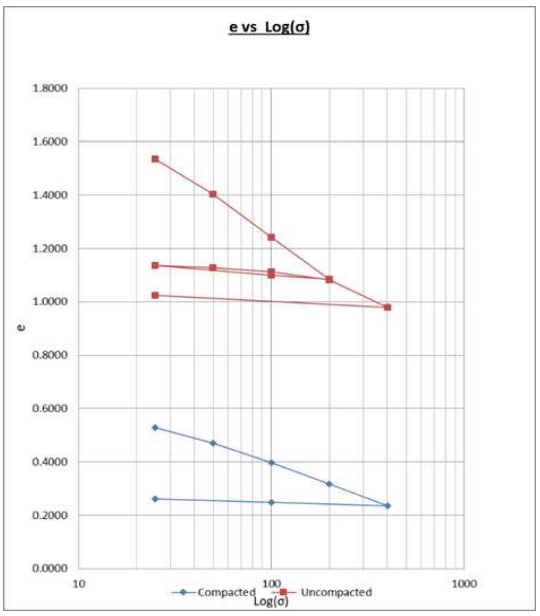

Fig. 5 e vs log (σ) curve for compacted and non-compacted MSW samples

Table 3. Compression index and recompression index values

Test Set	Values of compression index (C_c)	Values of recompression index (C_r)
Sample 1 (Compacted)	0.2373	-
Sample 2 (non-compacted)	0.4906	0.0537

The compression index of MSW that was subjected to dynamic compaction has reduced to about 50 % of that of the non-compacted MSW. But the recompression index of non-compacted sample was only about 10% of its compression index.

The C_r values represent the primary consolidation behaviour of a preloaded MSW. The much-reduced C_r values indicate that the reduction of primary consolidation settlement of MSW achievable by preloading is much greater than that achievable through the dynamic compaction.

3.2 *Variation of coefficient of volume compressibility (m_v)*

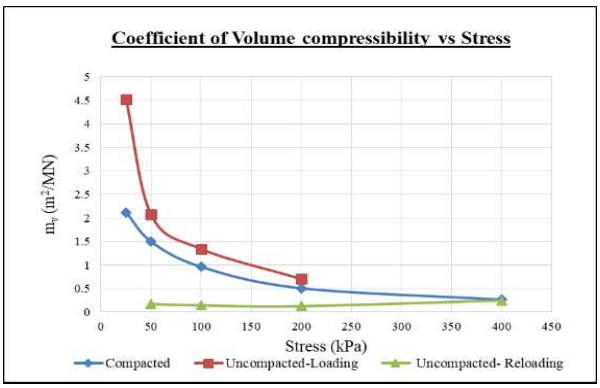

Fig. 6 Variation of volume compressibility

The coefficient of volume compressibility, m_v values decreased as the effective stress increases in-both compacted and non-compacted samples (Fig 6). The m_v value of non-compacted sample during reloading increments were much smaller than those of compacted samples. As the over consolidation ratio approached unity those values approached the values of compacted sample.

These results indicate that the compressibility of MSW can be reduced more by preloading as compared to the dynamic compaction.

3.3 *Variation of coefficient of secondary consolidation (c_α)*

The settlement curves of MSW are similar to those of peaty clay and a reduction of gradient could not be identified with time (Fig.7). This is an indication that MSW exhibit high secondary consolidation. Coefficient of secondary consolidation C_α values for different loading and reloading stages are presented in Fig 8. However, these magnitudes are lower than that of peaty clay.

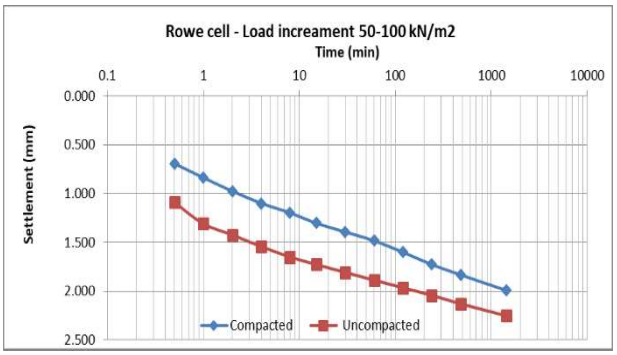

Fig.7 Settlement vs log (time) curve for compacted and non-compacted samples

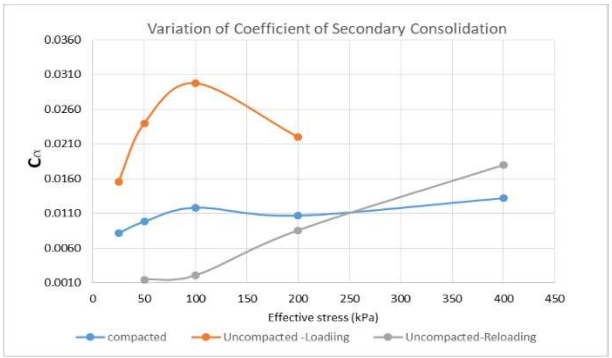

Fig. 8 Variation of coefficient of secondary consolidation

In general, $C_\alpha$values increased with the stress level in the loading increments. The dynamic compaction process has caused a significant reduction of coefficient of C_α. The preloading process has also caused a significant reduction of C_α. The $C_\alpha$values in reloading increments with higher over consolidation ratios were much smaller compared to those of compacted sample. In reloading increments $C_\alpha$values increased as the over consolidation ratio approached unity.

According to the Lewis et al. (2004), dynamic compaction was more effective in reducing the rate of secondary settlement of landfill as compared to the preloading. According to them C_α ranges from 0.0153 to 0.0513 with an average value of 0.0313 for the landfill material treated by dynamic compaction and C_α ranges from 0.0529 to 0.0817 with an average value of 0.0657 for the landfill material treated by preloading. These values are higher than the values observed during this study. Difference in the results may be due to the difference of the degradation stages and composition of the MSW.

3.4 *Variation of coefficient of consolidation (c_v)*

The coefficient of consolidation C_v is essential to predict the rate of settlement of MSW sites. The value of the coefficient of consolidation (C_v) is estimated here using laboratory consolidation test results.

In the soil, engineering practices Taylor's square root of time fitting method and Casagrande's logarithm of time fitting method are the two widely used methods to find coefficient of consolidation. However, when the shape of the settlement curves do not confirm the standard shapes proposed by the Casagrande and Taylor. Rectangular hyperbola method (Sridaran 1981, Selig et al 1985) and velocity method (Parkin 1978) can be used as better alternative methods. Hence, these two methods were considered to find the coefficient of consolidation for each loading step to identify the settlement characteristics of MSW.

Fig. 9 and fig.10 presents the variation of C_v values obtained. Values of coefficient of consolidation obtained by both methods are showing the same trend on increasing stress level. Apart from the initial increment of 0–25 kN/m^2 the coefficient of consolidation values were of the same order at higher stress levels. These values are quite high as compared to those of conventional soils.

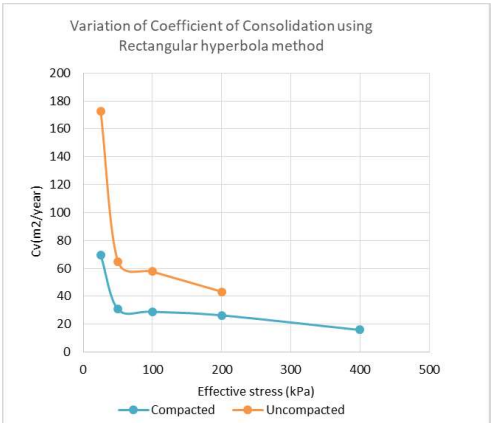

Fig.9 Variation of C_v (Rectangular hyperbola method)

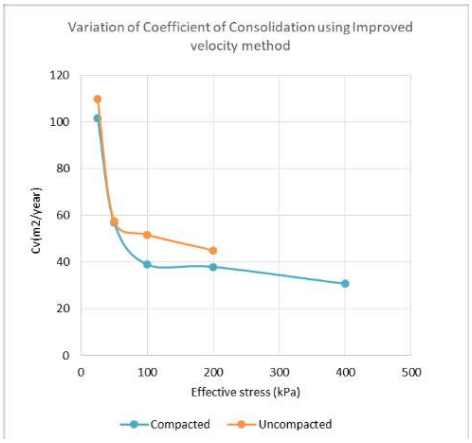

Fig.10 Variation of C_V (Improved velocity method)

C_V values obtained by both methods were of the same order at higher stress levels. The dynamic compaction process has caused a reduction of the value. The higher C_V values indicate that the pore pressure dissipation during an improvement process would be quite rapid.

4 CONCLUSION

Open dumping is the predominant method of MSW management in Sri Lanka. The failure to address issues in open dumping of MSW in a timely manner has resulted in unsanitary eyesores in Karadiyana, Bluemendhal, Meethotamulla, Kolonnawa etc. These sites, which are currently used as waste dump yards in urban areas, will have to be rehabilitated for various construction projects. It is important to understand the compressibility characteristics of waste material before embarking on these development projects.

Preloading and dynamic compaction both are possible methods in reducing the compressibility of waste material and in this study effectiveness of both methods were evaluated and compared.

Compression index of MSW that was subjected to dynamic compaction was reduced about 50 % of the compression index of the non-compacted MSW. Recompression index values of non-compacted MSW values are less than about 10% of compression index values of non-compacted MSW samples. Similarly, results obtained for coefficient of volume compressibility shows greater reduction by preloading compared to the dynamic compaction. Both preloading and dynamic compaction shows significant effectiveness in reducing the coefficient of secondary consolidation.

Compressibility characteristics of MSW can be improved significantly using both preloading and dynamic compaction. According to results observed in this study preloading can be considered as the more effective method. However, depending on the composition and the degradation level of the MSW sample used these results can be changed. Considering the time, it takes to achieve the required compressibility reductions by preloading, dynamic compaction can be considered as another advantageous option.

REFERENCES

Bjarngard, A., and Edgers, L. (1990). "Settlement of Municipal Solid Waste Landfills". The thirteenth Annual Madison Waste Conference, 192-205.

Bowders, J., Roth, N., Loehr, E., Russell, M., Klouzek, A., and Bouazza, M. (2001). "Municipal solid waste settlement". Missouri Waste Control Coalition Conference, Columbia Missouri.

Dixon, N., and Langer, U. (2006). "Development of a MSW classification system for the evaluation of mechanical properties". Waste Management, 26(3), 220-232.

Durmusoglu, E., Sanchez, I., and Corapcioglu, M. (2006). "Permeability and compression characteristics of municipal solid waste samples". Environmental Geology, 50(6), 773-786.

Environment Foundation (Guarantee) Limited."Status of Waste Management in Sri Lanka." (2021).<https://efl.lk/status-waste-management-sri-lanka.> (May 27, 2021).

Head, K. (1980). Manual of soil laboratory testing. Pentech Press, London.

Manassero, M., Van Impe, W. and Bouazza, A., 1996. Waste disposal and containment. In: International Congress on Environmental Geotechnics. A.A. Balkema, Rotterdam, pp.1425-1474.

Naveen, B., Sivapullaiah, P., and Sitharam, T. (2018). "Appropriate Method of Determination of Coefficient of Consolidation for Municipal Solid Waste". Geotechnical Testing Journal, 41(6).

Parkin, A. (1978). "Coeffcient of consolidation by the velocity method". Géotechnique, 28(4), 472-474.

Selig, E., Sridharan, A., and Prakash, K. (1985). "Improved Rectangular Hyperbola Method for the Determination of Coefficient of Consolidation". Geotechnical Testing Journal, 8(1), 37.

Sridharan, A., and Rao, A. (1981). "Rectangular Hyperbola Fitting Method for One Dimensional Consolidation". Geotechnical Testing Journal, 4(4), 161.

Stulgis, R., Soydemir, C. and Telgener, R., 1995. Predicting landfill settlement. In: Geoenvironment 2000: Characterization, Containment, Remediation, and Performance in Environmental Geotechnics. Pp.980–994.

Van Impe, W., and Bouazza, A. (1996). "Densification of domestic waste fills by dynamic compaction". Canadian Geotechnical Journal, 33(6), 879-887.

Wall, D., and Zeiss, C. (1995). "Municipal Landfill Biodegradation and Settlement". Journal of Environmental Engineering, 121(3), 214-224.

Watts, K., and Charles, J. (1990). "Settlement of recently placed domestic refuse landfill.". Proceedings of the Institution of Civil Engineers, 88(6), 971-993.

Zekkos, D., Kabalan, M. and Flanagan, M., 2013. Lessons Learned from Case Histories of Dynamic Compaction at Municipal Solid Waste Sites. Journal of Geotechnical and Geoenvironmental Engineering, 139(5), pp.738-751.

Stability analysis of Colombo Katunayake expressway (CKE) embankment using fly ash stabilized soil as embankment material

K. Mathumidah, S. Lavanyan and M. C. M. Nasvi

Department of Civil Engineering, University of Peradeniya, Sri Lanka

ABSTRACT: Rapid growth of highway construction in Sri Lanka has increased the demand and scarcity of high-quality aggregate materials. On the other hand, huge amount of fly ash (FA) is produced at Lakwijaya coal power plant and they end up in landfills posing severe environmental threats. Therefore, this study aims to predict the feasibility of using FA-stabilized marginal soil as an embankment material by analyzing the load-settlement and stability behaviour of two selected embankment sections at Colombo Katunayake Expressway (CKE) at chainages K2+600 and K6+850 numerically by using PLAXIS 2D and SLOPE/W. For this analysis 0, 10, 20, 30, and 40% of FA (by weight) with a marginal clayey soil, which does not satisfy the Road Development Authority (RDA) requirements for embankment material was used. According to the results, increasing FA from 0 to 30% resulted in reduction in vertical and lateral deformation and increase in FOS values of both embankment sections. Further increase beyond 30% resulted in 1% reduction in vertical settlement and 7% increase in lateral deformation at K6+850. Therefore, the optimum FA content based on the deformation and stability results is 30%.

1 INTRODUCTION

Colombo–Katunayake Expressway (CKE) is the second major highway in Sri Lanka that connects the International Airport at Katunayake to the capital city of Colombo has been constructed over soft soils, of which 53% of the land covers peat, organic soil, clays, and sludge (Zhang et al., 2010). Even though different types of soft ground treatments were implemented for CKE sections during the construction stage, considerable consolidation settlement was observed to be increasing with time (Nasvi and Krishnya 2019). Therefore, use of industrial waste materials for road embankment construction not only will provide solution to the waste disposal problem but also offers economical alternatives to traditional earth materials.

FA is a non-plastic material and pozzolanic in nature, proven as a best stabilizing material for years due to its self-cementing properties. Properties that make FA as a suitable material in replacement for fill materials in embankment construction include relatively lightweight, high shear strength, low compressibility, permeability, and self-cementitious characteristics. There are some literatures (Turan et al., 2019; Rajak et al., 2019) proposed FA content range of 5 to 40% to be favourable amount to stabilized the marginal soil. At the same time problems due to slope instability are very common and cause failure in the road embankments. Numerical modelling techniques such as Finite element method (FEM) and Limit equilibrium method (LEM) with excellent commercial software are gaining increasing popularity in slope stability engineering. PLAXIS 2D is FEM-based software that gives a more realistic indication of geotechnical problems involving settlements and slope stability. Aryal 2006 concluded that most preferably, a slope should be analyzed by FE methods, or else otherwise by LE-based M-PM.

2 RESEARCH METHODOLOGY

Two critical embankment sections along CKE alignment at chainages K2+600 and K6+850 as shown in Fig. 1 has been chosen for this study. A typical K2+600 embankment is 12m crest width with V:H ratio as 3:7 and K6+850 embankment is 16m crest width with V:H as 5:6.

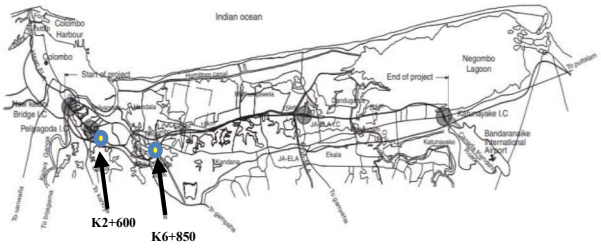

Figure 1: Location of the two embankment sections selected for the analysis

2.1 *FEM Analysis*

Stability and deformation analyses were performed using the finite-element program PLAXIS 2D (Professional version 8.2). For the foundation soil, three types of model configurations namely Mohr-Coulomb model (MC)-all soil layers in MC model, MC and Soft soil model (MC-SS)-peat, soft clay layers in soft soil model and other soil layers in MC model, MC, Soft soil, and Soft soil creep model (MC-SS-SSC)-peat soil layers in soft soil creep model, soft clay in soft soil model and other layers in MC model. The nonlinear behaviour of FA stabilized soil embankment fill was modeled using MC criterion.

The properties and filling sequence of the existing foundation soil at chainages K2+600 and K6+850 of CKE were referred from Nasvi & Krishnya (2019). This study aims to use the soft clayey soil that does not meet the RDA requirement for embankment material stabilized with FA as the embankment material for CKE embankment. As we were unable to conduct the experimental works due to Covid-19, situations we went through the existing literature (Bose 2012; Deb and Pal 2014; Rajak et al., 2019; Turan et al. 2019; Santos et al. 2011) and selected the soil sample from Rajak et al., 2019 by taking into account the requirements for type I and type II embankment material of standard specifications for Construction and Maintenance of Roads and Bridges/ICTAD SCA as the soil for this study. From that, FA proportions of 10, 20, 30, 40% were selected for this study and the required properties such as unit weight, cohesion, and friction angle of soil stabilized with these FA contents were obtained from the same literature. Other parameters required for *FA* stabilized soil, such as horizontal and vertical permeability (k_x and k_y), Poisson's ratio(v) and Young's modulus (E) were obtained from relevant literature (Boroumand and Baziar 2005; Buwa and Wayal 2016; Saride and Dutta 2016; Deb and Pal 2014) as these values were not reported in the original literature referred for FA stabilized soil properties. Table 1 provides the selected material properties for the FA stabilized soil.

Table 1: Properties of FA-stabilized embankment fill soil layers

	100S+0 FA	90S+10 FA	80S+20 FA	70S+30 FA	60S+40 FA
Υ_{sat} (kN/m^3)	21.57	21.06	20.55	20.18	19.93
φ'(°)	29	32	35	37	39
c'(kPa)	38.25	32.28	29.08	20.10	10.18
k_x&k_y (m/day)	7.5×10^{-6}	3.5 ×10^{-5}	8×10^{-5}	1.3×10^{-4}	1.7×10^{-4}
E (kPa)	1616	1656	1693	2461	3051
v	0.350	0.315	0.279	0.240	0.210

Owing to the symmetry of the problem only one-half needs to be modeled by geometry line in a working space of 20 m × 50 m, and standard fixities were used to define the boundary condition. According to the convergence analysis a very fine mesh was adopted to minimize the effect of mesh dependency. Initial stresses were generated using K_0 procedures or gravity loading. Staged construction of the embankment was effectively modeled followed by the application of overburden pressure on the embankment. The initial conditions include the existence of the phreatic level at a depth of 0.5 meters below the ground level in both embankment sections.

Following the validation, validated material model was employed for further analysis on effect of stabilization on Vertical settlement, lateral deformation, pore water pressure, stress variation, FOS and slip surface location at the final phase.

2.2 *Stability Analysis using LEM*

The FOS of FA-stabilized embankment sections were analyzed with five LEM techniques such as OM, BSM, JSM, SSM and M-PM using SLOPE/W 2012 software. The simple non-linear MC soil model was used as the material model for all the soil layers. Entry and exit method was chosen to define the slip surface. The critical slip surface was searched from thousands of possible slip surfaces by defining the input of 30 slices, 2000 iterations, and 4 increments for entry, 4 increments for exit. In stability analysis, validation of results was done by comparing the FOS values from PLAXIS 2D and SLOPE/W. Even though five different LEM techniques were used for FOS calculations MPM analysis type was selected as a precise prediction and further comparisons were done using it.

3 RESULTS AND DISCUSSION

3.1 *Validation of model with field Observation*

Figure 2 shows the vertical settlement value with time for different material models and observed settlement for section K2+600. According to the figure 2, settlement values predicted by both MC-SS and MC-SS-SSC models are consistent with the observed settlement at chainage K2+600 whereas MC model shows a significant difference compared to the observed settlement. As MC is a simple nonlinear model which assumes elastic perfectly plastic behaviour, it is not suitable for soil layers such as peat and soft clay. Although MC-SS and MC-SS-SSC capture the field behaviour reasonably taking into account secondary compression effects such as creep, which is mainly prominent in

peat soil, MC-SS-SSC model is selected as the best model for further analysis.

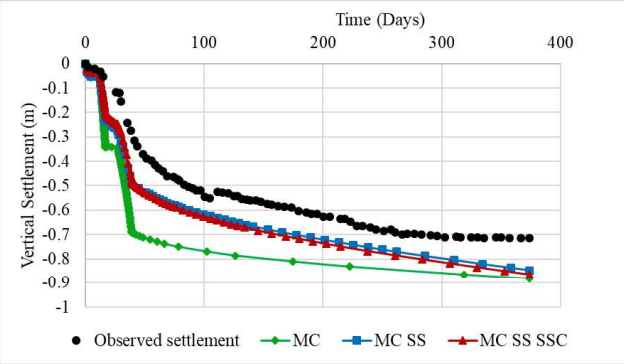

Figure 2: Variation of Vertical settlement with time for K2+600

3.2 *Effect of stabilization on settlement behaviour*

Figure 3 shows the percentage reduction in vertical settlement and lateral deformation for the embankments K2+600 and K6+850 after 374 and 765 days of construction respectively. According to it, FA stabilization of the marginal embankment material reduces the overall vertical and lateral deformation. This reduction is due to the cementitious reactions occurs between FA and soil in the presence of water result in the formation of cementitious gels (CSH and CASH) that create strong binding between particles and reduce the ability of soil-FA matrix to undergo deformation.

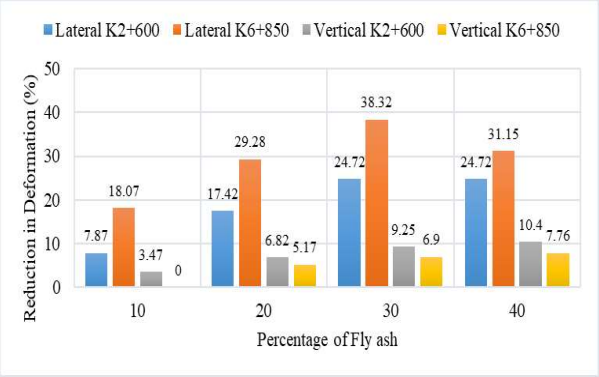

Figure 3: Percentage reduction in Vertical and lateral deformation with FA stabilization for both sections.

And also, it can be seen that 30% and 40% FA additions provided the maximum reduction in the lateral deformation and vertical settlement values respectively. Although 40% FA addition provided the highest reduction in vertical settlement, it was noted that the reduction in settlement is not significant beyond 30%. Percentage reduction for 30% addition is higher than that of 40% in lateral deformation is due to the increase of fines that tend to separate adjacent soil particles resulting in decrease interlocking between particles, reduce the compaction.

3.3 *Stability Analysis from PLAXIS 2D & SLOPE/W*

Table 2 shows the FOS results of two embankment sections with FA stabilization. It is obvious that FOS values from SLOPE/W are 10-40% higher than PLAXIS 2D and this is because, PLAXIS 2D incorporates strength reduction method that can effectively accommodate changes in the stress-strain distribution while LE method is based on static equilibrium that divide sliding mass into smaller sizes. In addition, this can be attributed to the different material models (MC & MC-SS-SSC in SLOPE/W and PLAXIS) used for similar embankment sections in both methods.

Considering the stability analysis results of PLAXIS 2D, optimum value of FA stabilization in both embankment sections is 30%. With 30% of FA addition, K2+600 section showed 7.6% and K6+850 section showed 1.6% increase in FOS values. FOS values of MPM analysis from SLOPE/W shows a decreasing trend with the increase of FA percentage at K2+600 section and increase up to 20% and reduction beyond 20% in section K6+850. This is due to the variation of soil-FA mix cohesion values which shows a sudden reduction from 30% FA and this shows that cohesion plays an important role in the stability calculations.

Table 2: FOS values for stabilized embankment from PLAXIS 2D and SLOPE/W

Mix proportion	FOS of stabilized soil embankment			
	K2+600 Section		K6+850 Section	
	PLAXIS 2D	SLOPE/W (MPM)	PLAXIS 2D	SLOPE/W (MPM)
100S+0FA	1.31	2.14	1.22	2.03
90S+10FA	1.33	2.12	1.23	2.05
80S+20FA	1.38	2.1	1.24	2.06
70S+30FA	1.41	1.94	1.23	1.92
60S+40FA	1.39	1.8	1.16	1.73

3.4 *Long-Term Stability Analysis of the FA-stabilized soil Embankment.*

Deformation and stability analysis analysis were performed for 30% FA-stabilized soil embankments for 5, 10, 15 years. Figure 4 shows the variation of vertical settlement and horizontal deformation of 30% FA stabilized soil embankment at K6+850 after 15 years. It is noted that after 15 years, vertical settlements at centre of the embankment in the two embankment sections are as high as 2.4 times that of the embankment after

construction. Variations of lateral deformations in both embankments are not significant and it is expected to reduce with time in section K2+600 and increase with time in section K6+850. The stability of both embankment sections tends to increase with time.

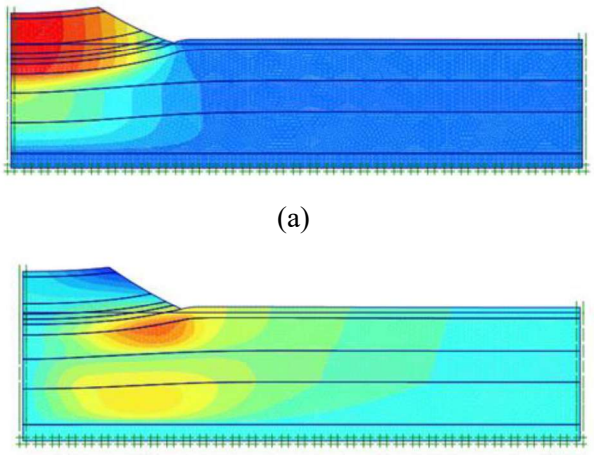

(a)

(b)

Figure 4: Variation of Vertical deformation of 30% FA-stabilized embankment section at K6+850 after 15 years.

4 CONCLUSIONS

The following conclusions are drawn based on the outcome of this research study,

- The vertical settlement and lateral deformation of the embankments reduce with the FA-stabilization compared to non-stabilized embankment and the percentage reduction in the vertical settlement and lateral deformation were 3 to 10% and 7 to 25% respectively for K2+600 section and 5-8% and 18-39% respectively for K6+850 section.
- The optimum FA content for reduced vertical settlement and lateral deformation of the embankment is 30% FA. Increase in the FA content beyond 30% shows further 1% reduction in the vertical settlement in both sections and 7% reduction in lateral deformation at K6+850.
- Based on the stability analysis, the FOS of these embankments increases with the FA content up to 30% and the percentage increase in FOS is 7.6% and 1.6% for K2+600 and K6+850 respectively.
- Considering long-term stability analysis of 30% FA-stabilized embankments, the FOS of both embankment sections tends to increase with time up to 15 years. Vertical settlements at centre of the embankment in the two embankment sections are as high as 2.4 times those after construction whereas lateral deformations in both embankments are not significant and it is expected to reduce with time in section K2+600 and increase with time in K6+850. This exposes that considerations on allowable maximum deformations need to be verified to confirm its feasibility to use as embankment fill material.

REFERENCES

Aryal, K.P. (2006). 'Slope Stability Evaluations by Limit Equilibrium and Finite Element Methods', Doctoral thesis. (http://hdl.handle.net/11250/231364).

Boroumand, A & Baziar, M.H (2005). Determination of compacted clay permeability by artificial neural networks, In Ninth International Water Technology Conference, IWTC9, Sharm El-Sheikh, Egypt pp. 515-526

Bose, B (2012). Geo engineering properties of expansive soil stabilized with fly ash, Electronic Journal of Geotechnical Engineering. 17(1):1339-1353

Buwa, V & Wayal, A.S (2016). Use of fly ash and lime for stabilization of soft soil, Electronic Journal of Geotechnical Engineering, 21(18):6235-6246

Deb, T. & Pal, S.K (2014). Effect of fly ash on geotechnical properties of local soilfly ash mixed samples, International Journal of Research in Engineering and Technology, 3(5):507-516

Nasvi, M.C.M & Krishnya, S (2019). Stability Analysis of Colombo–Katunayake Expressway (CKE) Using Finite Element and Limit Equilibrium Methods, Indian Geotechnical Journal, 49(6):620-634

Rajak, T.K, Yadu, L & Pal, S.K (2019). Analysis of Slope Stability of Fly Ash Stabilized Soil Slope, Geotechnical Applications, pp. 119-126.

Santos, F, Li, L, Li, Y & Amini, F (2011). Geotechnical Properties of Fly Ash and Soil Mixtures for Use in Highway Embankments, Proc. of the World of Coal Ash (WOCA) Conference, Denver, USA, pp. 125-136

Saride, S & Dutta, T.T (2016). Effect of fly-ash stabilization on stiffness modulus degradation of expansive clays, Journal of Materials in Civil Engineering, 28(12):04016166-1-12

Turan, C, Javadi, A, Consoli, N.C, Turan, C, Vinai, R, Cuisinier, O. & Russo, G (2019). Mechanical Properties Of Calcareous Fly Ash Stabilized Soil, In Eurocoalash 2019, 1:184-194.

Zhang, Q, Qin, X, Dong, H & Qu, D (2010). Foundation Treatments for Embankments Over Highly Compressible Peat in CKE Project, 5th Civil Engineering Conference in the Asian Region and Australasian Structural Engineering Conference 2010, 5: 1138-1141.

Prediction of Geotechnical Properties of Stabilized Soil Using Fly Ash Based Stabilizer Systems

K.M.D. Nimesha, N.A.N.M. Nissanka and M.C.M. Nasvi
Department of Civil Engineering, University of Peradeniya, Sri Lanka

ABSTRACT: This study was carried out in order to develop predictive models for geotechnical properties of fly ash stabilized soil systems; fly ash treated soil (FA-S) and fly ash geopolymer stabilized soil (FA-GP-S) using Artificial Neural Network (ANN). For this purpose, data bases were developed collecting data from many laboratory studies available in the literature. ANN models predicting Optimum Moisture Content (OMC) and Maximum Dry Density (MDD) of FA-S and the Unconfined Compressive Strength UCS of FA-S and FA-GP-S were developed. Models were then validated using independent data from several past studies. All the models exhibit good correlations between experimental and predicted results and also reasonable predictive abilities towards new data. Hence the obtained relationships may be useful in practical civil engineering applications.

1 INTRODUCTION

Due to the rapid increase in development, civil engineering constructions are increasingly located on land areas with problematic soil like expansive soil, collapsible soil, peat and landfills. One of the common methods used to improve the mechanical properties of them is the stabilization with chemical additives. The use of mineral additives such as fly ash, blast furnace slag, bottom ash and rice husk ash which are received as industrial by-products for chemical stabilization has become a popular research area mainly due to the low CO_2 emission and low cost associated with their production.

Fly ash is one of the abundant and versatile industrial by product (Senol *et al*., 2006) which is recommended in stabilizing problematic soil, in the form of mineral additives to the soil (Dissanayaka *et al*., 2017; Zha *et al*., 2008; Cokca, 2001; Rangaswamy, 2016) within their optimal dosage range. In addition, fly ash has been identified as a successful precursors for soil geopolymerization (Murmu *et al*., 2018; Phummiphan *et al*., 2015; Teerawattanasuk and Voottipruex, 2018; Cristelo *et al*., 2013; Phetchuay *et al*., 2016), which is a recent trend in chemical stabilization. However based on the review of previous papers, it can be identified that mechanical properties of stabilized soil are dependent on various parameters such as the type of soil and fly ash, activator type and dosage used for geopolymerization and temperature, and thus, determining relationships between these parameters and soil geotechnical properties is a challenging task. Several models have been developed using different tools and techniques to predict geotechnical properties of fly ash stabilized systems. Multi-Variable Regression (MVR) (Ling *et al*., 2019; Adhikari *et al*., 2019), Artificial Neural network (ANN) (Muzumder and Laskar, 2015; Ling *et al*., 2019; Leong et al., 2018) and genetic programming (Soleimani *et al*., 2017; Leong et al., 2018)) are some of the methods that have been used in previous works.

Some of the main limitations in previous models are the usage of data from one individual experimental program, and the unavailability of validation study.

Hence, this research focuses on addressing above knowledge gaps by developing predictive models for OMC, MDD and UCS of fly ash stabilized soil and UCS of fly ash based geopolymer stabilized soil. ANN is used in this study for developing the models considering its ability to handle multi-variable problems with complex non-linear relationships through the 'training' process.

2 DATA COLLECTION PARAMETER IDENTIFICATION

Data bases were developed collecting laboratory experimental data available in the literature. Only the soil classified as high plasticity clayey soil (CH) were preserved in the database, because the soil type considerably affects the quality of database. Experimental studies having used both class F and class C fly ashes were considered due to the limited availability of other parameters like the UCS of raw soil (UCS_o) data in the literature. Further, stabilized soil samples cured at only the ambient temperature were considered.

Table 1. Data sources and the number of data used for developing the models

Model	Data sources	No. of data
OMC-FA-S- & MDD-FA-S-	Murmu et al. (2018), Murmu & Patel (2020), Murmu et al. (2019), Pandya & Shah (2017), Bnal (2016), Mishra(2012), Ramlakhan et al. (2013), Gyanen et al. (2013), Athanasopoulou & Kollaros (2016), Anupam et al. (2013), Seyrek (2018), Bhat et al. (2018), Karim et al. (2015), Ahmad et al. (2015), Ozdemir (2016), Jafer (2015), Sezer et al (2006), Deb & Pal (2014), Sharma & Hymavathi (2016),	112
UCS-FA-S	Jafer et al. (2017), Mahedi et al.(2021), Geliga & Ismail (2010), Athanasopoulou & Kollaros (2016), Seyrek (2016), Turan et al. (2013), Karim et al.(2015), Dissanayake et al. (2017), Bose (2012), Deb & Pal (2014), Fusheng et al. (2008)	136
UCS-FA-GP-S	Cristelo et al. (2012), Cristelo et al. (2011), Murmu & Patel (2020),Debanath et al. (2019) Murmu et al. (2018),Murmu et al. (2019), Joshi et al. (2021)	154

OMC model for FA-S was developed with fly ash/ soil (w/w) and OMC of raw soil (OMC_0) as input parameters and MDD model with fly ash/ soil (w/w) and MDD_0 as input parameters. To develop the predictive model for UCS of FA-S, fly ash/ soil (w/w) and curing time (days) were selected as model input parameters and UCS-UCS_o as output parameter.

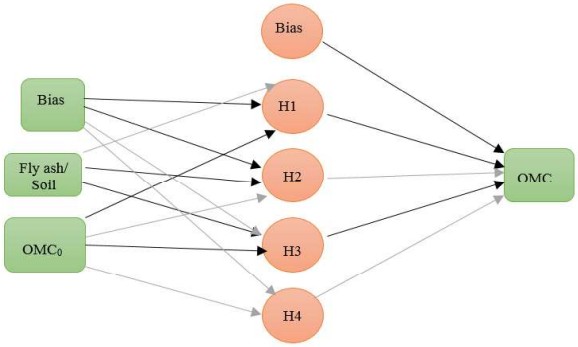

Fig. 1 OMC model architecture diagram for FA-S

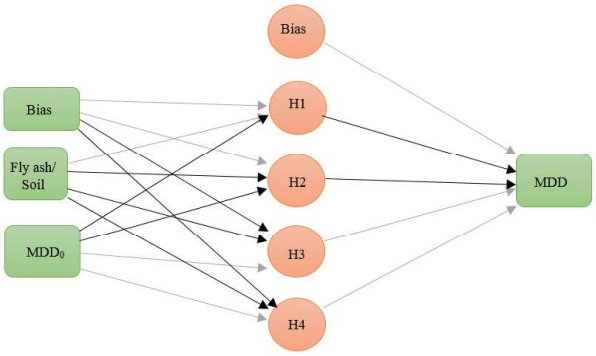

Fig. 2 MDD model architecture diagram for FA-S

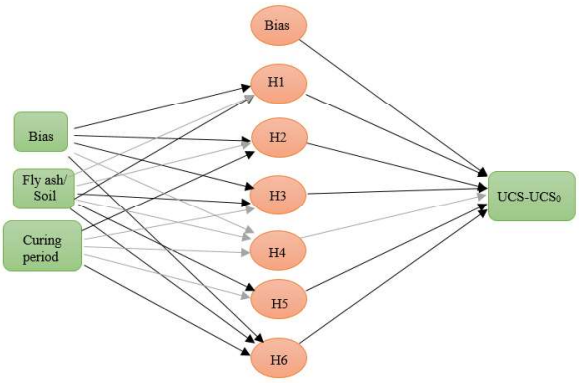

Fig. 3 UCS model architecture diagram for FA-S

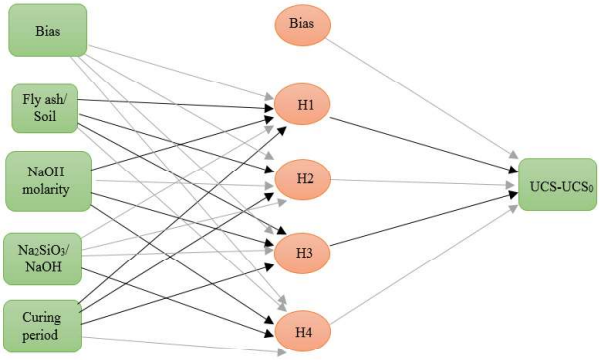

Fig. 4 UCS model architecture diagram for FA-GP-S

For UCS-model of FA-GP-S, previous studies on geopolymer stabilization where a combination of NaOH and Na_2SiO_3 was used as alkaline activator were considered. This is because it is the most commonly used activator yielding better strength values (Yaghoubi *et al.,* 2018). Fly ash/ soil (w/w), NaOH molarity, Na_2SiO_3/ NaOH (w/w) and curing period (days) were selected as model input parameters and (UCS- UCS_0) as output parameter. Data sources and the number of data used for training and validating the four models are summarized in Table 1. It should be noted that geopolymer based soil stabilization is still in its infancy and hence there are a limited number of published papers in this area. Hence the analysis was conducted using the limited numbers of data set available in the literature.

Table 2. Weights and biases of OMC-FA-S model

		Hidden layer				
		Bias	H (1)	H (2)	H (3)	H (4)
Input layer	Bias		-2.056	-1.363	0.852	-0.121
	F		0.122	-0.521	-0.511	0.296
	OMC_0		-1.011	1.336	-1.144	-0.058
Output layer		-0.458	-1.486	0.816	-0.740	0.343

Table 3. Weights and biases of MDD-FA-S model

		Hidden layer				
		Bias	H (1)	H (2)	H (3)	H (4)
Input layer	Bias		0.032	0.000	-0.164	-0.817
	F		0.241	-0.342	-0.276	-0.477
	MDD_0		-0.043	-0.473	0.062	0.675
Output layer		0.563	-1.024	-1.594	0.825	0.714

Table 4. Weights and biases of UCS-FA-S model

		Hidden layer						
		Bias	H (1)	H (2)	H(3)	H(4)	H (5)	H (6)
Input layer	Bias	-0.574	-3.448	-0.568	1.189	0.048	-0.556	-0.574
	F	1.556	0.404	-0.283	0.187	-0.249	-1.648	1.556
	C	-0.286	-4.430	0.001	0.089	0.149	-0.363	-0.286
Output layer		-1.802	-1.133	-1.106	-0.392	0.105	-0.131	-1.401

Table 5. Weights and biases of UCS-FA-GP-S model

		Hidden layer				
		Bias	H (1)	H (2)	H (3)	H (4)
Output layer	Bias		1.088	0.207	2.591	0.219
	F		-0.073	-0.774	-0.336	1.021
	M		-0.487	0.284	-1.189	-0.208
	S		0.790	1.273	0.992	-0.950
	C		-0.128	-0.054	-0.477	0.231
Output layer		1.673	-0.412	1.213	-1.905	0.916

3 MODEL DEVELOPMENT

A feed-forward multilayer perceptron ANN architecture having only one hidden layer was adopted in developing the models, and the optimum number of neurons in the hidden layer were determined by trial and error procedure. Standardization was used as the data scaling method for pre-processing. Hyperbolic tangent function and pure linear function were used as activation functions at hidden layer and output layer respectively. Batch training process together with scaled conjugate gradient optimization algorithm were adopted for training, due to the small number of data sets used for each model. The model performances were evaluated based on three criteria; coefficient of determination (R^2), mean squared error (MSE) and mean absolute percentage error (MAPE). These statistical parameters can be expressed mathematically using Eq. (1) to Eq. (3).

$$R^2 = \frac{(n\sum_i to - \sum_i t \sum_i o)^2}{[n\sum_i t^2 - (\sum_i t)^2][n\sum_i o^2 - (\sum_i o)^2]} \quad (1)$$

$$\text{RMSE} = \sqrt{\sum_{i=1}^{n} \frac{(t-O)^2}{n}} \quad (2)$$

$$\text{MAPE} = \frac{1}{n}\sum_{t=1}^{n} \left|\frac{t-O}{t}\right| \quad (3)$$

Where t is the target value, o is the output value and n is the number of data sets.

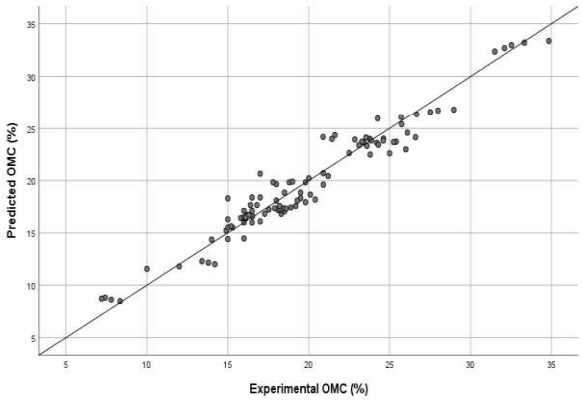

Fig. 5 Predicted vs. experimental data used for training OMC-FA-S model

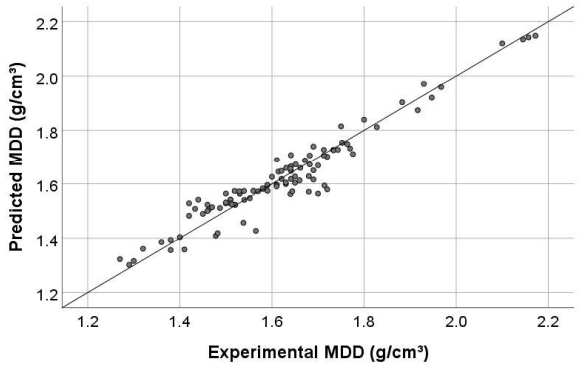

Fig. 6 Predicted vs. experimental data used for training MDD-FA-S model

Fig. 1-4 illustrate resulted ANN architectures for each model with the optimum number of hidden neurons. Weights and biases associated with each model is given in Table 2-5. Plots of predicted versus experimental results of all the studied properties are shown in Fig. 5-8. Best fitting lines having R^2 values of 0.973, 0.961, 0.815 and 0.963 for OMC, MDD, UCS models of FA-S and UCS model of FA-GP-S show good agreements with line of equity. This indicate better correlations between experimental and predicted results for all four developed models.

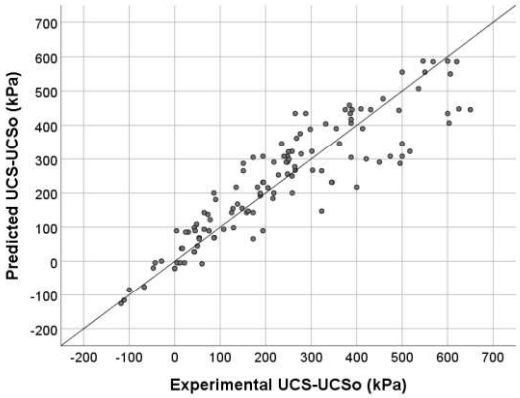

Fig. 7 Predicted vs. experimental data used for training UCS-FA-S model

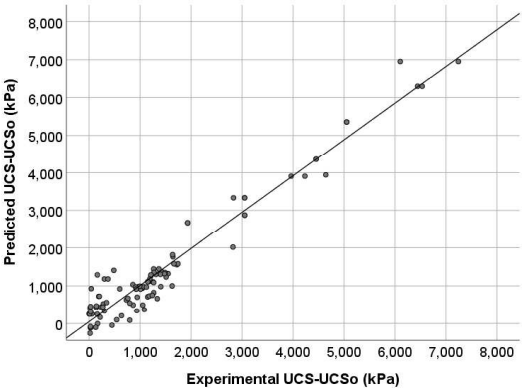

Fig. 8 Predicted vs. experimental data used for training UCS-FA-GP-S model

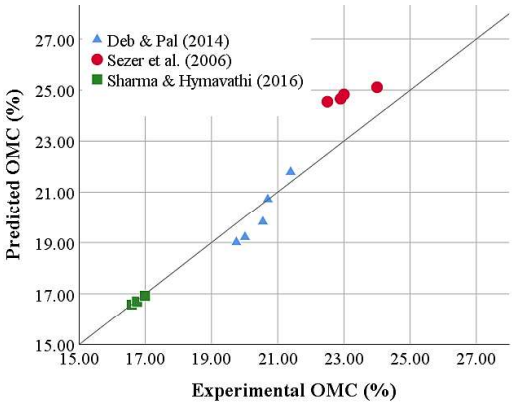

Fig. 9 Predicted vs. experimental data used for validating OMC-FA-S model

Table 6. Performances of developed models

Model	Data set	R^2	RMSE	MAPE
OMC-FA-S	Training	0.973	1.254	0.055
	Validation	0.970	1.073	0.036
MDD-FA-S	Training	0.961	0.047	0.022
	Validation	0.975	0.145	0.246
UCS-FA-S	Training	0.815	58.991	0.475
	Validation	0.702	127.013	0.432
UCS-FA-GP-S	Training	0.963	17.060	0.397
	Validation	0.842	66.290	0.378

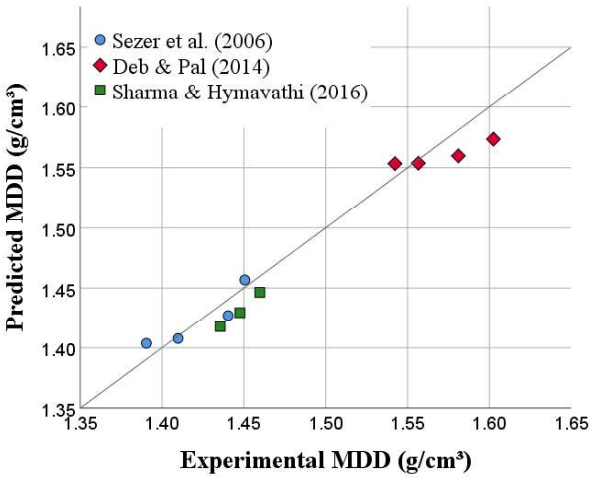

Fig. 10 Predicted vs. experimental data used for validating MDD-FA-S model

4 MODEL VALIDATION

Model validation was carried out to assess the predictive ability of each developed model using independent data from several past studies. Because this data set is not used for developing the model, the error associated with validation data gives an honest expression of the predictive ability of the models. As shown in Fig.9-12 predicted values of all the ANN models exhibits a reasonable correlation with the experimental values. The R^2 values associated with OMC, MDD and UCS models of FA-S were 0.970, 0.975, 0.702 and 0.842. Statistical performances of training and validation data for all ANN models are summarized in Table 6.

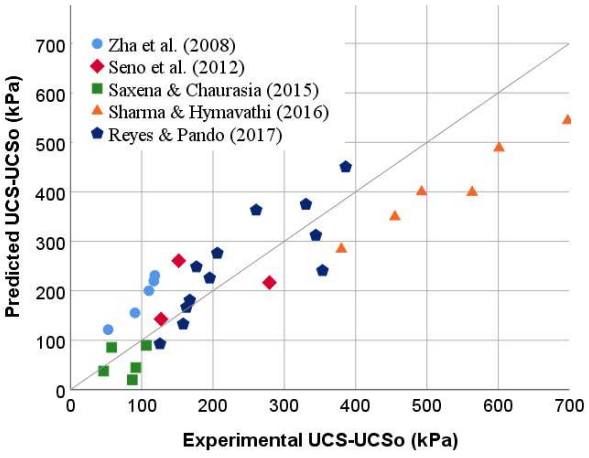

Fig. 11 Predicted vs. experimental data used for validating UCS-FA-S model

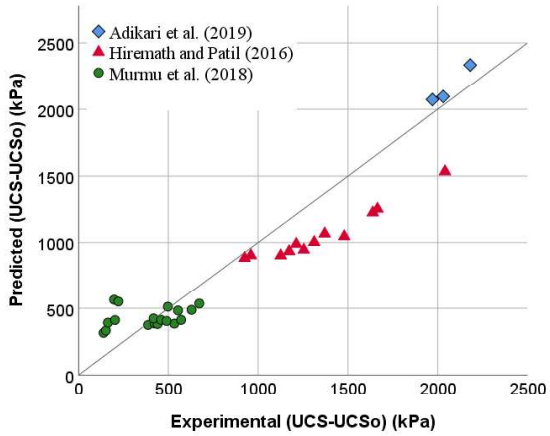

Fig.12 Predicted vs. experimental data used for validating UCS-FA-GP-S model

5 CONCLUSIONS

Following major conclusions can be derived from the study;

- All the ANN models were successfully developed with good correlation between experimental and predicted values.
- Developed models shows a reasonable predictive ability towards new data, suggesting that the models can be used as an alternative for conducting experimental studies to predict geotechnical properties of fly ash stabilized soil systems.

REFERENCES

Adhikari, B., Khattak, M.J. and Adhikari, S. (2019). Mechanical and durability characteristics of flyash-based soil-geopolymer mixtures for pavement base and subbase layers. International Journal of Pavement Engineering, 22(9), pp.1193–1212.

Ahmed, B. S., Gadouri, H., Ghrici, M., and Harichane, K. (2020) Best-fit models for predicting the geotechnical properties of FA–stabilised problematic soils used as materials for earth structures, International Journal of Pavement Engineering, 21:7, 939-953

Anak Geliga, E. and Awg Ismail, D.S. (2010). Geotechnical Properties of Fly Ash and its Application on Soft Soil Stabilization. Journal of Civil Engineering, Science and Technology, pp.1–6.

Anupam, A.K., Kumar, P. and Ransinchung R.N., G.D. (2013). Use of Various Agricultural and Industrial Waste Materials in Road Construction. *Procedia - Social and Behavioral Sciences*, 104, pp.264–273.

Athanasopoulou, A., George,K.(2016). Improvement of Soil Engineering Characteristics Using Lime And Fly Ash. Journal of Materials in Civil Engineering, 26(4), pp.773–775.

Binal, A. (2016). The Effects of High Alkaline Fly Ash on Strength Behaviour of a Cohesive Soil. *Advances in Materials Science and Engineering*, 2016, pp.1–11.

Binal, A., Bas, B. and Karamut, O.R. (2016). Improvement of the Strength of Ankara Clay with Self-cementing High Alkaline Fly Ash. *Procedia Engineering*, 161, pp.374–379.

Bose, B. (2012) "Geo-engineering properties of expansive soil stabilized with fly ash," Electronic Journal of Geotechnical Engineering, Vol.17, Bund. J, pp.1339-1353

Cokca, E. (2001). "Use of class C fly ashes for the stabilization of an expansive soil". Journal of Geotechnical and Geoenvironmental Engineering, 127(7), pp. 568-573.

Cristelo, N., Glendinning, S., Fernandes, L., Pinto, A.T., 2013. Effects of alkaline-activated fly ash and Portland cement on soft soil stabilisation. Acta Geotech. 8 (4), 395–405.

Debanath O.C., Rahman M.A and Farooq, S. M. 2019, Use of fly ash based geopolymer for stabilization of expansive soil. Construction Materials and Environment.

Deb, T. and Pal, S.K. (2014). Effect of fly ash on geotechnical properties of local soil-fly ash mixed samples. IJRET: International Journal of Research in Engineering and Technology, 3(5): 507–516.

Dissanayake, T. B. C. H., Senanayake S. M. C. U., Nasvi, M. C. M. (2017). Comparison of the Stabilization Behavior of Fly Ash and Bottom Ash Treated Expansive Soil. Journal of ENGINEER, (01):11-19.

Duxson, P., Fernández-JiméneZ, A., Provis, J. L., Lukey, G. C., Palomo, A., van Deventer, J.S. (2007). Geopolymer technology: the current state of the art. Journal of Materials Science, 42(9):2917-2933.

Erdal Cokca (2001) "Use Of Class C Fly Ashes for the Stabilization – of an Expansive Soil"Journal of Geotechnical and Geoenvironmental Engineering Vol. 127, July, pp. 568-573.

Fusheng, Z., Songyu, L., Yanjun, D., Kerui, C.,(2008), Behavior of Expansive Soil Stabilized with FA, Natural Hazards,vol 47(3), pp.509-523

Hiremath, P.,Patil, G.,(2016). Stabilization of Black Cotton Soil using Alkali Activated Fly Ash. –International Journal for Innovative Research in Science & Technology, 2349-6010

Jafer, H., Atherton, W., Sadique, M., Ruddock, F. and Loffill, E. (2018). Stabilisation of soft soil using binary blending of high calcium fly ash and palm oil fuel ash. *Applied Clay Science*, 152, pp.323–332.

Jafer, H., Atherton, W., Sadique, M., Ruddock, F. and Loffill, E. (2018). Stabilisation of soft soil using binary blending of high calcium fly ash and palm oil fuel ash. Applied Clay Science, 152, pp.323–332.

Leong, H.Y., Ong, D.E.L., Sanjayan, J.G., Nazari, A. and Kueh, S.M. (2018). Effects of Significant Variables on Compressive Strength of Soil-Fly Ash Geopolymer: Variable Analytical Approach Based on Neural Networks and Genetic Programming. Journal of Materials in Civil Engineering, 30(7), p.04018129.

Ling, Y., Wang, K., Wang, X. and Li, W. (2019). Prediction of engineering properties of fly ash-based geopolymer using

artificial neural networks. Neural Computing and Applications

Mahedi, M., Cetin, B. and White, D.J. (2021). Closure to "Cement, Lime, and Fly Ashes in Stabilizing Expansive Soils: Performance Evaluation and Comparison" by Masrur Mahedi, Bora Cetin, and David J. White. Journal of Materials in Civil Engineering, 33(9), p.07021013.

Mozumder, R.A. and Laskar, A.I. (2015). Prediction of unconfined compressive strength of geopolymer stabilized clayey soil using Artificial Neural Network. *Computers and Geotechnics*, 69, pp.291–300.

Murmu, A. L., Jain, A., Patel, A. (2019). Mechanical Properties of Alkali Activated Fly Ash Geopolymer Stabilized Expansive Clay. KSCE Journal of Civil Engineering, 23(9):3875-3888.

Murmu, A., Dhole, N., Patel, A. (2018). Stabilization of black cotton soil for subgrade application using fly ash geopolymer. Journal of Road Materials and Pavement Design, 21:867-885.

Murmu, A. L., Patel, A. (2020). Studies on the properties of Fly Ash-Rice Husk Ash Based Geopolymer for Use in Black Cotton Soils. International Journal of Geosynthetics and Ground Engineering, 6:38

Ozdemir, M.A. (2016). Improvement in Bearing Capacity of a Soft Soil by Addition of Fly Ash. *Procedia Engineering*, 143, pp.498–505.

Phetchuay, C., Horpibulsuk, S., Arulrajah, A., Suksiripattanapong, C., Udomchai, A., 2016. Strength development in soft marine clay stabilized by fly ash and calcium carbide residue based geopolymer. Appl. Clay Sci. 127–128, 134–142.

Phummiphan, I., Horpibulsuk, S., Sukmak, P., Chinkulkijniwat, A., Arulrajah, A., Shen, S. (2015). Stabilization of marginal lateritic soil using high calcium fly ash- based geopolymer. Journal of Road materials and pavement design, 17(4):877-891.

Rangaswamy, K. (2016). Influence of burnt ash additives on stabilisation of soft clay soils. Innovative Infrastructure Solutions, 1(1).

S. Soleimani, S. Rajaei, P. Jiao, A. Sabz, S. Soheilinia, New Prediction Models for Unconfined Compressive Strength of Geopolymer Stabilized Soil Using Multi-Gen Genetic Programming,Measurement (2017)

Senol, A., et al., 2006. Soft subgrades' stabilization by using various fly ashes.Resources, Conservation and Recycling, 46 (4), 365–376.

Seyrek, E. (2018). Engineering behavior of clay soils stabilized with class C and class F fly ashes. *Science and Engineering of Composite Materials*, 25(2), pp.273–287.

Sezer, A., İnan, G., Yılmaz, H.R. and Ramyar, K. (2006). Utilization of a very high lime fly ash for improvement of Izmir clay. Building and Environment, 41(2), pp.150–155.

Sharma, R. K., and J. Hymavathi. 2016."Effect of Fly Ash, Construction Demolition Waste and Lime on Geotechnical Characteristics of a Clayey Soil: A Comparative Study."Environmental Earth Sciences 75 (5): 377. doi:10.1007/s12665-015-4796-6.

Teerawattanasuk, C., Voottipruex, P. (2018). Comparison between cement and fly ash geopolymer for stabilized marginal lateritic soil as road material. International Journal of Pavement Engineering, 20:1264:1274.25. Whitlow, R., 2001. Basic Soil Mechanic, 4th Edition. Prentice Hall, England.

Turan, C., Javadi, A., Vinai, R., Shariatmadari, N. and Farmani, R. (2020). Use of class C fly ash for stabilization of fine-grained soils. *E3S Web of Conferences*, 195, p.06001.

Yadu, L., and Tripathi, R. K. (2013) Stabilisation of soft soil with Granulated Blast Furnace Slag and Fly Ash. *International Journal of Research in Engineering and Technology,* 2 (2), P.115-119.

Yaghoubi, M. J., Arulrajah, A., Disfani, M. M., Horpibulsuk, S., Bo, M. W.,Darmawan, S. (2018). Effects of industrial by-product based geopolymers on the strength development of a soft soil. Journal of Soil and foundations, 58:716-728.

Zha, F., Liu, S., Du, Y. and Cui, K. (2008). Behavior of expansive soils stabilized with fly ash. Natural Hazards, 47(3), pp.509–523.

Pavement Degradation Model for Road Infrastructure in Sri Lanka

M.M.N.T. Meghasooriya, K.M.N.M. Jayarathna, and S.K. Navaratnarajah
Department of Civil Engineering, University of Peradeniya, Sri Lanka

ABSTRACT: Pavement degradation prediction is essential for road management systems to predict the most effective maintenance time. The existing degradation prediction models are calibrated for conditions most suitable for that particular country. Therefore, it cannot be used directly for the local condition. In Sri Lanka, this is causing many difficulties in planning maintenance activities of road infrastructure. Therefore, in this study, a pavement degradation model for unpaved road infrastructure in Sri Lanka is proposed using the data collected at three unpaved roads in the Naula Pradeshiya Saba area. The analysis consists of identifying performance parameters, condition stages of the road sections, Transition Probability Matrix (TPM), and finally prediction of the road lifetime and level of maintenance requirements. The developed Unpaved Condition Index (DUPCI) is proposed as the performance parameter which includes all the possible deterioration types of gravel roads such as potholes, corrugations, overexposed aggregates, erosion, roadside drainage, and rutting. Model calibration and validation were done using the collected data for Sri Lankan unpaved roads.

KEYWORDS: Pavement degradation, Maintenance, Markov Model, Unpaved Condition Index

1 INTRODUCTION

Pavement maintenance is one of the most important tasks after the construction. Every country adopts various pavement management systems (PMS) which are consist of many prediction models developed in their state or calibrated models from other states. Model is depending on the road types such as unpaved, paved, and rigid pavements. Among various models that developed in many countries, the Australian Road Research Board (ARRB) models, Highway Development and Management (HDM) models, and Technical Recommendations for Highway Manual 20 (TRH20) model are widely used.

Pavement degradation models are widely used in PMSs to predict when maintenance will be required. Models can predict the degradation with time as well as the lifetime economic evaluation. After the construction, long-term funding requirements for pavement maintenance can be estimated with the sense of the lifetime of the road (George et al., 1989). Also, Saha and Ksaibati (2017) concluded that models are used to decide the best maintenance type such as re-graveling, blading, reconstruction, and major drainage repair considering cross-section, roadside drainage, rutting, potholes, loose aggregates, dust, corrugation, and ride quality. The model can be used for any country after it is calibrated to local conditions. Calibration is essential because universal degradation models can vary from country to country with many factors. Better prediction can be obtained by calibrated models for local conditions.

Age of the pavement, traffic volume, and weight, thickness of last overlay, strength, and condition of pavement structure, surface deflection, and construction quality are the affecting factors for pavement degradation (George et al., 1989). Among them, age was identified as significant in predicting pavement deterioration. Giummarra et al (2007) found that plasticity factors, traffic, rainfall, and material properties can be considered as the affecting factors. Furthermore, Zyl et al (2007) recommend taking pavement material properties, climate, and road geometry as the affecting factors for TRH-20, HDM-4, and ARRB models. HDM-4 and ARRB models incorporate all four major fields of input, but geometry is omitted from the TRH-20 Model. For road geometry, HDM-4 uses the gradient and the curvature whereas ARRB incorporates only the gradient. Wijk et al (2011) compared gravel loss prediction models such as TRRL Model, South African Model, Australian Model, and Highway Design and Maintenance model. According to the review of literature, a summary of the affecting factors can be identified as traffic volume age of pavement, the thickness of last overlay, material properties of wearing course (plasticity factor, material type, particle size distribution), climate (rainfall, wet zone, and dry zone, Weinert N-value, wind), and road geometry (average rise and fall, gradient of the road, average curvature).

George et al (1989), Chamorro and Tighe (2011), and Abaza (2015) used combined performance parameters to predict the lifetime of a road.

Giummarra et al (2007), Wijk et al (2011), Aleadelat et al (2019), and Uyz (2011) reported individual performance parameters to rate the condition of the road. Combined performance parameters are related to the overall condition of the road which is suitable for combined maintenance procedures. Individual performance parameters identify each degradation individually and distinct maintenance is proposed such as blading and re-graveling.

2 MARKOV APPROACH

Prediction of performance is done by two types of models: deterministic and stochastic (probabilistic). Deterministic models include primary response, structural performance, functional performance, and damage models according to George et al (1989). Stochastic models are based on probability which is applied widely because of the consideration of uncertainty. Markov approach and survivor curves are two main approaches for stochastic models as suggested by Carnahan et al (1987) and Lytton (1987). Markov approach is mainly consisting of four main steps: performance parameter selection, condition stages identification, transition probability matrix development, and finally Markov chain development to predict the lifetime of a road. Markov chains can be identified as homogeneous and non-homogeneous chains based on the transition probability matrix used. According to Abaza (2015), the homogeneous Markov model assumes steady-state transition probabilities over the entire analysis period which presents a major drawback for predicting future pavement conditions. The non-homogeneous Markov model deploys different transition probabilities for each transition which can lead to superiority in predicting future pavement conditions. But as concluded by Butt et al (2011), this required more data and time to develop TPM for each transition. In this research homogenous Markov modeling is used for final analysis.

2.1 *Performance parameter selection*

Individual performance parameters identify each degradation individually. Therefore separate models are needed to identify specific deterioration types. Maintenance activity might recover many degradations but some other deteriorations might not be recovered. Combined performance parameters are related to the overall condition of the road which is suitable for combined maintenance procedures. Prediction is done considering all the degradation types including all parameters into one model. Both types of performance parameters are presented in Table 1.

Table 1. Performance parameters

Individual Performance Parameters	Combined Performance Parameters
Roughness Rating	Unpaved Road Condition Index (URCI)
Structural Strength Rating	Unpaved condition Index (UPCI)
Rutting Rating	Unpaved Pavement Condition (UPC)
Cracking Rating	
Stone Loss Rating	

Eaton et al (1987) reported Unpaved Road Condition Index (URCI) combined performance parameter developed by the U.S. Army Corps of Engineers. This index consists of properties of the cross-section. Roadside drainage, corrugations, dust, potholes, rutting, and loose aggregate into a value between 0 and 100. Common Unpaved Condition Index (UPCI) model for both gravel and earth roads with and without roughness was used in Chamorro and Tighe (2011). But Unpaved Pavement Condition (UPC) was defined only as a function of age by Saha and Ksaibati (2017).

2.2 *Condition stages*

Condition stages represent the level of road degradation. Each stage has a fixed range of performance parameter ratings useful in identifying the transitions from one stage to another. The number of stages depends on the degradation rate of the road. Five condition stages and seven condition stages are the most ideal number of stages (Aleadelat et al., 2019).

2.3 *Transition probability matrix (TPM)*

The transition probability matrix (TPM) consists of the probabilities of transitions from upper stages to the same stage or lower stages after a considerable period. Each probability is computed as a percentage of the total number of sections transferred to the total number of sections considered. TPM which is composed of the diagonal probability in addition to extra probabilities concerning the first raw of the TPM has been used (Aleadelat et al., 2019). Along the main diagonal represent the probabilities of pavements remaining in the same condition states and entries above the main diagonal denote the probabilities of pavements transmitting to the worse condition states after one condition. Similarly, entries below the main diagonal indicate the probabilities of pavement transiting to the better condition which cannot happen. This is the most common method of developing the transition probability matrix. But cumulative probability matrixes are also defined by calculating the cumulative probability per row in each TPM (Chamorro and Tighe, 2011).

2.4 *Markov chain*

Markov chain is developed to predict life by calculating the transferring fractions for the considered period in TPM. Homogenous TPM assumes that the transition probabilities for each period are equal. Therefore, the prediction of the condition rating for an equal period can be computed by continuing the multiplication using the same TPM. Equally distributed TPM is required for a better prediction.

3 DATA COLLECTION

Lion Rock Road(1), Naula Road(2), and Inamaluwa Road(3) were selected for data collection as shown in Fig 1. All three roads are maintained directly by Naula Pradeshiya Sabha. The following aspects were considered selecting roads for this study. The selected roads should have many characteristics to implement the analysis. Road sections should not be improved by any maintenance work during the data collection period. Also, the selected roads should represent all the introduced stages. Straight road sections were selected to avoid degradation due to additional friction forces imposed on the horizontal curves of the roads.

Fig. 1 Map of the selected roads

As stated previously, many factors affect gravel road degradation. But if the condition is rated using few or one factor, or one condition parameter, the entire effect cannot conclude in the model. Also, the models consist of condition parameters that are recommended to use rather than models with factors because parameters consist of the effect of all factors. Therefore Unpaved Condition Index (UPCI) was selected as the most appropriate performance parameter to rate the gravel roads in Sri Lanka because it consists of many degradation parameters which give overall condition with less use of measuring instruments.

The index consists of six degradation measurements such as corrugation, potholes, erosion, rutting, exposed oversize aggregate, and crown condition. First, each road was divided into 100 m sections and three sections among them were selected which represent the condition of the entire road. UPCI values were assigned to subdivided sections with 10m in length. UPCI needs several in situ measurements to calculate the current condition of each section. Three data sets were collected in three different periods, two for TPM development and the other one for validation. UPCI has performed a technique of reducing the maximum possible rating of 10 by the measured degradations as shown in Equation (1).

$$UPCI = 10 - 1.16CR - 2.25PT - 1.47ER - 0.33RT - 1.56OA - 1.58CW \quad (1)$$

UPCI shows a linear variation for each parameter. But the effect of each parameter on the overall condition is different and proportional to the magnitude of parameter coefficient showing higher coefficients for highly affecting parameters in road degradation. All coefficients should be negative to reduce the rating from 10 to null, but should not be less than 0. Corrugations (CR) are measured as the mean vertical deformation observed in a section in centimeters. But corrugation was not observed in any section of selected three roads during the entire investigation time. Potholes (PT) are calculated as the product of the mean diameter in meters, maximum depth in meters, and the number of potholes in a sample section. Erosion (ER) is a dummy variable, considered as 1 if either erosion depth or width is greater than or equal to 5 cm. Measuring the depth and width of the erosion can be conducted as same as pothole diameter and depth measurements. Rutting (RT) or transverse deformations caused by the loose aggregate, measured as the mean vertical deformation of five readings for each 10 m subsection using a straight bar in centimeters. Exposed oversized aggregate (OA) is another dummy variable, considered as 1 when oversized aggregates with mean diameters greater or equal to 10 cm are observed as a generalized phenomenon within the sample section. Crown condition (CW) which is the average between drainage and transverse profile condition, both defects are rated as 0 when observed in good condition, 0.5 in fair condition, and 1 in poor condition.

4 DATA ANALYSIS

UPCI model is calibrated to United States road conditions. Therefore model calibration is required for Sri Lankan conditions before lifetime prediction in Sri Lankan gravel roads. To find the actual rating of

the road, a Visual and Direct Measurement (VDM) method was used as proposed by Woll et al (2011). UPCI model was calibrated equating VDM values as the dependant variable. But it was observed that the R-sq is only 63% indicates that something remains in the residuals that can be removed by a more appropriate model. Therefore all variables, their interaction terms, and square terms were subjected to stepwise regression. Concluding the analysis results, the authors are proposed a developed model called Developed Unpaved Condition Index (DUPCI) shown in Equation (2) with R-sq of 78% for gravel road condition rating in Sri Lanka which was calibrated for the dry zone.

$$\begin{aligned} DUPCI = {} & 9.009 - 1.169RT - 0.752ER \\ & - 0.6264RT \times OA + 1.602RT \times CW \\ & - 0.1232PT \times ER - 2.465CW^2 \end{aligned} \quad (2)$$

DUPCI shows a maximum rating of 9. Therefore the number of condition stages was reduced to 4 including very good, good, poor, and fail stages and new ranges of ratings were proposed by the authors as showed in Table 2.

Table 2. Condition stages

Stage	UPCI Range
Very good	9 - 7
Good	7 - 5
Poor	5 – 3
Fail	3 - 1

Initially, separate analyses were conducted for each road preparing 3 transition probability matrixes. During the first data collection, it was observed that all sections of the Lion Rock road are comprised of very good and good stages. After the second data collection TPM was developed as shown in Table 3. Hence the initial conditions only belong to higher stages, TPM consists of probabilities only at the upper triangle of the matrix.

Table 3. Transition probability matrix for Lion Rock Road

	VG	G	P	F
VG	0.421	0.526	0.052	0.000
G	0.000	0.909	0.090	0.000
P	0.000	0.000	0.000	0.000
F	0.000	0.000	0.000	0.000

Table 4 is concluded the TPM for Naula Road. Similar to Lion Rock road only very good and good sections were identified at the first data collection. All very good sections have transferred to each stage and good sections have remained in the same condition.

Table 4. Transition probability matrix for Naula Road

	VG	G	P	F
VG	0.545	0.318	0.091	0.045
G	0.000	1.000	0.000	0.000
P	0.000	0.000	0.000	0.000
F	0.000	0.000	0.000	0.000

Inamalua Road was in poor condition during the first visit. According to the TPM, all 30 sections have been distributed within every stage but more sections were related to lower stages as indicated in Table 5.

Table 5. Transition probability matrix for Inamaluwa Road

	VG	G	P	F
VG	0.400	0.200	0.000	0.400
G	0.000	0.563	0.438	0.000
P	0.000	0.000	0.750	0.250
F	0.000	0.000	0.000	1.000

Fig. 2 shows the lifetime predictions of Lion Rock Road, Naula Road, and Inamaluwa Road. Lion Rock Road shows better variation showing a complete failure after 80 months from the construction.

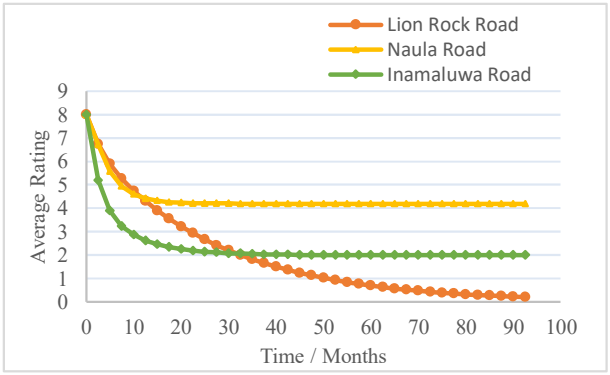

Fig. 2 Pavement lifetime prediction for individual analysis

The lifetime of the Naula Road consists of better prediction during the 1st few and the final rating is converged to rating 4. But Markov chain has the capability of prediction until the complete degradation occurred with accurate TPM. Therefore it can be concluded that the matrix is not complete enough for a better prediction. Inamaluwa Road also shows the same variation as Naula road.

Individual analysis of Lion Rock, Naula, and Inamaluwa roads do not show complete behavior during the entire life because the number of transitions is not enough. The main reason for this is an inadequate number of sections selected for the analysis. Also, the selected period might be not enough to

show each stage's transitions. Therefore combined analysis was conducted to overcome difficulties and data deficiency faced during the individual road analysis. All data were concluded to develop one TPM which defines the entire selected region as shown in Table 6. The developed Markov chain is shown in Table 7.

Table 6. Transition probability matrix for combined analysis

	VG	G	P	F
VG	0.400	0.200	0.000	0.400
G	0.000	0.563	0.438	0.000
P	0.000	0.000	0.750	0.250
F	0.000	0.000	0.000	1.000

Table 7. Markov chain

Stage	Month	VG	G	P	F	Average Condition
0	0.0	1.000	0.000	0.000	0.000	8.00
1	2.5	0.468	0.404	0.064	0.064	6.55
2	5.0	0.219	0.501	0.170	0.046	5.53
3	7.5	0.103	0.474	0.256	0.057	4.81
4	10.0	0.048	0.407	0.308	0.071	4.20
5	12.5	0.022	0.333	0.327	0.080	3.65
6	15.0	0.011	0.266	0.323	0.083	3.14
7	17.5	0.005	0.209	0.304	0.081	2.67
8	20.0	0.002	0.163	0.276	0.076	2.26
9	22.5	0.001	0.127	0.245	0.069	1.89
10	25.0	0.001	0.098	0.213	0.061	1.57
11	27.5	0.000	0.076	0.182	0.053	1.29
12	30.0	0.000	0.059	0.154	0.046	1.06
13	32.5	0.000	0.045	0.129	0.038	0.86
14	35.0	0.000	0.035	0.107	0.032	0.70
15	37.5	0.000	0.027	0.088	0.027	0.57
16	40.0	0.000	0.021	0.072	0.022	0.46
17	42.5	0.000	0.016	0.059	0.018	0.37
18	45.0	0.000	0.012	0.048	0.015	0.30
19	47.5	0.000	0.010	0.039	0.012	0.24
20	50.0	0.000	0.007	0.031	0.010	0.19
21	52.5	0.000	0.006	0.025	0.008	0.15
22	55.0	0.000	0.004	0.020	0.006	0.12
23	57.5	0.000	0.003	0.016	0.005	0.09
24	60.0	0.000	0.003	0.013	0.004	0.08

The time difference between the first two data collections is 2.5 months. Therefore chain was developed for 2.5 month time intervals. Fig. 3 shows more acceptable lifetime predictions than individual predictions. The final value of the rating is converged to 0 confirmed that the matrix selected for the analysis has enough transitions between every stage.

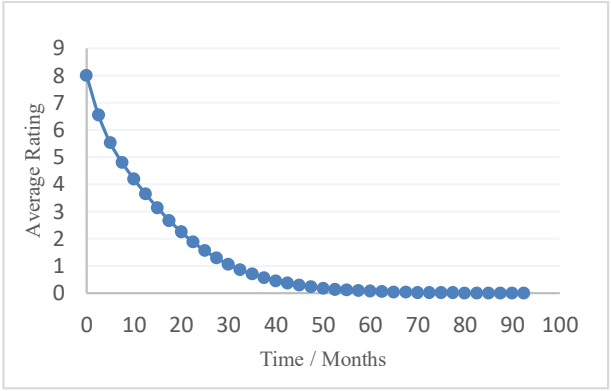

Fig. 3 Pavement lifetime prediction for combined analysis

Two data sets were used to build the Markov chain from 1st data collection until the fail condition. The Markov chain can predict future conditions with time but not backward. Therefore the predicted lifetime is not included in the time from construction to 1st data collection. According to the data records of Naula Pradeshiya Sabha, all the roads were graveled in February 2019. The third data set was used to validate the proposed model for Sri Lankan gravel roads. Considering the condition rating of a gravel road just after the construction is 9, all four data sets were plotted in the lifetime prediction graph for validation as shown in Fig. 4.

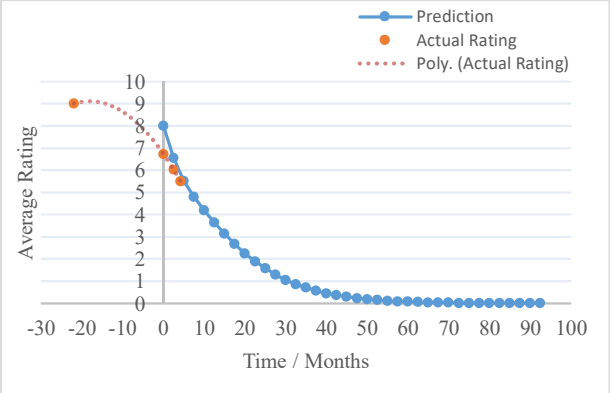

Fig. 4 Pavement lifetime prediction validation

The actual mean rating trends to go with the predicted lifetime confirming the model is applicable. Hence all the calibration was done using roads in the dry zone of Sri Lanka, this model is applicable only for the dry zone roads. According to the results, a gravel road in the dry zone, Sri Lanka is completely failed within 7 years. But with the experience at the site, the author proposes rehabilitation when a road reaches rating 5, the stating rating of poor condition stage. Therefore rehabilitation should be done after 2.5 years after construction. Reconstruction is proposed when the road reached to fail condition-stage which starts at a rating of 3.

5 CONCLUSIONS

According to the observed results, rehabilitation is required to commence at the rating of 5. According to the prediction curve, it is 2.5 years after the construction. Reconstruction is proposed after 3 years from the construction when the road reaches rating 3. Another important conclusion is corrugations were not observed during the entire investigation period on all roads. According to the analysis in this study, Markov analysis can be used for forward prediction but not backward. During the study period, considerable variation was noticed in rutting and potholes making them the most significant factors affecting road degradation. The effect of erosion is only considered after a certain depth. But the same impact is considered in UPCI and DUPCI for different scales of erosion. According to the measured ratings, the road does not show any noticeable degradation during the first 7 months. Noticeable degradation was observed during higher condition stages and degradation of road sections which having lower stages showed slow degradation. It was observed, the silt accumulation in potholes begins reducing the depth of the potholes after some time of degradation happened. UPCI and DUPCI don't consider the smaller exposed over-size aggregates. This might be caused for errors in calculations of rating. Therefore it is recommended to consider the factor OA as a function of the area or diameter of exposed aggregates. Rutting is measured as the maximum depth relative to the road centerline and edge. Road edge can degrade only due to environmental factors such as rainfall. But the center can be degraded due to traffic which causing errors in measurements of rutting depth. Taking rutting depths relative to the reference point by using a leveling instrument can avoid this error. Proper TPM can be defined using data of more sections. The number of transitions from each stage to lower stages contributes to proper distributions in transition probabilities. Also, it is recommended to take a higher number of lengthy sections rather than selecting small sections to observe better degradation. Selected gravel roads had average daily traffic of less than 50. The predicted lifetime is relevant to less ADT and the same analysis can be conducted to higher ADT ranges, different climate zones, and different terrains. Also, all the required data were collected manually using a leveled bar and measuring ruler. Then the readings might be different from observer to observer. Therefore a sensor network or echo-sounder system can be developed to take measurements by scanning the road similarly to the bathymetry survey which is done to identify the topography of a river bed.

ACKNOWLEDGMENTS

The authors would like to appreciate the support of the Road Development Authority (RDA), Provincial Road Development Authority (PRDA), Kundasale, and Naula Pradesiya Sabha.

REFERENCES

Abaza K., (2015)., Simplified Staged Homogenous Markov Model for Flexible Pavement Performance Prediction, Department of Civil Engineering, Road Materials and Pavement Design, 2015, Vol. 17, No. 2, 365–381.

Aleadelat W., Wulff S., and Ksaibati K., (2019)., Development of Performance Prediction Models for Gravel Roads Using Markov Chains, American Journal of Civil Engineering, vol 7, no. 3, 2019, pp. 73-81.

Butt A., Shahin M., Feighan K., and Carpenter S., Pavement Performance Prediction model using the Markov Process, Transportation Road Research Board, 1123, 2011, 12-19.

Carnahan J. V., Davis W. J., Shahin M. Y., Keene P. L., and Wu M. I., (1987)., Optimal Maintenance Decisions for Pavement Management, Journal of Transportation Engineering, ASCE, Vol. 113, No. 5, 1987, pp. 554-572.

Chamorro A. and Tighe S. L., (2011)., Condition Performance Models for Network-Level Management of Unpaved Roads, Journal of the Transportation research board, No. 2204, Transportation Research Board of the National Academies, Washington, D.C.2011, pp. 21-28.

Eaton R. A., Gerard S., and Datillo R. S., (1087)., A Method for Rating Unsurfaced Roads, Transportation Research Record Journal of the Transportation research board, No 1106, Washington, D.C., 1987, USA.

George K.P., Rajagopal A. P., and Lim L. K.,(1989)., Models for Predicting Pavement Deterioration, Department of Civil Engineering, University of Mississippi, 1989, Miss 38677.

Giummarra G. J., Martin T., Hoque Z., and Roper R., (2007)., Establishing Deterioration Models for Local Roads in Australia, Journal of the Transportation Research Board, No. 1989, Vol. 2, Transportation Research Board of National Academies, Washington, D.C., 2007, pp. 270-276.

Lytton R. L., (1987)., Concepts of Pavement Performance Prediction Modeling, Proc. North American Conference on Managing Pavements, Toronto, Canada, Vol. 2, 1987.

Saha P. and Ksaibati K., (2017)., Developing an Optimization Model to Manage Unpaved Roads, Journal of Advanced Transportation, Volume 2017, Article ID 9474838.

Uys R., (2011)., Evaluation of Gravel Loss Deterioration Models Case Study, Transportation Research Record: Journal of the Transportation Research Board, No. 2205, Transportation Research Board of the National Academies, Washington, D.C., 2011, pp. 86–94.

Wijk L. V., Williams D., and Serati M., (2011)., Roughness deterioration models for unsealed road pavements and their use in pavement management, International Journal of Pavement Engineering.

Woll J.H., Surdahl R., Marquez R., Everett R., and Andresen R., (2011)., Road Stabilizer Product Performance: Seedskadee National Wildlife Refuge, U.S. Central Federal Lands Highway Division, Lakewood. November 23, 2011.

Zyl G. V., Uys R., and Henderson M., (2007)., Applicability of Existing Gravel Road Deterioration Models Questioned, Journal of the Transportation research board, No. 1989, Vol. 1, Transportation Research Board of the National Academies, Washington, D.C., 2007, pp. 217-225.

Engineering Behavior of Gravel Compaction Piles (GCP) under Drained Condition

I.G.C.D. Dhanasekara and N.H. Priyankara
Department of Civil and Environmental Engineering, University of Ruhuna, Sri Lanka

ABSTRACT: Peaty clay is a poor soil material according to the geotechnical engineering due to high compressibility, high water content and very low shear strength. Therefore, it is necessary to improve the peat clay soils through any kind of a ground improvement method prior to the construction on it. Gravel compaction piles are one of the most commonly used method for improve poor ground conditions. Many research studies have been carried out to understand the various parameters that influence the overall performance of granular column improved composite ground using physical modelling, mathematical analysis and full-scale testing. However, this research study highlights the influence of the pre-consolidation pressure of the surrounding soft soil and length of the granular pile on the stability of the granular pile improved composite ground.

KEY WORDS: Gravel Compaction Piles, Aggregate Base Cause

1 INTRODUCTION

Gravel Compaction Piles (GCP) are one of the most commonly used methods to improve soft soil. Further, this technique can be defined as one of the environmentally and economically acceptable method. Gravel compaction piles were successfully used as a ground improvement technique in many projects in Sri Lanka.

Generally GCPs were used to improve soft soils up to a depth of 5-10m. But when the soft soil thickness is more than 13m, this technique was failed in one of the major projects in Sri Lanka due to lack of knowledge on drainage condition, stiffness of surrounding soft clay and maximum possible GCP length. However, only very limited number of researches were carried out to study the engineering behavior of granular piles in Sri Lankan soft peat clay. Therefore, this research study was conducted to investigate the influence of length of gravel compaction pile and pre-consolidation pressure of soft clay on stability of GCP improved ground.

Many studies based on physical modelling, mathematical analysis and full-scale testing have been carried out in order to understand and predict the behaviour of Gravel compaction piles. Some of these research studies have identified various parameters that influence the overall performance of this technique. Laboratory studies by Hughes and Withers (1974), Charles and Watts (1983), and Bachus and Barksdale (1984) have contributed considerably to understanding the behaviour of Gravel compaction piles. The ultimate bearing capacity obtained from full-scale tests on single gravel compaction piles was more than three times that of the untreated ground. However, there was little difference between the ultimate bearing capacity of the sand pile compared with that of the gravel pile.

Bouassida (1977) has studied the increase in shear strength and the reduction of settlements of the reinforced clay with respect to the reconstituted clay. Laboratory and field tests and theoretical analysis by Gung-Xin et al (2000) have shown that confining pressure is directly affected to the modulus and strength of the gravel column composite ground. In addition, the lateral interaction between column and surrounding soil is caused by the dilatancy of the gravel. Kaolin samples with partially and fully penetrating columns were tested by Sivakumar (2004) under undrained conditions. In that research study, area replacement factor of column was 10%, and two different methods of installation and types of loading were tested. If the column length longer than approximately five times their diameter, they did not indicate further increases in their load carrying capacity. The column length may have a significant influence on the stiffness of the composite material.

Experimental studies have identified most of the specific parameters that control the behaviour of a vertically loaded gravel column included composite soft soil. However, previous studies do not highlight the influence of surrounding pre-consolidation pressure and the gravel compaction column length on stability of composite ground. Therefore, this research study was carried out to investigate the effect of these parameters on the shear strength characteristics of soft soil reinforced by compacted sand columns. For this reason, triaxial compression tests were conducted on composite soil specimens consisting of soft clay which is tak-

en from Nilwala flood plain reconstituted from slurry and reinforced in the centre by a compacted sand column. The results were compared with the results for the untreated ground.

2 METHODOLOGY

Steel mould which having 200mm height and 100mm internal dimeter was used to prepare the test specimens as shown in Figure 1. The prepared remolded sample is depicted in Figure 2.

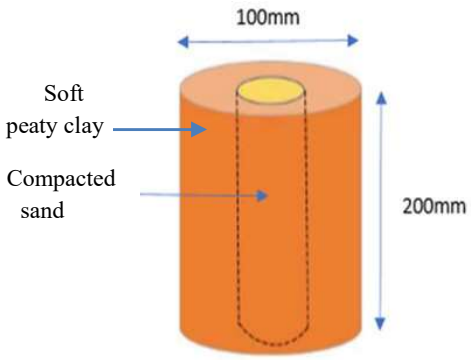

Fig. 1 Sample preparation

Fig. 2 Remolded sample

The prepared remoulded sample was preconsolidated using the modified oedometer apparatus as shown in Figure 3.
After preconsolidation, sample were subjected to triaxial Consolidated Undrained (CU) test by simulating field condition. Under laboratory conditions, granular pile length was kept constant as 200mm, i.e. height of triaxial sample. In order to simulate the field condition, granular pile diameter to length ratio was changed as shown in Table 1.

Fig. 3 Modified oedometer apparatus for apply preconsolidation

Table 1. Simulation of field condition in the laboratory

In Field	In Laboratory
Diameter=0.7m length = 10m Diameter / Length Ratio = 0.07	Diameter=16mm length = 200mm Diameter / Length Ratio = 0.07
Diameter=0.7m length = 6m Diameter / Length Ratio = 0.116	Diameter=23mm length = 200mm Diameter / Length Ratio = 0.116

Series of CU triaxial tests were conducted by varying preconsolidation pressure and granular pile diameter. In addition, CU triaxial test was conducted for unimproved peaty clay to study the effect of granular pile installation on improvement of shear strength characteristics of composite ground. The triaxial test conditions are depicted in Table 2. Under each test case, Mohr-Coulomb diagram was developed and corresponding shear strength parameters were determined.

Table 2. Triaxial test condition

Pre-consolidation pressure (KPa)	Confining pressure- 50,100,150 kpa	
	Granular pile diameter	Without granular pile
20	16mm	-
40	16mm	-
60	16mm, 23mm	Unimproved

According to the Table 2, 15 remolded samples were prepared with three confining pressures. Triaxial testing apparatus used for this research study is shown in Figure 4.

Fig. 4 Triaxial testing of remolded samples

3 RESULTS AND DISCUSSION

3.1 *Effect of preconsolidation pressure on shear strength parameters*

In order to study the effect of preconsolidation pressure on shear strength parameters, preconsolidation pressure was varied by keeping the granular pile diameter constant as 16mm. It can be seen that with the increase of pre-consolidation pressure, there is no significant amount of change in Undrained Friction angle, but Effective Friction angle is decreased due to higher disturbance in the samples as shown in Figure 5. With the increase of pre-consolidation pressure, there is no significant amount of change in Undrained Cohesion, but effective cohesion is increased with the preconsolidation pressure as shown in Figure 6.

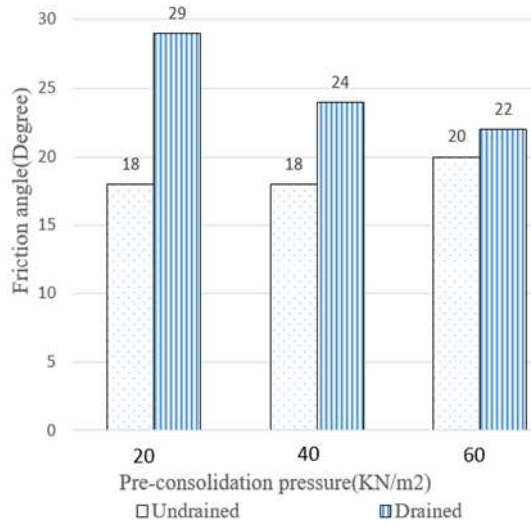

Fig. 5 Variation of friction angle with pre-consolidation pressure

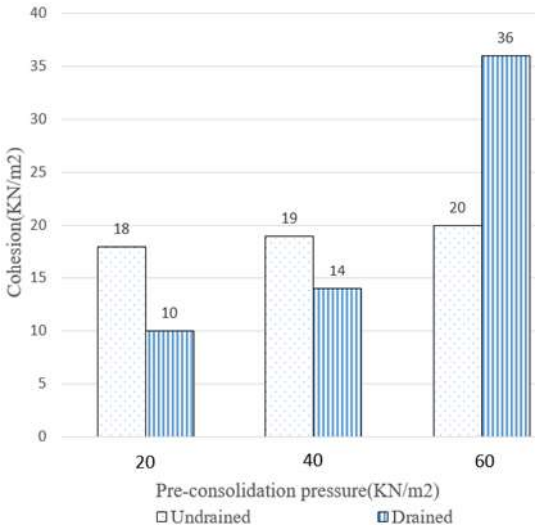

Fig. 6 Variation of cohesion with pre-consolidation pressure

3.2 *Effect of granular pile length on shear strength parameters*

In order to study the effect of granular pile length on improvement of shear strength parameters on GCP improved ground, preconsolidation pressure was kept constant as 60 kpa and vary the granular pile diameter as shown in Table 1. Here effect of length of granular pile was taken by varying the diameter of the granular pile with maintaining the diameter to length ratio as constant for field condition and the laboratory condition as shown in Table 1. Further, results were compared with the peaty clay without inclusion of granular pile. With the increase of column diameter i.e. increasing granular column diameter/length ratio, both Undrained and Effective friction angles are increased as indicated in Figure 7. Similarly. With the increase of

column diameter, both Undrained and Effective cohesions are increased as shown in Figure 8 (Here increase the pile diameter in the laboratory means decreased the pile length in the field according to the Table 1).
Based on above results, it can be concluded that short granular columns with composite ground have higher undrained and Effective strength parameters than that of long sand columns with composite grounds.

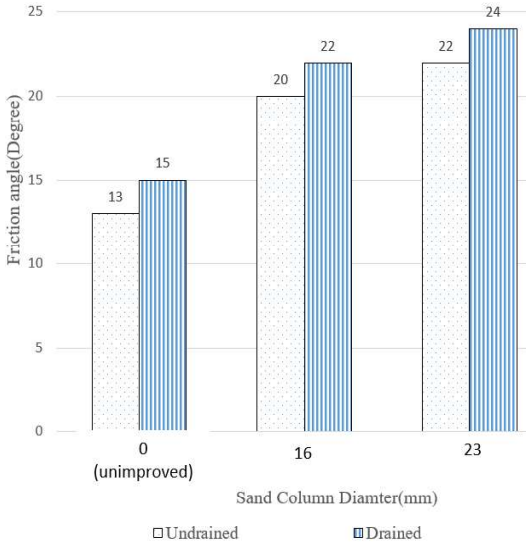

Fig. 7 Variation of friction angle with Column diameters

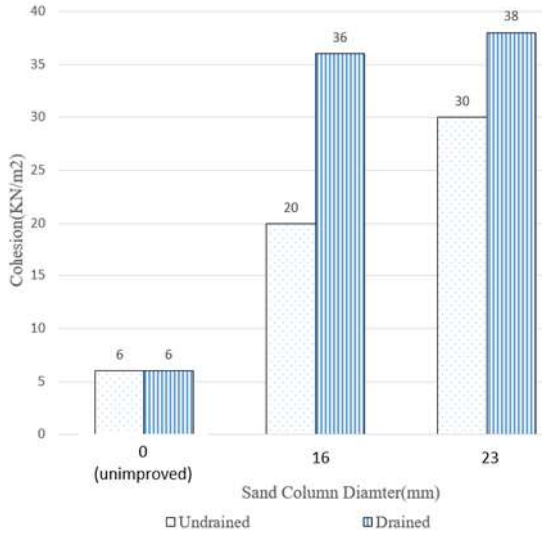

Fig. 8 Variation of cohesion with Column diameter

4 CONCLUSION

This research study was conducted to achieve mainly two objectives. One was to investigate the effect of pre-consolidation pressure of surrounding soft soil on the strength-deformation characteristics of gravel compaction pile improved composite ground. The second objective was to investigate the effect of length of gravel compaction pile on the strength-deformation characteristics of gravel compaction pile improved composite ground. Based on the series of laboratory experiments, following conclusions can be drawn;

1) Pre-consolidation pressure does not significantly affect to the undrained shear strength parameters of composite ground.
2) Pre-consolidation pressure and effective friction angle have inversely proportional relationship (i.e. drained friction angle decreases with the increase of preconsolidation pressure).
3) On the other hand, effective cohesion increases with the preconsolidation pressure.
4) Undrained and effective strength parameters have inversely proportional relationships with sand compaction pile lengths, i.e. increase the pile length decreases the shear strength parameters or other hand when the pile length is minimum the shear strength of the composite soil is maximum.

Consolidated drained test should be carried out in the future for further study. Here in this research study, two lengths of sand compaction piles were used. If we use more lengths of sand compaction piles, clear and accurate results can be predicted. Recommend to carried out tests using ABC material as column raw material due to ABC material is used frequently in the construction industry. In this research study, stability check of the composite sample was not considered. Therefore, stability check of composite ground with the sand pile lengths should be done.

REFFERENCES

BARKSDALE R. D and BACHUS R. C. Design and Construction of Stone Columns, Vol. I. Federal Highway Administration, Washington, DC, 1983, Report No. FHWA/RD-83/026.

CHARLES J. A. and WATTS K. S. Compressibility of soft clay reinforced with granular columns. Proceedings of the 8th European Conference on Soil Mechanics and Foundation Engineering, Helsinki, 1983, 1, 347–352.

GUNG-XIN L., HUANG W.-F. and UGAI K. Interactions between column inclusion and surrounding soil in composite ground. Institute of Lowland Technology, Saga University, Japan, 2000, 2, No. 1, 23–34.

SIVAKUMAR V., MCKELVEY D., GRAHAM J. and HUGHES D. Triaxial tests on model sand columns in clay. Canadian Geotechnical Journal, 2004, 41, No. 2, 299–312.

BARKSDALE R. D and BACHUS R. C. Design and Construction of Stone Columns, Vol. II: Appendixes. Federal Highway Administration, Washington, DC, 1983, Report No. FHWA/ RD-83/026.

Variation of Shear Strength Characteristics of Sri Lankan Residual Soils

D.M.S.W. Dissanayake and N.H. Priyankara
Department of Civil and Environmental Engineering, University of Ruhuna, Sri Lanka

ABSTRACT: By cause of significant rainfall account for the changes in climatic conditions, rainfall-induced landslides have resulted frequently within Sri Lanka where most of the slopes are made of residual soils. The complex behaviour and limited studies on unsaturated residual soils have led to difficulties of effective mitigatory actions for slope instabilities. Thus, from this research study, fundamental characteristics of unsaturated residual soils and their relationship in between were developed. Using the collected residual soils, Soil Water Characteristic Curve and Permeability function were developed by conducting series of laboratory tests using tensiometer method and variation of shear strength parameters over moisture content were developed using direct shear tests. The developed curves were compared with empirical models. Results illustrated the cohesion and friction angle were increased up to optimum moisture content and reduce after with the increase of saturation. Permeability was higher under lower suctions. Analysis showed the reduction of Factor of Safety with the continuation of rainfall and with the increase of rainfall intensity.

KEY WORDS: Matric suction, Soil Water Characteristic Curve (SWCC), Tensiometers, Direct shear

1 INTRODUCTION

Slope stability problems during wet season carried by rainfall induced lands slides is an issue for most of tropical countries including Sri Lanka. In Sri Lanka, most of the slopes are made of residual soils and current solutions for slope failures can't be considered as economical and accurate. In dry season where the soil is in unsaturated state, due to additional shear strength provided by negative pore water pressure or matric suction, natural as well as cut slopes have higher stabilities. But in rainy season due to water infiltrate in to air voids of unsaturated soils, matric suction within the soil will be reduced. Therefore, due to the additional strength loss slope will fail. Hence study of unsaturated residual soils is a need for country's issue. Thus, there is a need of proper understanding about the behaviour of shear strength of unsaturated soils during rainy season with the change of matric suction.
Hence from this research study a relationship in-between matric suction and shear strength was developed and slope stability analysis model was created.

2 LITERATURE REVIEW

According to Fredlund and Rahardjo (1993), unsaturated soil has four phases as soil, water, air, air-water interface/contractile skin. Hence are completely different from saturated soils. Contractile skin is the air water interface which acts like an elastic membrane. It has the ability to exert a tensile pull which is called the 'surface tension'. In unsaturated zone of soil pore water pressure is determined by capillarity and also called as tension or "Matric Suction". Matric suction is the difference of pore air pressure (U_a)and pore water pressure (U_w).

Most convenient way to understand the behaviour of unsaturated soil is using SWCC which is the relationship of matric suction and volumetric water content. Volumetric water content can be taken from the gravimetric moisture content using the following equation,

$$\theta_w = \omega \frac{\rho_d}{\rho_w} \quad (1)$$

Where, $\boldsymbol{\omega}$ is Gravimetric moisture content, $\boldsymbol{\rho_d}$ is Dry density of soil and $\boldsymbol{\rho_w}$ is for Density of water
According to the situation the soil is facing it has two curves as wetting and drying. Figure 1 below shows a typical SWCC. There are two important terms which can be found from the SWCC,

- Air Entry Value (AEV) – point of air starts to enter soil replacing water

- Residual zone – where only chemically bounded water is present

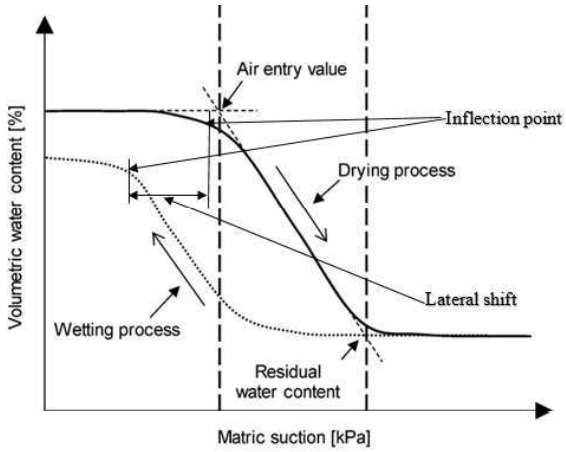

Figure 1: Typical Soil Water Characteristic Curve (www.semanticscholar.org)

According to the available literature related to unsaturated soils and SWCCs accounts for following hysteresis nature of dying and wetting curves.

- The contact angle for wetting is larger than that of drying
- The presence of entrapped air bubbles during soil wetting
- Ink bottle effect of soil pores

The larger contact angle of soil-water interface during wetting path results in reducing the suction at that particular degree of saturation as the value of cosine of the contact angle decreases with increasing contact angles. The entrapped air bubbles which are present as a result of the ink- bottle effect causing from non uniformity in shape and sizes of interconnected pores, eventually dissolve with water. This results in producing a lower suction during wetting path, compared to drying path. Therefore, wetting curve will be left shifted.

In order to obtain the variation of matric suction during shearing, Jotisankasa et al (2010) and Kankanamge et al (2018) had used a tensiometer connected to the top cap of a shear box. From that a relationship between matric suction and shear strength had been made. Also, had identified the change of apparent cohesion with matric suction. All these relationships had shown nonlinear variation even with different regression values.

3 METHODOLOGY

After the sample collection physical properties were found using basic tests. Then SWCC was developed using tensiometer method and was compared with two empirical models. In order to get continuous tensiometer readings and weight measurement an Arduino setup was used.

Figure 2 and 3 shows the set up used to obtain SWCC. For drying curve, a fully saturated sample was allowed to dry in air until it become fully dried. For wetting curve, a fully dried sample was continuously wetted until it become fully saturated. The base method used was the method outlined by prof. Apiniti Jotisankasa, Jotisankasa et al (2010). Three tensiometers were connected to the sample on three elevations.

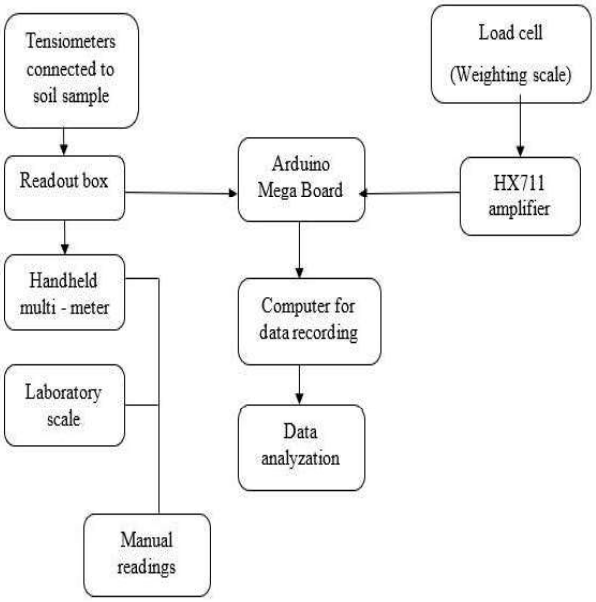

Figure 2: Component connection to obtain SWCC

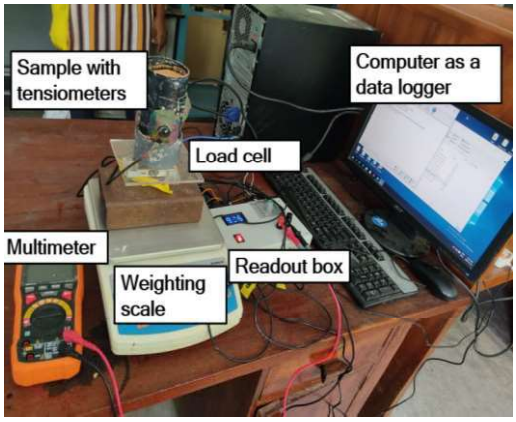

Figure 3 : Setup used to obtain SWCC

In order to obtain shear strength parameters series of direct shear tests were carried out using automated direct shear apparatus by changing saturation of an equal mass of soil. Suction of each soil sample was measured at the end of each test and relationship between matric suction and shear strength was developed. To obtain shear strength parameters of samples, moisture content was changed from 0% saturation to 100% saturation under six saturation levels as 0%, 20%, 40%, 60%, 80%, 100%. Each of sample was loaded with three Normal load cases, 12.73kN/m^2, 25.46kN/m^2, 38.197kN/m^2.

All tests were conducted under drained conditions with a shearing rate of 0.125mm/min according to Vasanthan (2015). Calculated amount of water was added to the base sample and moisture content at the beginning and end was checked. Permeability function was developed using the data collected from SWCC tests by incorporating them with following equations from literature.

$$\mathbf{i} = \frac{\mathbf{d}(\mathbf{z} - \frac{\mathbf{s}}{\gamma_w})}{\mathbf{dz}} \quad (2)$$

Where, **z** is elevation head of each tensiometer relative to the base of sample, **s** is matric suction and γ_w is unit weight of water.

$$\mathbf{v} = \frac{\mathbf{dV_w}}{\mathbf{Adt}} \quad (3)$$

Where, $\mathbf{dV_w}$ is change of volume of water in soil sample (can be calculated by change in soil mass), **A** is cross section area of sample and **dt** is elapsed time.

The value of permeability at any suction and volumetric water content can then be calculated by,

$$k = v/ i \quad (3)$$

k- Hydraulic conductivity

Then slope stability analysis was done using experimental results using SEEP/W and SLOPE/W softwares

4 RESULTS AND DISCUSSION

4.1 *Basic soil properties*

From the Sieve analysis test particle size distribution was obtained as 71% passing from 0.075mm sieve. With the help of basic property tests, according to Unified Soil Classification System (USCS), soil was classified as CL- Inorganic clay of low to medium plasticity. Table 1 shows the summery of the basic physical properties.

Table 1: Summary of Physical properties

Test	Parameter	Value
Saturation test	Fully saturated moisture content	70%
Specific gravity test	Specific gravity (GS)	2.602
Hydrometer analysis	Clay content (0.002mm passing)	30%
Atterberg limit test	Liquid Limit	49%
	Plastic limit	28%
Proctor compaction test	Optimum moisture content	21%
	Maximum dry density (kN/m^3)	14.75

4.2 *SWCC test results*

Figure 4 shows the obtained SWCC from the tensiometer method (wetting and drying) and from the empirical methods Arya- Paris and Zapata. For the comparison for both drying and wetting paths, curves related to middle suction data are considered here; as those two curves show lesser scattering.

For both wetting and drying curves shape of the SWCC came more relatable with the shapes of literature, but small scattering nature was obtained and can be related with the sensitivity of the Arduino set up.

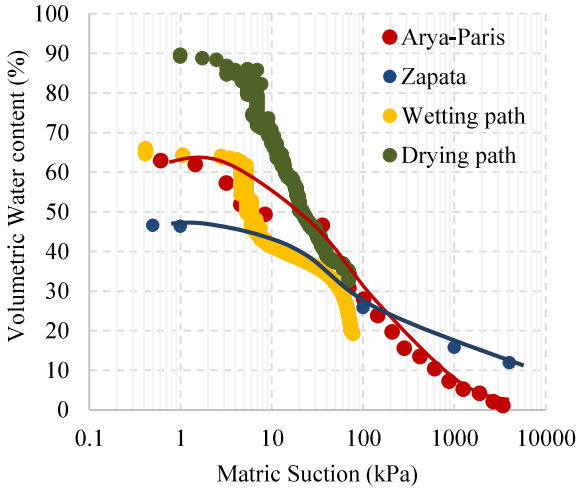

Figure 4: SWCC developed for the soil

Table 2 shows the important points found from obtained SWCC. Experimental curves and modelled curves are not completely tallying.

These two empirical methods were related to numerical equations and as the input parameters only particle size gradation and plasticity indexes were needed. Therefore, these can relate to a range of that particular type of soil.

Table 2: Important points of SWCC

Curve	Air Entry Point		Inflection point		Residual water content	
	Volumetric water content (%)	Suction (kPa)	Volumetric water content (%)	Suction (kPa)	Volumetric water content (%)	Suction (kPa)
Arya and Paris	60	4.01	60	4.01	3.5	1200
Zapata	45	3.9	45	3.9	-	-
Wetting path	65	4.2	65	4.2	-	-
Drying path	86	4.2	86	4.2	-	-

4.3 *Direct shear tests*

Figure 5 shows the variation of shear strength parameters; they increase and reach maximum values at optimum moisture contents (where it has the best particle arrangement) and then gradually decrease with the increase of saturation

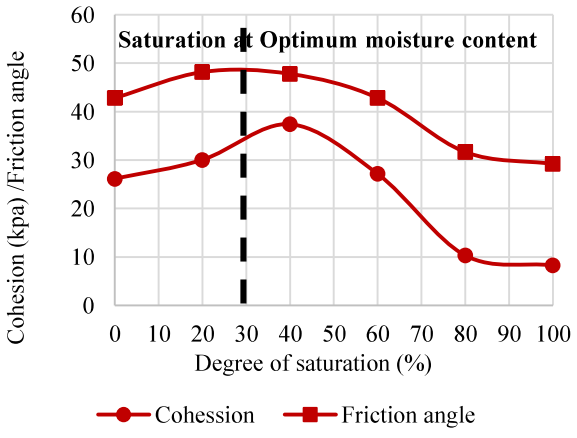

Figure 5: Variation of shear strength parameters

When the soil is fully dry, the compaction it can achieve is less hence lesser strength. But with the increase of moisture up to optimum moisture content, particles will well packed and will achieve its maximum shear strength.

Then further increase of the moisture from the optimum value will cause the flocculated structure to become dispersed structure causing loss of matric suction hence loss of its shear strength.

Figure 6 shows the relationship of cohesion and matric suction where cohesion increase with matric suction in a nonlinear way; where similar kind of results obtained by Jotisankasa et al., 2010 and Kankanamge et al.,2018.

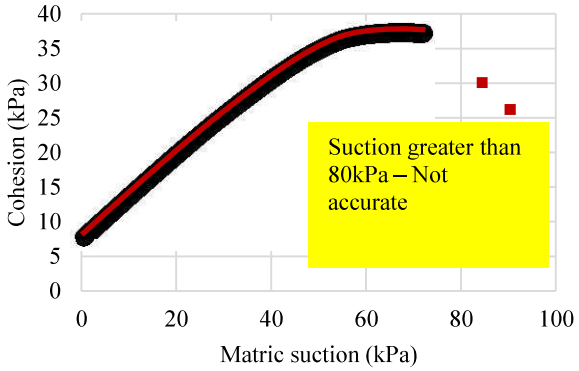

Figure 6: Relationship of cohesion and matric suction

1.1. *Permeability function*

Figure 7 shows the permeability function obtained.

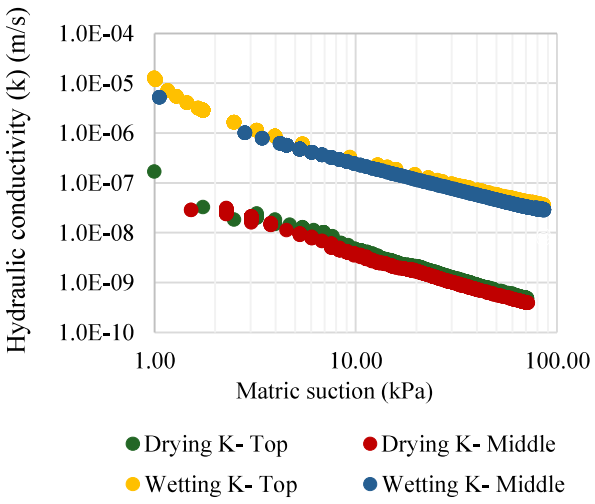

Figure 7: Permeability function

Permeability of the soil increase as it gets saturated gradually due to filling of the voids inside it. Therefore, at the beginning of wetting soil has lower permeability – water has plenty of voids to fill. When time passes and if wetting continued permeability will increase with the time.

The hydraulic conductivity decreases with increase of suction.

1.2. *Slope stability analysis*

As the initial condition, SEEP/W transient analysis was done without a rainfall on an imaginary slope consisting of two layers (Figure 8); residual soil-clay and weathered rock. For the material properties of the residual soil experimental results were given as follows.

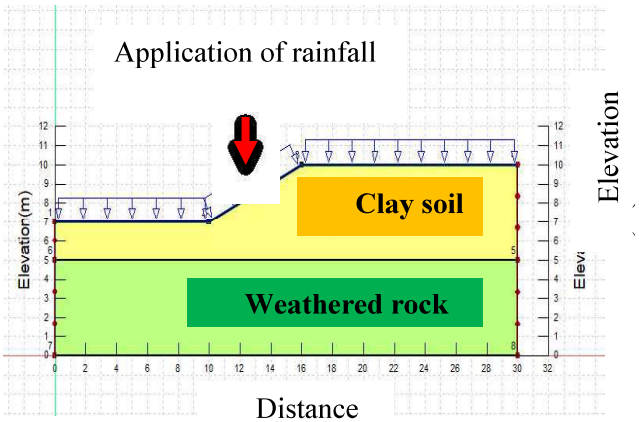

Figure 8: Slope geometry used for the analysis

- **Residual soil – clay**

  Soil properties (material parameters) were taken as saturated/ unsaturated condition.
  For the hydraulic functions - Permeability function and Volumetric water content function Drying middle tensiometer data were given as it showed less scattering than other experimental results.

- **Weathered rock**

  Material parameters were taken according to Kankanamge et al (2010) as saturated condition. And saturated permeability was taken as $1\times 10^{-9} m/s$

Then taking this initial analysis as a parental analysis, another transient analysis was done for the same slope for different rainfalls as, 25mm/day, 50mm/day, 75mm/day, 100mm/day ,200mm/day ,300mm/day. Rainfall was given for 7 days.
Then pore water pressure distribution for a selected section of the slope was obtained.

Figure 9 shows the pore water pressure variation obtained.

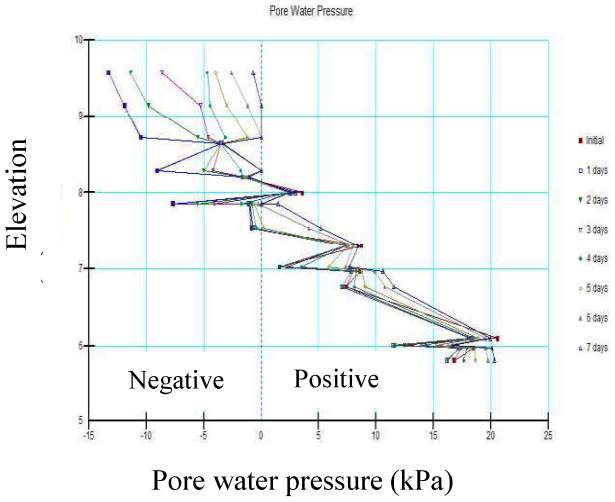

Figure 9: Pore water pressure distribution

From the pore water pressure distribution, it can be clearly seen that pore water pressure goes from negative values to positive values as the rainfall continue. It depicts why slopes are unstable during rainy season; due to loss of negative pore water pressure or matric suction slope losses its strength against falling.

Then for Slope stability analysis, second transient analysis of applied rainfall was used as parental analysis for a limited slope stability analysis. Spenser method was used using SLOPE/W software. Then factor of safety was obtained.

Figure 10 shows the results obtained from slope stability analysis.

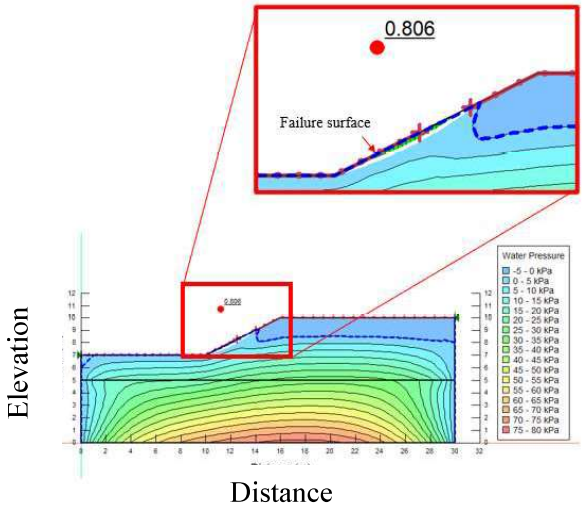

Figure 10: Results of slope stability analysis for 25mm/day

Factor of safety against time was plotted using the SLOPE/W software.

Following figure (Figure 11) shows the variation of factor of safety with the continuation of the rainfall.

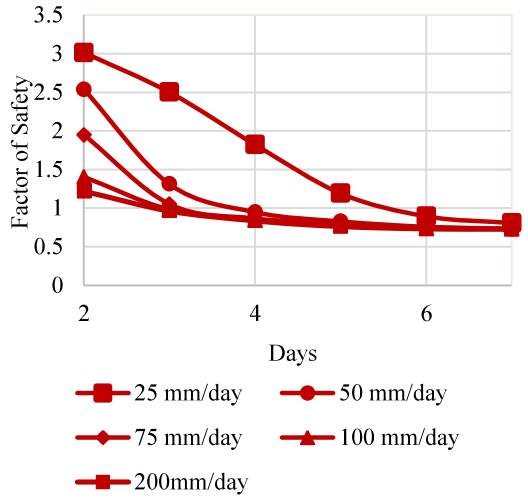

Figure 11: Variation of factor of safety

From the analyzed results of factor of safety (Figure 11) it is clear that with the increase of rainfall intensity slopes tends to be unstable in a lesser time period. Similar kind of results had been obtained by Kankanamge et al (2018).

5 CONCLUSIONS

Cohesion of soil decrease with the increase of saturation depicting that slope fail in wet season; shear strength of soil reduces as it gets more and more saturated. Friction angle also showed similar variation.

Obtained SWCCs from experimental data can be used as base data for an early warning system. Although both curves showed scattering nature due to the Arduino setup sensitivity, as both of the curves indicate field conditions; Wetting curve – soil get saturated indicating behaviour of soil mass during rainy weather conditions and Drying curve – soil getting desaturated indicating behaviour of soil mass during dry weather conditions, these data can be used for future analyses.

From the permeability function, permeability increases at lower suctions and decrease when suction increases. Here it can be concluded that water infiltrate more with the increase of saturation of the soil.

Modeled analysis of the experimental data further shows the reason of slopes fail during wet season with the continuation of the rainfall and with the increasement of rainfall intensity. Factor of safety decrease as the rainfall continues and also with the increase of rainfall intensity further showing the slope stability during rainy weather conditions. Further development of this analysis can be used for an accurate early warning system.

REFERENCES

1. Arya, L. and Paris, J., 1981. A Physicoempirical Model to Predict the Soil Moisture Characteristic from Particle-Size Distribution and Bulk Density Data. *Soil Science Society of America Journal*, 45(6), pp.1023-1030.

2. Estimation of Soil Water Characteristic Curves in Hong Jung < https://www.semanticscholar.org/paper/Estimation-of-Soil-Water-Characteristic-Curvs-in-Hong-Jung> (April.8,2021)

3. Fredlund, D.G. & Rahardjo, H., 1993, Soil mechanics for unsaturated soils, John Wiley & Sons Inc.,Newyork

4. Jotisankasa, A., Tapparnich, J., Booncharoenpanich, P., Hunsachainan, N. and Soralump, S., 2010. Unsaturated Soil Testing for Slope Studies. < http://www.gerd.eng.ku.ac.th/Paper/Paper_Other/SlopeConference2010/27_Unsaturated%20Soil%20Testing_Jotisankasa.pdf> (Aug.12,2020)

5. Kankanamge, L., Jotisankasa, A., Hunsachainan, N. and Kulathilaka, A., 2018. Unsaturated Shear Strength of a Sri Lankan Residual Soil from a Landslide-Prone Slope and its Relationship with Soil–Water Retention Curve. *International Journal of Geosynthetics and Ground Engineering*, 4(3).

6. Kankanamge, L., Karunarathna, S.W.B.S., Kulathilaka, S.A.S., Bandara, K.N. (2010). "Rainfall induced Shallow Landslides in Sri Lanka: Development of Rainfall Thresholds Using the Fundamentals of Unsaturated Soil Mechanics" <https://www.researchgate.net/publication/338447883_Rainfall_Induced_Shallow_Landslides_in_Sri_Lanka_Development_of_Rainfall_Thresholds_Using_the_Fundamentals_of_Unsaturated_Soil_Mechanics > (April.8,2021)

7. Vasanthan, N., Idirimanna, N. and Kulathilaka, S., 2015. Establishment of Fundamental Characteristics of Unsaturated Sri Lankan Residual Soils. <http://dl.lib.mrt.ac.lk/handle/123/11673> (Jul.20,2020)

Shear Strength Characteristics of Municipal Solid Waste in Meethotamulla Dump Site

M.A.G.P. Perera and N.H. Priyankara
Department of Civil and Environmental Engineering, Faculty of Engineering, University of Ruhuna, Hapugala, Galle

ABSTRACT: Disposal of Municipal Solid Waste (MSW) has become a serious problem in all over the world which is influenced by the rising population and rapid urbanization. Most of the developing countries have tended open dumping as a waste disposal method and due to the higher valuation of prime lands, open dumps are expanded in vertical direction. Therefore, physical, chemical and shear strength properties of MSW are timely important to overcome stability failures of the dump sites during the operational period and after the closure of the dump sites. In order to represent the aging effect of MSW, waste samples were extracted from Meethotamulla dump site at different depths. The shear strength parameters of MSW were analyzed using Direct shear test which was conducted at the different moisture contents and dry densities. The obtained results revealed that MSW experience a higher friction angle due to presence of soil aggregates and fabric.

KEY WORDS: Cohesion, Internal Friction Angle, Municipal Solid Waste, Open Dump Sites, Shear Strength, Waste Composition

1 INTRODUCTION

In United State of America, 54% of solid waste is being landfilled and in Japan, there is a higher trend of incinerating solid waste, using advanced technologies (Reddy et al., 2008). The best example for open dump sites in developing countries is the world's largest garbage mound in Indonesia, which is considered as a ticking time bomb. This is a clear indication that due to absence of advanced technologies and a higher amount of cost requirement; open dumping is the most popular method of waste disposal in developing countries like Sri Lanka.

Usually, open dump sites receive all types of heterogeneous solid waste, consists of biodegradable waste, non-biodegradable waste and residual fines from the municipal areas without sorting (Nawagamuwa et al., 2013). Due to the decomposition of biodegradable solid waste, settlement would be induced during the operational stage of the dump sites which is directly affected by the stability of the garbage mounds. In addition, due to scarcity of land and higher demand for prime lands around Colombo municipal area, the existing dump sites are expanded in the vertical direction. Therefore, proper planning and monitoring is essential to overcome the disasters and failures of garbage mounds.

There was a sudden failure of Meethotamulla dump site in 2017 which affected the surrounding environment, destroying human lives, public property and several infrastructures at the South-Western side of the garbage mound (NBRO, 2017). Such incidents clearly illustrated that it is necessary to follow proper technical procedure to maintain solid waste dump sites. The assessment of the current stability condition, planning closure of the open dump sites and converting them to public parks, requires physical, chemical and engineering characteristics of solid waste. Further, these parameters are varying with time due to degradation of solid waste.

Although a number of international researches were conducted to find out the geotechnical properties of MSW, very limited number of researches in Sri Lankan context were performed on the ageing effect. As a result, this research was conducted to determine the physical, chemical and shear strength properties of MSW in Meethotamulla dump site, considering the ageing effect.

Fig. 1 Meethotamulla dump site after failure

2 LITERATURE REVIEW

According to Reddy et al., 2008, research study conducted on finding geotechnical properties of MSW in Orchard Hills Landfill, USA, cohesion varies in the range of 31-64kPa and drained friction angle varies in the range of 26^0-30^0. The variation of shear stress over shear strain under different normal stresses of MSW in USA is illustrated in Figure 2.

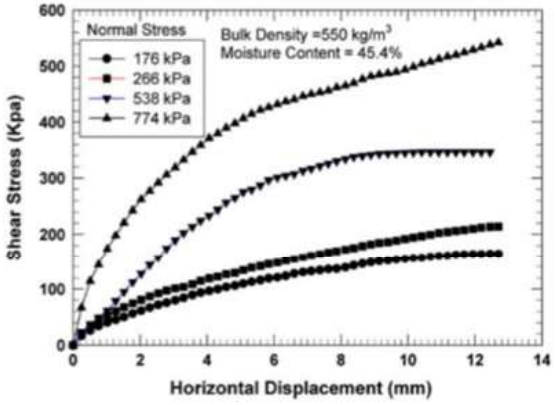

Fig. 2 Test results of Direct Shear test (Reddy et al., 2008)

In Sri Lankan context, these shear strength parameters are in different ranges due to the various consumption patterns, disposal methods and climatic changes. Cohesion varies from 10-25kPa and angle of friction varies from 18^0-21^0 for MSW in Colombo Municipal Council area (Nawagamuwa et al., 2013). Based on the results of Balasooriya et al., 2015, cohesion and angle of friction varies from 14-49kPa and 21.8^0-49.7^0 respectively for MSW in different regions of Sri Lanka. The variation of shear stress over shear strain under different normal stresses of MSW in Hambantota is illustrated in Figure 3.

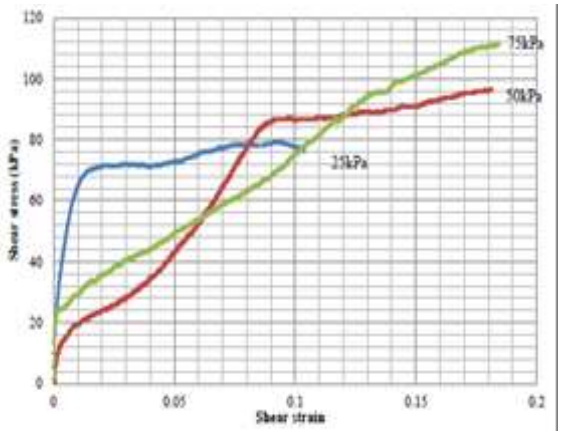

Fig. 3 Direct shear test result for same sample (Balasooriya et al., 2015)

3 METHODOLOGY

3.1 *Collection and Preparation of Samples*

Waste samples were collected from the Meethotamulla dump site during the restoration phase. Four number of disturbed waste samples were collected from Meethotamulla dump site at four different depths to represent the aging effect of MSW. After air-drying the extracted samples, they were laid on the dry concrete surface and large debris were subdivided into small parts. The procedure of reducing the samples was carried out according to the quartering method and 5-10kg of samples were taken to the laboratory experiments.

3.2 *Physical and Chemical Properties of MSW*

Initially, compositions of waste materials were determined for each sample and then particle size distribution was checked using Sieve Analysis test. In order to determine the Specific Gravity and Compaction characteristics of MSW, Pycnometer test and Automated Proctor Compaction test were performed. pH, Electric Conductivity and Volatile Organic content were determined using Glass-electrode pH meter, Electrical conductivity sensor of pH meter and Muffle Furnace.

3.3 *Shear Strength Properties of MSW*

Samples were prepared for the direct shear test to obtain the shear strength parameters based on the results obtained from the Standard Proctor Compaction Test. This test was carried out according to the ASTM D3080 which is equivalent to JGS 056. The maximum particle size for the direct shear test was selected as 9.5mm. A constant strain rate of 0.125mm/min was used to shear the sample at different normal stresses of 25kPa, 50kPa and 75kPa. For each normal load, variation of shear strain, shear stress and vertical displacements were recorded in the data logger attached to the direct shear apparatus. The Automated direct shear apparatus used for the test is shown in the Figure 4.

Fig. 4 Automated Direct Shear Apparatus

4 RESULTS AND DISCUSSION

After performing the laboratory experiments, physical, chemical and shear strength properties of MSW were determined considering the aging effect. The obtained results were analyzed as below.

4.1 *Physical Properties of MSW*

4.1.1 *Waste Composition*

The comparison of waste composition with aging is shown in Figure 5.

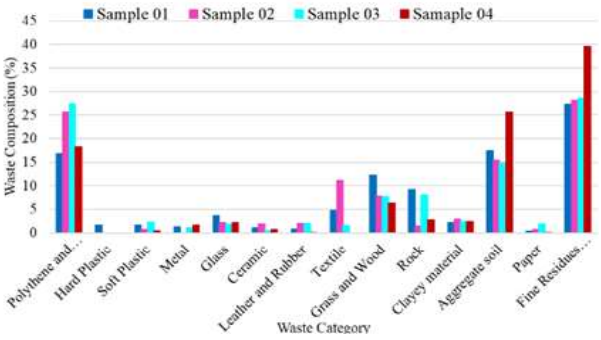

Fig. 5 Composition with Aging

The largest portion of the waste materials is consisted of aggregate soil, fine residues and polythene and pet bottles. Sample 04 which is having the bottom waste consisted with more fine residues (Particle size<9.5mm) than the other samples and percentage of fine residues is increasing with the depth. Due to the decomposition of organic waste materials, fine particles can be accumulated at the bottom of the garbage mound. When extracting waste from the several depths, cover soil layers which are used to reduce animal attraction, bad odor and displeasing view of open dumps, can be easily mixed with the waste materials. These are the possible reasons for having the large amount of aggregate soil and fine residues.

4.1.2 *Particle Size Distribution*

The particle size distribution curves for different waste samples are illustrated in the Figure 6.

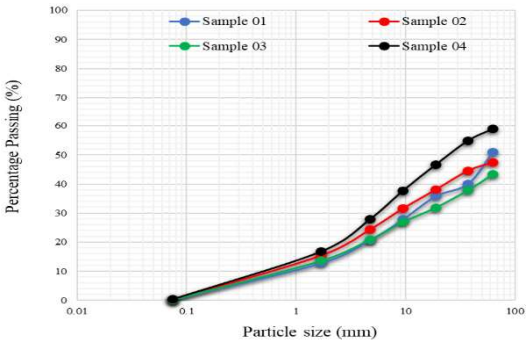

Fig. 6 Particle Size Distribution Curves for Four Different Samples

It can be observed that more than 40% of the particle sizes are greater than 63mm and it includes most of the elongated, large debris such as polythene, pet bottles, hard plastics, metal, glass, ceramic, leather, textile, yard waste, wood, clayey materials and rock etc.

4.1.3 *Specific Gravity*

It can be noted that specific gravity values are greater than 2.0 and they are considerably high as the most of the waste materials were mixed with soil. Also, it is a noticeable factor that specific gravity values are increasing with the depth and this was proven through another existing researches done by Piumali et al., 2017.

4.1.4 *Bulk Unit Weight*

Based on the results, it can be seen that bulk unit weight gradually increases with the depth. However, average bulk unit weight of the MSW of Meethotamulla is about 5.1 kN/m^3.

4.1.5 *Saturated Moisture Content*

Saturated moisture content of MSW is between the range of 350-400%.

4.2 *Chemical Properties of MSW*

4.2.1 *pH Value*

pH values of all samples are greater than 7.0. It means that these waste materials show the behavior of base. But usually, fresh MSW shows the acid behavior due to the higher number of acidic components such as chemicals, electric equipment and spoiled kitchen matters etc. But there were only decomposed waste materials and most of the waste portion could be visualized as aggregate soil, gravel and fine residues. Hence, the reason of base behavior of MSW is presenting the fully and partially decomposed waste materials.

4.2.2 *Electric Conductivity (EC)*

EC values are greater than 2.0 in top waste layers and they are considerably high. It means MSW shows the electric conduction properties. Also, the values obtained for the Electric Conductivity for MSW is decreasing with the depth of the dump site.

To verify these higher EC values of MSW, total ion concentration was determined. When preparing samples, it could be identified colour changing and after completing the experiment, there is a value for ion absorbance. Hence it can be concluded that MSW samples consist of metallic concentration to some extent.

4.2.3 *Volatile Organic Content*

It can be observed that all samples show same volatile organic content irrespective of the depth. and they were around 38-39%.

Summary of physical and chemical properties of MSW at different depths is shown in Table 1.

Table 1. Physical and Chemical Properties of MSW

Sample	Bulk Unit Weight (kN/m3)	Gs (Large particles)	Gs (Small particles)	pH	EC Value (mS/cm)	Volatile Organic Content (%)
1	6.22	2.16	2.10	7.54	2.96	39.1
2	4.78	2.20	2.16	7.60	2.03	39.0
3	4.28	2.24	2.21	7.39	1.81	38.8
4	8.19	2.25	2.23	7.61	1.17	38.7

4.3 *Compaction Characteristics of MSW*

Based on the results, it can be noted that the maximum dry unit weight is 11.2kN/m3 and the optimum moisture content is 38%. The variation of dry unit weight over moisture content is illustrated in Figure 7.

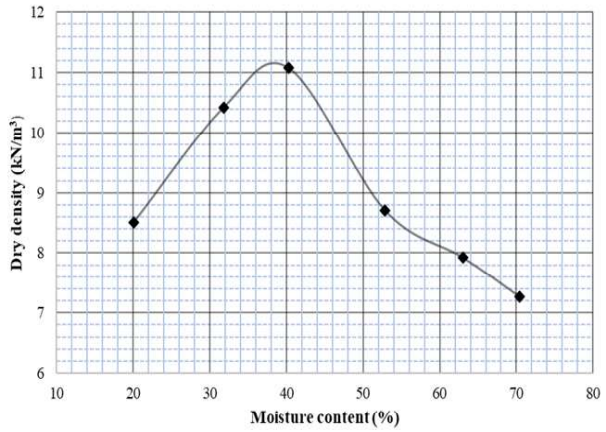

Fig. 7 Proctor Compaction Curve

4.4 *Shear Strength Properties of MSW*

Shear strength properties can be varied with time due to the biodegradation of MSW and it is affected on the stability of a garbage mound. Therefore, it is important to obtain the shear strength parameters of the MSW, considering the effect of aging.

In order to achieve this objective direct shear test was conducted on top and bottom waste samples, varying the moisture content and compaction. The aging effect is represented by using four different samples which were extracted from four different depths.

The samples were prepared based on the compaction curve developed as shown in Figure 7. 5 different samples were prepared for direct shear test representing w_{opt}±6%, w_{opt}±3% and w_{opt} where wopt is the optimum moisture content.

4.4.1 *Effect of Sample Preparation Method*

Waste is a heterogeneous material. When using different samples for the direct shear tests under a particular moisture content, properties of the samples would be varied due to the varying of composition of solid waste. Therefore, the compaction would be changed in preparing samples. It was reported that shearing at higher normal stresses results lower shear strengths due to the effects of pre-shearing in the previous loading stage.

In order to verify the effect of staged testing in MSW, direct shear test was carried out in two different cases; using same samples for shearing and using different samples for shearing. After testing under the lower normal stress, the same sample was re-sheared while increasing the normal stress. In this case properties of the waste materials would not be changed.

Then the second scenario was carried out, using separate samples for the shearing. In this case properties of waste may change due to the heterogeneous natures of the waste. The Figure 8 represents the comparison of shear stress Vs shear strain behavior for top waste at W_{opt}-6% (Sample 01) of moisture content. Due to the similar behavior of two different
scenarios, same samples were used for shearing at three different normal stresses.

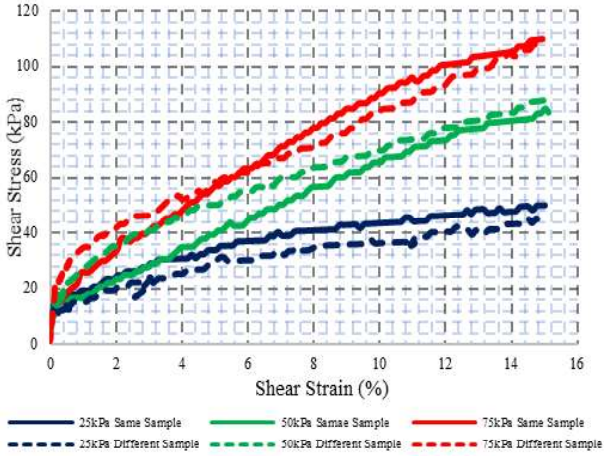

Fig. 8 Shear Stress Vs Shear Strain (Sample 01)

4.4.2 *Effect of Strain levels on Shear Strength Properties*

It can be observed that only the strain hardening behavior in waste. There was no any clear indication of strain softening behavior of waste.
Generally, in soil, it can be clearly identified the strain softening behavior. Therefore, the maximum stress can be obtained at a certain shear stain level. But in the case of waste only, the strain hardening was observed and hence it was decided to define different strain levels to develop failure envelop. It was considered 15%, 10% and 5% as the different strain levels to obtain shear stresses.

4.4.3 *Shear Strength Properties*

After obtaining the shear stress values at the three different strain levels, failure envelopes were developed between the shear stress and the normal stress. Then by developing failure envelops, shear strength parameters were calculated under different strain levels. The obtained cohesion varies from 9-27kPa and angle of friction varies from 17^0-54^0 within 5-15% of strain levels. Table 2 presents the summary of shear strength properties of the MSW.

When 15% shear strain level is used, the internal friction angles gave high values which tend to rock type nature. Therefore, 10% shear strain level is the most suitable strain level to get the shear stresses and Stark et al., 2009 also recommended the 10% of shear strain level for waste materials.

4.4.4 *Shear Strength Properties Vs Moisture Content*

The variation of Friction angle and cohesion with the moisture content at 10% of shear strain is shown in Figure 9. Cohesion is increasing and then decreasing with moisture for all the strain conditions. Friction angle is decreasing and then increasing with moisture for all the strain conditions.

4.4.5 *Dilatancy Behavior of MSW*

Dilatancy is the effect of swelling the waste sample while shearing. This effect was clearly observed at the higher normal stresses and the results of dilatancy behavior of top waste are illustrated in the Figure 10. According to the data presented, dilatancy angle is varied 5^0-10^0.

Table 2. Summary of Shear Strength Properties

Moisture Content (%)	Top Waste					
	15% strain		10% strain		5% strain	
	c' (kPa)	φ' (deg)	c' (kPa)	φ' (deg)	c' (kPa)	φ' (deg)
W_{opt}-6%	22	49.6	20	42.3	19	28.6
W_{opt}-3%	23	49.2	21	41.6	20	27.6
W_{opt}	13	48.8	12	39.8	11	27.1
W_{opt}+3%	11	52.7	10	45.0	9	33.3
W_{opt} +6%	10	54.0	9	46.4	12	34.5
Moisture Content (%)	Bottom Waste					
	15% strain		10% strain		5% strain	
	c' (kPa)	φ' (deg)	c' (kPa)	φ' (deg)	c' (kPa)	φ' (deg)
W_{opt}-6%	26	50.5	22	43.6	20	27.2
W_{opt}-3%	27	49.6	24	39.8	22	20
W_{opt}	24	46.5	22	38.6	19	16.5
W_{opt}+3%	23	51.3	20	45.0	18	33.7
W_{opt}+6%	20	53.1	18	46.7	16	38.6

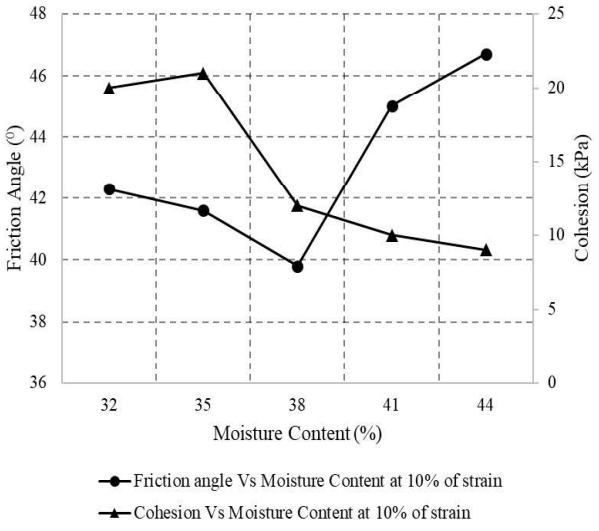

Fig. 9 Variation of Friction angle and Cohesion with Moisture Content

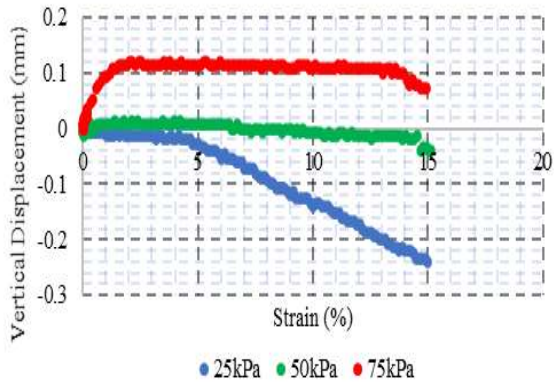

Fig. 10 Vertical Displacement Vs Shear Strain

4.5 *Effect of Fabric on Shear Strength Properties*

The effect of fabric on shear strength properties was reported by Yamawaki et al., 2016 by conducting series of laboratory tests. According to the Yamawaki et al., 2016, the relationship between shear strength and tensile strength gives by Equation 1.

$$T=N*\tan\phi + \tau(z)*l \quad (1)$$

T - Total shear resistance exerted on the failure surface (kN/m)
N – Normal Load applied on the failure surface (kN/m)
Φ – Internal friction angle (0)
τ(z) – Tensile resistance exerted on the slip surface (kN/m^2)
l – Considered length along the slip surface (m)

There is a clear relationship between tensile resistance and shear resistance, according to the Equation 1. Therefore, higher tensile resistance creates higher shear strength parameters. According to the results of Waste Composition, it was observed that there was a higher percentage of textile in MSW in Meethotamulla dump site. This is the main reason for obtaining higher friction in the MSW.

5 CONCLUSIONS

- pH values are greater than 7.0 because waste was fully decomposed.
- Specific gravity values are high due to the large composition of fine residues and they are increasing with aging.
- Electric conductivity of top waste is high due to the presence of metals and they are decreasing with aging.
- Shear strength properties are significantly high due to the presence of large amount of aggregate soil and textile. Fabric acts as a reinforcement material in solid waste due to the higher amount of tensile strength.
- The highest cohesion is obtained near to the optimum moisture content.
- The lowest internal friction angle is obtained after the optimum moisture content.

REFERENCES

Balasooriya, B. L. C. B., Priyankara, N. H., Alagiyawanna, A. M. N., Kawamoto, K. and Ohata, H. (2015). "Geotechnical properties of landfill solid waste in dry zone of Sri Lanka." In: proceedings of the International Conference on Geotechnical Engineering (ICGE-Colombo 2015), pp. 281-284.

National Building Research Organization Ministry of Disaster Management, (2017). "Meethotamulla Rehabilitation."

Nawagamuwa, U.P., Gunaratne, W. D. S. P., Kirubajiny, P., Thiviya, T. and Priyadharshana, H. K. A. (2013). "Study on the Geotechnical properties of Open dumps in Sri Lanka.", Vol. 0, No. 0.

Piumali, A. B. K.T., Saito, T., Priyankara, N. H., Alagiyawanna, A. M. N. and Kawamoto, K. (2017). "Characterization of physical, chemical and compaction properties of buries municipal waste at three dumping sites in Sri Lanka." In: proceeding Geomate Conference, pp. 343-350.

Reddy, K., Hettiarachchi, H., Parakalla, N., Gangathulasi, J. and Bogner, J. (2008). "Geotechnical properties of fresh municipal solid waste at Orchard Hills Landfill, USA." Waste Management, Vol. 29, No. 2, pp. 952-959.

Stark, T. D., Sarihan, N. H., Li, G., 2008 "Shear Strength of Municipal Solid Waste for Stability Analysis." Environmental Geology.

Yamawaki, A., Omine, K., Doi, Y. and Kawasaki, M., (2016). "Slope Stability of Solid Waste Layers in Japan and Asia." Modern Environmental Science and Engineering, Vol. 2, No. 1, pp. 23-30.

Moderately Loaded Structures Supported on Soil-Cement Columns

A.Yoganathan and N.H. Priyankara
Department of Civil and Environmental Engineering, University of Ruhuna, Sri Lanka

ABSTRACT: Construction on soft soil is one of the crucial task due to its unfavorable behavior. In order to improve soft soil, implementing the effective and economical method to overcome the problematic nature of soil has become more challenging. Installation of soil-cement column is one of the most efficient and economical method practiced in most of the countries. In this research, the effect on compressive strength due to effect of size, shape of the sample at different percentage of cement at different curing period were analyzed. To improve soft soil, rather than installing soil-cement column, in-situ mixing is also an effective way. Comparison of strength and the area improved through both methods have been investigated. At later part, laboratory model setup was prepared compensating the actual field condition using a scale down factor and maximum load and settlement the columns could bear were analyzed. From the results obtained it can be concluded that compressive strength increased with the size of the sample and strength obtained for in-situ mix sample is much greater than pre-cast sample

KEY WORDS: Soil-cement columns, Deep mixing, In-situ mixing, Pre-cast soil-cement columns, Stabilizing agent.

1 INTRODUCTION

Nowadays scarcity of land has enforced the Engineers to construct on soft soil. Due to unfavourable behaviour of soft soil, several methods have been practiced improving the soil. In order to construct moderately loaded buildings on soft soil, installation of piles would be an option to transfer structural loads to underlying hard stratum which is not an economical and efficient method. Therefore for thin soft soil layer thickness of 4 to 7m, to bear moderately loaded buildings, installing soil-cement columns by replacing pile will be much economical and efficient method which is been widely practiced all over the world.

However, this method is very rarely applied in Sri Lanka. Comparing with other stabilizing agents, cement is much economically and environmentally feasible agent as it could react with water in any soil as it does not rely on minerals prevailing in soil (Makusa, 2012). It is a general practice to check the mix proportions of soil-cement in the laboratory prior to implement in the field. As such effect of shape and size of soil-cement sample plays a major role in compressive strength (Talaat et al., 2020). Peat soil was used in this research where formation of peat occurs naturally at low temperature under anaerobic (Ahamed, Z., 2005). It is one of the problematic soils due to its unfavourable behaviour such as high compressibility, low bearing capacity, high water content and etc (Venuja et al., 2017).

1.1 *Objectives*

1. Investigate the effect of shape of the soil-cement sample on unconfined compressive strength.
2. Deformation behavior of soil-cement treated ground due to moderately loaded structures.
3. Investigate the secondary consolidation behavior of soil-cement treated ground.

2 METHODOLOGY

In order to accomplish the objectives, basic properties of peaty clay soil were investigated at first. To find the effect of shape on soil-cement sample, small cylinders (50×100mm), cube (150mm) and large cylinders (150×300mm) with different curing period (7,28 and 90 days) at different cement dosage (10%, 20% and 30%) were casted. To compare the load bearing capacity and the area improved in both in-situ and pre-cast soil-cement sample, a scale down dimension of the model setup and soil-cement columns were prepared compensating the actual soil-cement sample used in the field. Both hand and driller mixed sample were analyzed for in-situ mixing by connecting to augur. Thereafter an apparatus was fabricated to install the casted columns and to find the settlement and maximum

load it could bear. After load was applied, columns were extracted and analyzed.

2.1 *Casting soil-cement columns*

For each mix proportions, constituents were measured and whole mixture was mixed for about 10 to15 minutes with addition of water to cement ratio 0.5 using small mortar mixer for small cylinders and large mechanical mixer for cubes and large cylinder. Thereafter mixture was transferred into the prepared mold in three layers and tampered using tampering rod. Each layer was tampered for 25 times in order to remove the voids. Casted soil-cement samples are shown in figure 1.

Figure 1 Casted soil-cement samples

To investigate the load bearing capacity of in-situ and pre-cast soil-cement column, Using augur soil and binder was well mixed and in-situ soil-cement columns were prepared. For pre-cast soil-cement columns, 30% cement dosage was used as it gives more strength and as it is practiced in field. Casted soil-cement columns with size 25×265mm is shown in figure 2.

Figure 2 Casted soil-cement columns

2.2 *Fabrication of model setup*

A model ground was prepared considering the scale down factor using a cylindrical tube. To compensate the field setup compacted lateritic soil was placed at bottom representing the hard stratum. On top of hard soil layer peat was filled up to 265mm representing actual height of layer 6m. Prepared pre-casted sampled were installed in the model ground and augur was used in the model setup in order to prepare in-situ soil-cement columns. Thereafter steel box connected with loading frame was fabricated to install the prepared soil-cement columns. Similar procedure was followed to install soil-cement columns in the steel box. The model ground is shown in figure 3.

Figure 3 Model ground

2.3 *Method of loading*

After curing period, load was applied on samples. To find the compressive strength tri-axial setup was used for small cylinders and compression testing machine was used for cube and large cylinders.

3 RESULTS AND DISCUSSION

3.1 *Determination of basic properties*

Prior to addition of stabilizing agent, basic properties of peat were identified as listed in Table 1.

Table 1 Basic property of peat

Basic property	Value
Bulk unit weight	10.44 kN/m^3
Liquid limit	150%
Plastic limit	65%
Linear shrinkage	15%
Plastic index	85%
Organic content	69%
Saturated moisture content	481%
Specific gravity	1.87

3.2 *Unconfined compressive strength*

Based on the results obtained, it can be concluded that, unconfined compressive strength increases with the increase in cement content. Further curing period is attributed to the hydration of cement. As such, unconfined compressive strength of soil-cement mixture increases with the curing period. Variation of compressive strength with the effect of curing period and different cement percentage for the small cylinder, cube and large cylinder is shown in Figure 4.

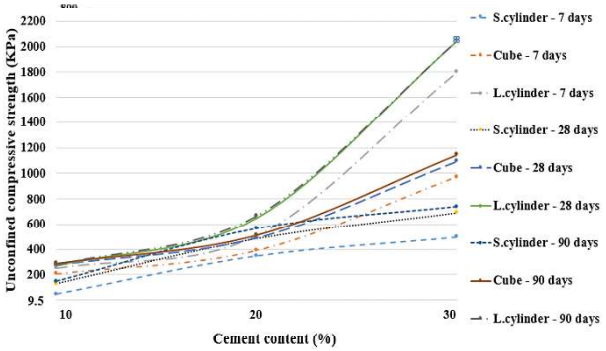

Figure 4 Variation of compressive strength with different curing period

This behavior is further explained with respect to the bar charts illustrated in Figure 5 to Figure 7. It can be observed that with increasing cement content, the unconfined compressive strength of soil-cement mixture increases irrespective of the size and shape of the sample. This increase in strength with increasing cement content is attributed to the hydration of cement on curing and filling of its product in the pores of the matrix thereby enhancing the rigidity of its structure by forming a large number of rigid bonds connecting clay particles. Compressive strength of cube samples stabilized by 20% and 30% cement is 1.79 and 4 times higher than the cubes stabilized with 10% cement and similarly for large cylinder, strength obtained with the addition of 20% and 30% cement is 2.3 and 7.5 times the cylinder stabilized with 10% cement respectively.

In a manner similar to that of concrete, the compressive strength of cement treated clay increases with time. The rate of increase of strength is generally rapid in the early stage of the curing period. Thereafter, the rate of increase of strength decreases with the time. When comparing compressive strength ratio obtained in 7 and 90 days with respective to 28 days, compressive strength obtained in 7 days is 0.75 to 0.85 times the strength obtained in 28 days and 1 to 1.1 times the 28 days strength has been obtained in 90 days, therefore even after 28 days small increment in compressive strength can be observed in soil-cement mixtures, unlike concrete. Strength ratio at 7 days and 90 days with respect to 28 days strength is shown in Table 2;

Table 2 Strength ratio of samples with respect to28 days strength

Shape	7 days	90 days
Small cylinder	0.72	1.12
Cube	0.8	1.04
Large cylinder	0.85	1.02

3.3 *Effect of shape and size on compressive strength*

3.3.1 *Variation of compressive strength between cube and large cylinder*

Along with curing period and cement content, effect of shape too plays a major role in compressive strength of the samples. For concrete samples, variation of compressive strength increases with the decreasing of the size of the specimen (Yakkali et al., 2015).Strength ratio obtained at different cement dosage between cube and large cylinder with respect to strength of large cylinder at 7, 28 and 90 days of curing period is illustrated in Table 3.

Table 3 Strength ratio between cube and large cylinder

Cement content (%)	Curing Period (Days)			Average
	7	28	90	
10	0.8	1.0	1.0	0.96
20	0.7	0.7	0.7	0.76
30	0.5	0.5	0.5	0.54

Table 3, it clearly shows that, with the increase of cement dosage the strength ratio between cube and large cylinder is decreasing. With addition of 10% cement compressive strength obtained between both sample is almost same. Based on above results, it can be concluded that cube specimens resist less in terms of vertical stress than that of cylindrical specimens when the curing period is larger.

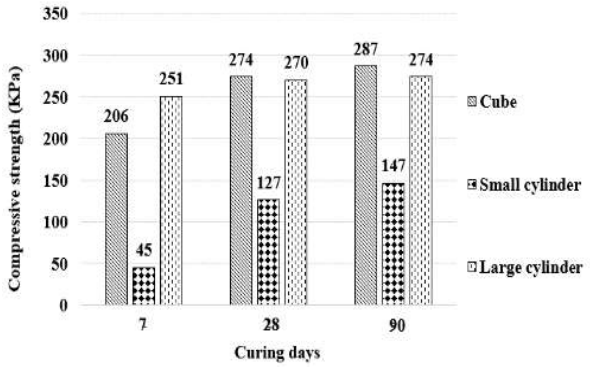

Figure 5 Variation of compressive strength at 10% cement dosage

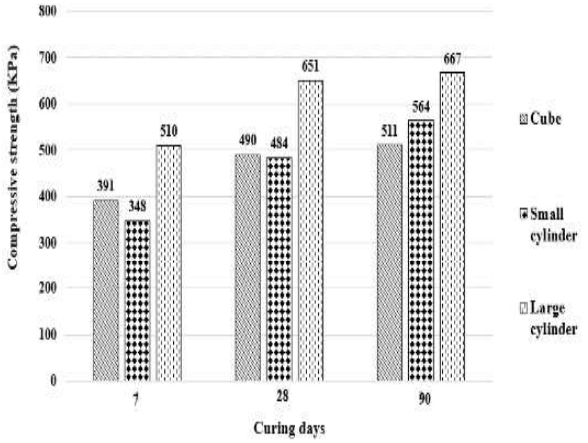

Figure 6 Variation of compressive strength at 20% cement dosage

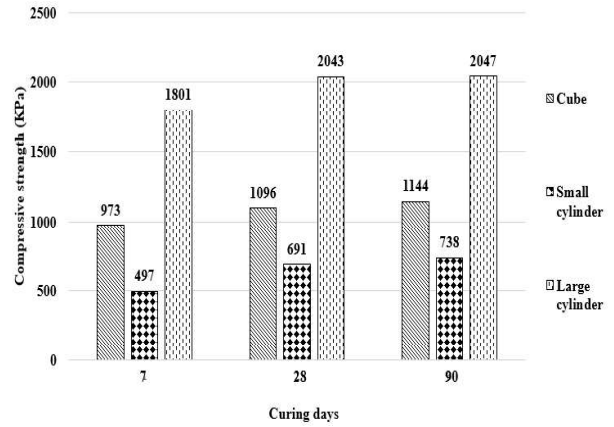

Figure 7 Variation of compressive strength at 30% cement dosage

3.3.2 *Variation of compressive strength between small and large cylinder*

Compressive strength ratio between small cylinder (50×100mm) and large cylinder (150×300 mm) after 7, 28 and 90 days at different cement dosage is depicted in Table 4

Table 4 Strength ratio between small cylinder and large cylinder

Cement content (%)	Curing Period (Days)			Average
	7	28	90	
10	0.2	0.4	0.5	0.37
20	0.7	0.7	0.9	0.76
30	0.3	0.3	0.4	0.33

It can be observed that large specimens indicate greater compressive strength than that of smaller specimens. Strength increment ratio due to addition of 20% cement with respect to 10% cement is about 2.8 in small cylinders whereas it is about 1.4 in large cylinders irrespective of curing period. An opposite behavior to above observations can be seen when 30% cement added to soft peaty clay. Strength increment ratio due to addition of 30% cement with respect to 10% cement is about 4.4 in small cylinders whereas it is about 6.5 in large cylinders irrespective curing period.

Even though the specimen shape is same and size is different, the slenderness ratio between these two sample is same which is equal to 2. However, based on the results obtained it can be noted that even under the same slenderness ratio under same soil-cement mixture, large specimens indicate greater strength than smaller specimens. This clearly indicates the importance of selection of correct sample size on specimen preparation to decide the mix proportion.

3.3.3 *Comparison of compressive strength of soil-cement mixture under different samples preparation method*

The comparison of the specimen shape and size on compressive strength is graphically presented in Figure 8 with respect to cube and cylinders.

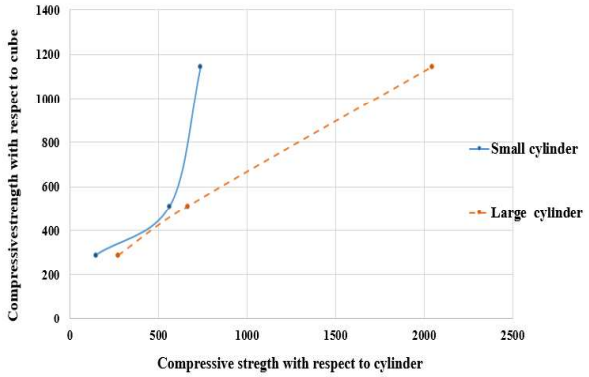

Figure 8 Comparison of specimen shape and size on compressive strength

The above behavior is further expressed with respect to average strength ratio as shown in Table 5 and Figure 9.

Table 5 Variation of strength ratio with different size and shape of the sample

Sample	Cement content		
	10%	20%	30%
Small cylinder vs Large cylinder	0.5	0.76	0.32
Small cylinder vs Cube	0.49	0.99	0.59
Cube vs Large cylinder	0.96	0.76	0.54

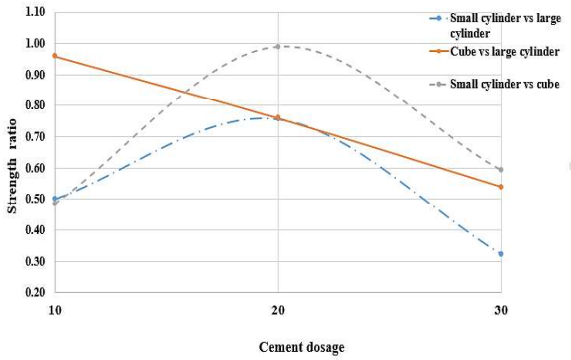

Figure 9 Variation of strength ratio with the effect of shape and size

When comparing the compressive strength obtained for small cylinder with both large cylinder and cube, variation is much similar, as shown in Figure 9. But linear variation can be seen when comparing the compressive strength obtained in cubes and large cylinders. When cement dosage increased compressive strength obtained for large cylinders increased more than cubes. When cement dosage is less, compressive strength of all three sample were almost same and at high dosage of cement significant effect on compressive strength was observed.

3.4 *Failure pattern*

After curing period, compressive strength was found. Here axial load was applied vertically, and the samples failed at maximum load. When the ultimate capacity of compression zone is reached the flexural failure occurred. In cubes fracture is provoked by the stress concentration near corner of the cubes and inclined micro cracks appear and merge near corner which intensify crack pattern. In cylinder crack pattern has occurred in vertical direction (Viso et al., 2008). Failure pattern obtained for small cylinder, cube and large cylinder is shown in Figure 10. This clearly indicates that crack pattern is sensitive to the shape of the sample.

Figure 10 (a) Crack pattern of small cylinders

Figure 10 (b) Crack pattern of cubes

Figure 10 (c) Crack pattern of large cylinders

3.5 *Comparison between in-situ and pre-cast soil-cement column*

The results obtained from both in-situ and pre-cast method is shown below in Table 6. From the results obtained, it can be concluded that strength resisted by driller mixed soil-cement sample is nearly 4 times the strength obtained by pre-cast sample and nearly 3 times the strength obtained by the hand mixed sample.

Table 6 Comparison of in-situ and precast sample

Data	Pre-cast	In-situ (Hand mix)	In-situ (Driller mix)
Maximum load	10 KN	13.9 KN	42.8 KN
Strength	0.58 MPa	0.81 MPa	2.48 MPa
Settlement	10.58 mm	18.08 mm	10.21 mm

After strength was applied, columns were extracted and the area improved were analyzed. A bulged shape column was obtained and more area was improved at middle part of the column in both hand and driller mixed sample.

3.6 *Loading on soil-cement column on treated ground*

After 6 columns were installed at equal space, load was applied via hydraulic jack. Figure 11 depicts the maximum settlement and load resisted by the columns.
By observing the results obtained, defect free columns were observed which resisted a maximum load of 525N at 10.7mm settlement, maximum strength applied on the columns were 62.5 KPa which shows that it could resist the load of a moderately loaded building.

4 CONCLUSIONS

Increase in population and urbanization has led the Engineers to even construct on soft soil. Therefore, installation of soil-cement columns will be one of the effective and economical way to improve soft soil. From the research it has been found that, with the increase of cement dosage and curing period compressive strength of soft soil can be increased. Compressive strength obtained after 7 days is 0.75 to 0.85 times than that of 28 days strength and 1.0 to 1.1 times the strength of 28 days is obtained after 90 days. Compressive strength obtained for cube is 0.96 times the strength obtained by large cylinder at 10% cement dosage. Therefore, compressive strength of large cylinder is greater than the cubes. Further it was found that larger the sample size has greater the strength. Strength of in-situ sample is 4 times the strength of precast sample due to more area improvement in in-situ mixing. Further it can be concluded that 6m columns could withstand the load of moderately loaded building. Further studies such as secondary consolidation behavior of the soil-cement columns by varying the pattern of installation should be analyzed in future.

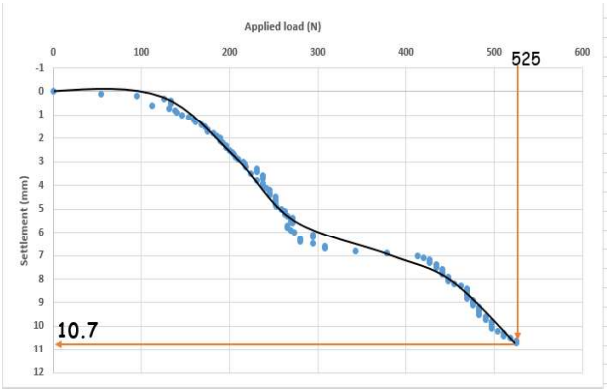

Figure 11 Applied load vs settlement

REFERENCES

Ahamed, Z., 2005. Compressibility and shear strength behaviour of peat soil in sarawak. *Faculty of Engineering, University of Malasiya Sarawak*, 24, pp.1-24.

del Viso, J., Carmona, J. and Ruiz, G., 2008. Shape and size effects on the compressive strength of high-strength concrete. *Cement and Concrete Research*, 38(3), pp.386-395

Makusa, G., 2012. SOIL STABILIZATION METHODS AND MATERIALS. *Diva-portal.org*, diva2:997144, pp.1-38.

Talaat, A., Emad, A., Tarek, A., Masbouba, M., Essam, A. and Kohail, M., 2021. Factors affecting the results of concrete compression testing: A review. *Ain Shams Engineering Journal*, 12(1), pp.205-221.

Venuja, S., Mathiluxsan, S. and Nasvi, M., 2017. Geotechnical Engineering Properties of Peat, Stabilized with a Combination of Fly Ash and Well Graded Sand. *Engineer: Journal of the Institution of Engineers, Sri Lanka*, 50(2), p.21.

Yakkali, S. and Reddy, D., 2015. Development of Compressive Strength Conversion Factors for Concrete. *International Journal & Magazine of Engineering, Technology, Management and Research*, (ISSN No: 2348-4845), pp.1-6.

Strength Mobilization in Quarry Dust Mixed Sri Lankan Dredged Clays in Early Curing

S.H.L.T. Priyankara and W.M.N.R. Weerakoon

Department of Civil and Engineering, University of Sri Jayewardenepura, Sri Lanka

ABSTRACT: Natural properties of dredged clay such as high-water content, high compressibility, and low strength are making them as unsuitable material for geotechnical applications. Therefore, the dredged soils must be pre-treated prior to application. In this study, quarry dust was chosen as a binder for stabilization because of its better interlocking properties, no hazardous constituents and high shear strength properties. Series of unconfined compressive strength tests and direct shear tests were carried out to investigate strength mobilization of quarry dust mixed non marine dredged clay during the early stages of curing from 1 hour to 28 days by varying quarry dust content as 10%, 20%, and 40% by volume. According to the results, the strength mobilization process can be divided into 3 stages; the first stage-within one day after curing, the second stage one day to 7 days, and the third stage 7 days to 28 days. The mixtures gained nearly shear strength of 100 kPa except for dredged clay with 10% mixtures by 28 days of curing. For samples cured from 7 to 28 days, the strength values obtained from both direct shear test (DST) and unconfined compression test (UCT) were compared and a fair agreement was identified.

KEY WORDS: Dredged clay, Quarry dust, Stabilization, Strength mobilization, Early curing

1 INTRODUCTION

Dredged soils are generally considered as soft clayey soils. A huge quantity of soil is dredged annually for the construction of infrastructures such as ports, navigation channels, coastal defense, and related activities such as land reclamation and beach nourishment. Dredged clay is often considered as problematic soil because of its low strength rendering in its naturally occurring condition. So, it is generally considered as a waste material that is disposed to the inland facilities. There are some issues related to disposing of dredged soil such as the high cost for construction of closed dumping facility, lack of closed dumping facilities, and various negative impacts on the environment. To minimize those issues, it is needed to have a sustainable solution that is capable of converting dredged soil into alternative green products for the construction industry.

Dredged soils cannot be directly use as a basement for construction projects since it has low shear strength and high compressibility which are the reason for majority of the problems encountered (Suaathi and Kaliannan 2016; Makusa 2015). Therefore, it is needed to stabilize the soil before application in the construction industry.

There are various binders used to stabilize the dredged clay, such as cement, lime, fly ash, steel slag, rice husk ash, etc. It is important to study strength mobilization at an early stage using those binder materials for various geotechnical applications such as determination of the thickness of the treated clay placed on submerged embankments or slope of manmade barriers as strength increases with curing time (Kang et al. 2015). However, studies on strength mobilization of dredged clay at the early curing stage are limited to few binder materials (Kang et al. 2015) such as cement and steel slag. Those binder materials have some drawbacks as soil stabilizers. These traditional binders especially the cement and lime production process generate around 7% of artificial CO_2 emissions, because of carbonate decomposition (Gartner 2004; Matthews et al. 2009). Another main issue is the cost of binder material (Pourakbar and Huat 2017). In order to overcome those issues, geotechnical Engineering researchers are more focused to find out sustainable materials for soil stabilization. Quarry dust can be considered as one of the promising sustainable stabilizing materials.

Quarry dust is a waste material generated from the aggregate crushing industry. Disposing of quarry dust is a generally difficult task due to various environmental and public health issues (Rahaman et al. 2013). Quarry dust's physical properties, chemical constitutions, and mineralogy vary with the aggregate type and production source but relatively consistent at quarry location (Wood and mark 1993 cited in Choudhary et al. 2015). Better interlocking properties of quarry dust are caused to enhance the strength of week soil (Anand et al. 2020; Onyelowe et al. 2012). Hence there are many studies to find out the applicability of quarry dust as a dredged clay stabilizer (Kiran et al. 2016).

Those studies mainly focused on shear strength parameters, CBR value, and index properties, etc. (Kanoo et al. 2014; Venkateswarlu et al. 2015a; Venkateswarlu et al. 2015b).

There are limited number of studies on the strength enhancement of dredged clay by using quarry dust. However, from those studies, it was identified that quarry dust can be used as an effective stabilization material. Priyankara et al. (2009) was investigated that when applied quarry dust percentage is more than 60% there is no significant variation in shear strength and 20%-60% identified as an effective range. Prakash and Paul (2016) also proved the strength enhancement ability of quarry dust with dredged clay. According to Onyelowe et al. (2012), dredged clay can be used as a road base material by strength improving with 30% quarry dust.

According to previous studies, it can be concluded that strength mobilization of dredged clay has not been studied with quarry dust in the early curing stages. So, this research aims to investigate Strength mobilization in quarry dust - mixed Sri Lankan dredged clays at early curing by using direct shear apparatus. This will help to determine the combination of clay and quarry dust which will lead to greater strength enhancement. It will be caused to enhance the reusing opportunities of two waste materials for engineering applications such as backfill materials, embankment, and sub-base in road construction, land reclamation, and other applications. This utilization will help to solve environmental problems and health-related issues arising from these two materials.

Due to the complexity of the solidification process which depends on quarry dust and clay properties, it is very difficult to predict the eventual strength of the quarry dust –clay mixture. As a result, detecting signs of eventual solidification early in the curing process would make laboratory mix tests and initial design easier as it facilitates conducting many shorter period trials without waiting for standard 28 -day curing.

2 METHODOLOGY

2.1 *Materials*

2.1.1 Dredged clay

Non-marine dredged clay obtained from the canal dredging process in Sri Lanka was used in this study as a dredged clay. They were dredged and then sieved through 425m to remove coarser particles and ensure homogeneity of the specimen. The clay was slurry in the sampling states, with water contents exceeding the liquid limits. Liquid limit, plastic limit and particle density ware measured. Physical properties of this non-marine dredged clay are summarized in Table 1.

Table 1. Physical properties of non-marine dredged clay

Property	Value
Liquid Limit	40.0%
Plastic Limit	22.7%
Plastic Index	17.3%
Specific Gravity	1.97

2.1.2 Quarry dust

Quarry dust were sieved through 4.75 mm sieve to remove the coarser particles and it will ensure the homogeneity of the prepared samples. Particle density is determined as 1828.41 kg/m^3.

2.2 *Sample preparation*

The mechanical test samples were prepared by combining various proportions of clay and quarry dust. The content of quarry dust (α) is expressed using a volume-based ratio, as follows:

$$\alpha = \frac{v_Q}{v_Q + v_c} \times 100\%$$

Where, v_Q is the volume of dry quarry dust and v_C is the wet non-marine dredged clay.

Quarry dust content (α), was used as, 10%, 20%, and 40%, in this research to investigate the influence of various quarry dust content on the strength of the quarry dust-clay mixture. To prepare specimens, the water content of a non-marine dredged clay sample was first increased to 1.5 times its liquid limit by adding water. Distilled water was added to the clay sample to maintain similar normalized water content as non-marine dredged clays. Then the required amount of quarry dust was added into the non-marine dredged clay, and it was mixed about three minutes by using a spatula. Until from 1 hours to 1 day curing time, specimen is prepared in the shear box having dimensions of a 100 mm x 100 mm x 25 mm in size for DST. For rest of curing times, after mixing, the quarry dust-mixed non marine dredged clay was poured into the cylindrical mold having similar dimensions and cure under room temperature. In addition to DST, specimens having dimensions diameter 50 mm and height 100 mm were prepared for unconfined compression test (curing time greater than 7 days).

2.3 *Laboratory testing methods*

The samples were remained in a very soft state, just after mixing. As the specimen was not strong enough to stand on its own, traditional laboratory experiments like unconfined compression tests

(UCTs) and triaxial compression tests were not performed at the early stage of curing. Hence, direct shear test was conducted according to the ASTM D3080/D3080M–11 for specimens prepared for curing periods varying from 1 hour to 28 days.
In this research, the shearing rate was kept at a constant value of 2 mm/min.

The UCT was carried out following ASTM D2166 for specimens prepared for 7 days – 28 days of curing. The applied loading rate was 2% per minute, and data on load-displacement was automatically logged for later analysis and processing.

3 STRENGTH MOBILIZATION

3.1 *Strength (S_u) mobilization with curing time*

Figure 1 shows undrained strength, S_u, mobilization at different quarry dust contents (10, 20, and 40%), with curing time, from 1 hour to 28 days. The strength mobilization was divided into few stages depending on the patterns in each series. The mobilization of strength can be divided into three phases. Even though a relatively higher strength mobilization is recorded by the 10% quarry dust mixed samples, no significant strength improvement was observed for first stage of curing, lasting approximately 1 day for the mixture. This stage could represent the initial solidification of clay in the presence of quarry dust. For steel slag-treated soils, a similar tendency was observed by Weerakoon (2018).

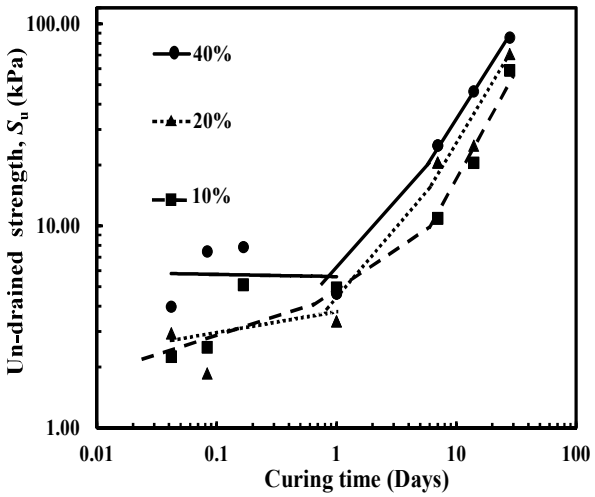

Fig 1- Strength (S_u) mobilization with curing time

The observed second phase period was approximately 1 to 7 days for all the quarry dust content at this stage. The strength suddenly increased and their strength values varied from 3 kPa to 25 kPa. Strength mobilization rates at this stage are higher than those are at the initial stage. However, the strength mobilization rate of 10% quarry dust mixture is relatively lower than other clay mixtures. So, shear strength values of 20% quarry dust mixture are exceeded than the relevant values of 10% quarry dust mixture.

Strength improvement in the third stage continued to a greater rate than in the earlier stages. It seems that at longer curing times, greater strengths can be detected. These progressively increased strength increment rates are coinciding with the investigation done by Weerakoon (2018) with steel slag and non -marine dredged clay. This increased strength increment pattern at longer curing periods did not change with the steel slag gradation. The similar tendency may be observed in the quarry dust mixed samples. The mixtures gained nearly 100 kPa except for dredged clay with 10% mixtures by 28 days of curing. According to this study, non-marine dredged clay produces sufficient strength for engineering applications.

3.2 *Strength mobilization patterns with Quarry dust content*

Shear strength was increased with the quarry dust content at each curing period as shown in Figure 2. The optimum quarry dust content was not identified for the strength development. This increasing pattern coincided with the results obtained by Sridharan et al. (2006). Addition of quarry dust caused to increase the interlocking with the dredged clay. But there was not considerable strength enhancement up to 1 day of curing. That means bond between non-marine dredged clay and quarry dust needs more than one day, to initiate the solidification process.

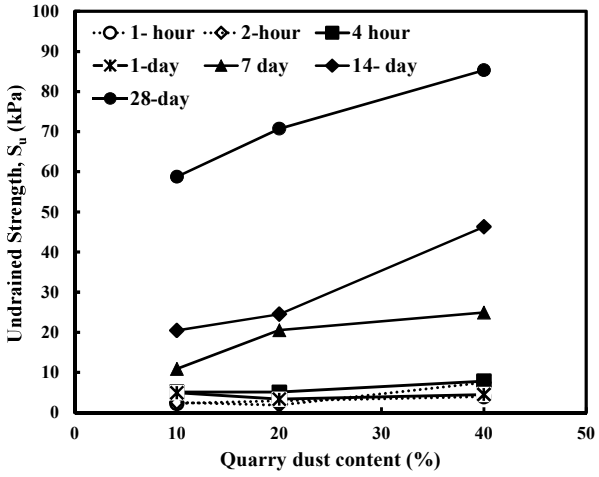

Fig 2- Relationship between Shear strength and Quarry dust content

3.3 *Comparison of strength obtained by direct shear test and unconfined compression test*

A comparison was made with the undrained strength values determined by the direct shear tests (DSTs) and undrained strength($q_u/2$) obtained by

the unconfined compression tests (UCTs) for a curing time of 7 to 28 days as shown in the Figure 3. S_u, measured from the DST is higher than that from the UCT for most of the data points. Since, S_u obtained from two types of tests were not match with the 1:1 ratio line, two deviation lines were introduced. The maximum deviation line within 122% difference was introduced for strength higher than approximately 15 kPa and the 80% deviation line for strength approximately lesser than 15 kPa.

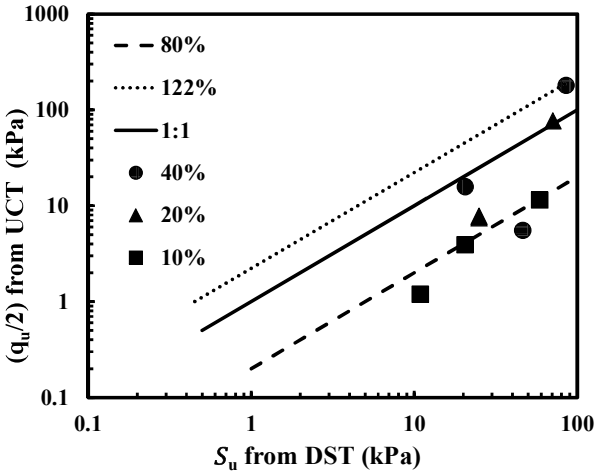

Fig 3- Relationship between strength obtained by direct shear test and unconfined compression test

Most of the data points match with the 80% deviation line. That is due to samples for UCT were remaining soft state during the curing period. Lack of hardness is mainly caused to reduced unconfined compressive strength at 7 days and 14 days curing time. So, S_u obtained from DST reached higher values than those from UCT. This tendency usually can be seen from samples with 10% of quarry dust content.

Some of the few data points which are having S_u approximately greater than 15 kPa are matching with the 122% deviation line. Here S_u obtained from UCT are greater than those are from DST. This scenario happens with curing times greater than 14 days and 28 days. Other reasons are the anisotropic properties of the specimens and the loading rates were different among the UCT and the DST which account for the UCT's systematically higher strength.

As a result, at low and high strength levels, the undrained strength determined by using direct shear and unconfined compression tests demonstrated a different degree of strength comparison agreement.

4 CONCLUSIONS

In order to eliminate waste products, this study looked at the nature of strength mobilization in quarry dust-mixed non-marine dredged clay by direct shear and unconfined compressive test for geotechnical engineering applications. The strength mobilization characteristics of dredged clay mixed with quarry dust were continuously investigated from 1 hour to 28 days of curing in this research with the use of direct shear apparatus since the direct shear test could be used on samples that are in a slurry state. Maximum shear strength values with the curing time could be seen from 40% quarry dust content while increasing the shear strength as increasing of quarry dust content. The mixtures gained nearly 100 kPa except for non-marine dredged clay with 10% mixtures by 28 days of curing. According to this study, non-marine dredged clay produces sufficient strength for engineering applications.

On the specimen cured from 7 to 28 days, the strength obtained using two separate test methods such as direct shear test (DST) and unconfined compression test (UCT) was compared. The strength obtained from a direct shear test and an unconfined compression test that is less than 15 kPa indicates fair agreement.

REFERENCES

Anjana Prakash and Anju Paul., (2016)., A Study on Stabilization of Marine Dredged Soil Using Quarry Dust, International Journal of Scientific Engineering and Research, 4:83–86.

Choudhary, A.K., Roy, N. and Sinha, A.K (2015) Utilization of Quarry Dust and Plastic Wastes in Highway Pavement Construction: Portland, Oregon 2015, Geosynthetics, pp 80–86.

Gartner, E., (2004)., Industrially interesting approaches to "low-CO_2" cements, Cement and Concrete Research, Cement and Concrete Research, 34:1489–1498.

Kang, G., Takashi Tsuchida and A.M.R.G. Athapaththu., (2015)., Strength mobilization of cement-treated dredged clay during the early stages of curing, Soil and Foundations, 55:375–392.

Kanoo, B., Das, S., Das, R. and Kalita, P.P. (2014), Quarry dust a promising geomaterial for improving the geo technical properties of soil.

Makusa,G.P. (2015). "Stabilization-Solidification of High-Water Content Dredged Sediments Strength, Compressibility and Durability Evaluations", Doctoral Thesis.

Matthews, H. D., Gillett, N. P., Stott, P. A. and Zickfeld, K., (2009)., The proportionality of global warming to cumulative carbon emissions. Nature, 459:.829–832.

Onyelowe Ken, C., Okafor, F. O. and Nwachukwu, D. G., (2012)., Geophysical use of quarry dust (as admixture) as applied to soil stabilization and modification-a review, Earth Sciences, 1: 6–7.

Pourakba, s. and Huat,B.K., (2017)., A review of alternatives traditional cementitious binders for engineering improvement of soils, International Journal of Geotechnical Engineering, 11:206–216.

Priyankara,N.H., R. M. S. D. Wijesooriya, S. N. Jayasinghe, W. R. M. B. E. Wickramasinghe and S. T. A. J. Yapa.,(2009)., Suitability of Quarry Dust in Geotechnical Applications to Improve Engineering Properties, Engineer,42:7–13.

Suaathi, A. and Kaliannan, P. (2016), "Light solidification of Kuala Perlis dredged marine soil via admixtures of GGBS – cement and sand: 1-D compressibility study", Doctoral Thesis.

Venkateswarlu, H., Prasad, D.S.V. & Raju, P., (2015)., Study on Behaviour of Expansive Soil Treated with Quarry Dust, International Journal of Engineering and Innovative Technology (IJEIT*)*, 4:193–196.

Weerakoon, W.M.N.R. (2018). "Characteristics of stiffness and strength mobilization in steel slag-mixed dredged clays from immediately after mixing", Doctoral Thesis.

Investigation of the shear strength characteristics of materials by experimental and numerical analysis

A.R.M.C.P.B. Amunugama, D.G.L.S. Kulasekara
Department of Civil Engineering, South Eastern University of Sri Lanka

ABSTRACT: The Eastern Province of Sri Lanka is a place where hard to find laboratory facilities. Research focuses on the investigation of the shear strength properties of materials by experimental and numerical analysis. The research group concentrated on developing a numerical model for specific tests and investigating soil properties. Further, laboratory tests were conducted under BS and ASTM standards to validate the Plaxis model. Plaxis was utilized to develop the numerical model and the numerical model leads to a significant reduction in the number of laboratory sessions. Direct shear, CBR, Proctor compaction, and PSD tests were conducted at the Geotechnical and Highway laboratories in the South Eastern University of Sri Lanka. That allows the constructors to continue their geotechnical testing inside the region without reaching outside for the geotechnical laboratories. Further, this leads to reduce time and cost of the constructor.

KEYWORDS: Direct Shear Test, CBR Test, Cohesion, Frictional angle, Shear Stress, Plaxis, Numerical Model

1 INTRODUCTION

1.1 *Research Problem*

The Eastern province is one of the rapidly emerging provinces heading towards aurora of development. Shear strength and physical properties are the prominent details required in the designing structures implemented on the soil. The availability of laboratory facilities in the Eastern Province is less than expected, and research on soil testing in the Eastern Province has not been conducted to a satisfactory level. The study mainly concentrated on investigations based on the shear strength and physical soil properties in the Eastern province in Sri Lanka.

1.2 *Aim*

Characterization of shear strength properties of loose soils in Eastern region in Sri Lanka.

1.3 *Objectives*

(i) Investigate the shear strength properties of soils by conventional and indirect laboratory tests.
(ii) Development of correlations for the determination of shear strength properties of soils.
(iii) Develop a numerical model for specific tests to monitor soil behavior and look for soil properties accordingly.

1.4 *Scope*

A software-based numerical model was developed using Plaxis software version 8.6 to determine the shear strength properties of loose soils in Eastern province, Sri Lanka. Samples were taken from the Galoya river bank and the coastal zone of the South Eastern University of Sri Lanka. The numerical model was validated from laboratory tests under BS and ASTM standards. All laboratory tests were conducted at the Geotechnical, Highway, and Materials Laboratories of Southeastern Engineering University, Sri Lanka.

1.5 *Significance*

The research allows reducing the effort on laboratory tests by introducing a reliable numerical model. When there is a significant amount of laboratory tests to perform, can be reduced the test frequency with the assistance of the numerical model. Also the cost of laboratory tests is significantly reduced.
This research outcome permits designers to follow BS and ASTM standards easily in the Eastern province.
This research allows performing easy observation of the shear strength of loose soils. Further will be supportive to the contractors who are practicing construction without suitable geotechnical assessments. Laboratory test results always depend on the laboratory apparatus and the operator's skill set. When the Eastern province is concerned, the availability of skilled operators is more or less than required. Furthermore, it can be operated as a training solution for the laboratory staff themselves to verify procedure is up to standards.

2 LITERATURE REVIEW

2.1 *Introduction*

Cohesion and the friction angle are defined as shear strength parameters of soils. Effective stress, drainage conditions, rate of strain, and heteromorphic conditions of soils represent different shear strength parameters (Roy & Bhalla, n.d.).

When concerned about soil failures due to shear, shear strength remains a vital factor in the design and construction. Knowledge and reliable data of a particular soil underneath must recognize before the project's initiation.

2.2 *Soils in Eastern Province*

The Eastern province of Sri Lanka consists of its identifiable significances considering the soil condition of the region. The geological considerations of the Eastern province belong to the Vijayan complex as categorized according to the geological map of Sri Lanka (A.Kröner, et al., 2013).

2.3 *Failure of Soils*

Soil failures are categorized into three particular failure modes, and these categories can be identified as a general shear failure, local shear failure, punching shear failure.

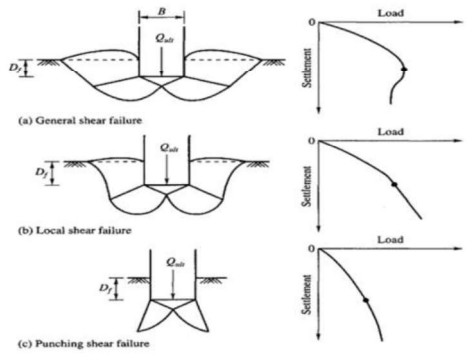

Fig. 1 Failure modes of soils (Eddybrbs, 2019)

2.4 *Bearing Capacity equations*

Terzaghi developed the equation in 1943 proposed by Prandtl in 1921. Further, he extended his theory to include the weight of soil and the effect of soil above the foundation on the bearing capacity of the soil strata.

The Terzaghi equation,

$$q_{ult} = cN_c + qN_q + \frac{1}{2}\gamma BN_\gamma (1)$$

For a circular footing,

$$q_{ult} = 1.3cN_c + qN_q + 0.3\gamma BN_\gamma (2)$$

For a square footing,

$$q_{ult} = 1.3cN_c + qN_q + 0.4\gamma BN_\gamma (3)$$

For a rectangular footing,

$$q_{ult} = cN_c\left[1 + 0.3\frac{B}{L}\right] + qN_q + \frac{1}{2}\gamma BN_\gamma\left[1 - 0.2\frac{B}{L}\right] \quad (4)$$

2.5 *Shear Strength properties*

Cohesion: The intermediate attraction between soil particles in the soil. When fines are prominent in the soil structure, it displays cohesive characteristics. Cementation, electrostatic and electromagnetic attraction, and primary valence bonding and adhesion are the main sources of cohesion between soil particles (Gautam, 2018).

Friction angle: Cementation, electrostatic and electromagnetic attraction, and primary valence bonding and adhesion are the main sources of cohesion between soil particles (Gautam, 2018).

2.6 *Numerical methods*

Plaxis 2D version 8.6 was utilized for numerical modeling of the soil characteristics. Plaxis is a computer program that allows the modeling of soil using a finite element analysis method. The Plaxis program defines soil behaviors using different soil models. Mohr-Coulomb model is elected for this study because it is frequently applied. Young's modulus, poisons ratio, cohesion, internal friction angle, and dilatancy angle was included as data for this step. Plaxis 2D comprises three steps; input, calculation, and output. In this study, a test model was developed utilizing the Plaxis software, and subsequently, it is verified by performing additional tests.

3 METHODOLOGY

Creating a numerical model for soils in the Eastern province in Sri Lanka was the target in this research. Primarily shear strength properties and some other relevant properties were obtained for the development of the model. These parameters were obtained using a series of laboratory tests. Soil samples were obtained from two different locations at Ampara district for laboratory testing. At least three separate tests were carried out to increase the accuracy of the results.

Initially, soils were classified by following the USCS classification system. Subsequently, soil index properties such as moisture content, liquid limit, plastic limit, and specific gravity were also identified using laboratory tests under ASTM and BS standards. Then shear strength properties were obtained using the direct shear test. Afterward, a proctor compaction test was performed to attain the optimum moisture content and maximum dry density. Further, the CBR test was performed for the samples according to the proctor compaction results.

Finally, a software-based model was developed for these two soils using the obtained data in Plaxis connect edition V20 software. Several parameters were obtained using existing literature due to the unavailability of necessary equipment. Comparison between CBR and numerical model values was performed to evaluate the model accuracy.

4 RESULTS AND DISCUSSION

4.1 *Introduction*

Laboratory tests and numerical analysis were performed in the line with research methodology.

4.2 *Laboratory test program*

4.2.1 *Index property tests*

Particle size distribution test:

The test was conducted for both sea sand and river sand samples. From that, the soil samples were classified according to USCS.

Pycnometer test for specific gravity:
Specific gravity was obtained for both river sand and sea sand

.

Table 1. Summary of specific gravities

Soil sample	Average specific gravity (Gs)
River sand	2.61
Sea sand	2.65

4.2.2 *Indirect strength property tests*

CBR test and proctor compaction tests were performed as indirect strength properties.

Proctor compaction test:

Table 2. Dry density and saturated density

Soil sample	γ_{dry}	γ_{sat}
River sand	16.32	19.97
Sea sand	15.91	19.63

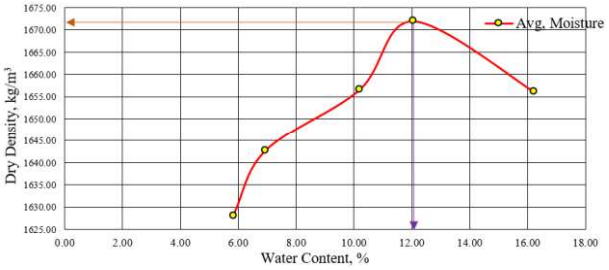

Fig. 2 Proctor compaction test curve for sea sand

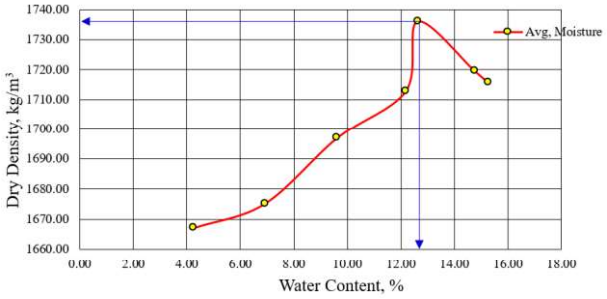

Fig. 3 Proctor compaction test curve for river sand

CBR test:

CBR tests were conducted for both River and Sea sand samples for few test iterations. The samples were tested for Optimum moisture content as well as full dried conditions. This CBR behavior of sea sand was unique because no research has encountered this behavior for a CBR test.

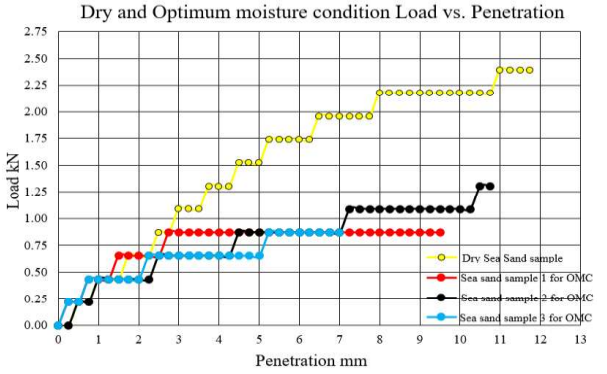

Fig. 4 Dry vs. Optimum moisture condition CBR curve for Sea Sand

In the Optimum moisture CBR samples, the stress was increased with the penetration. After considerable penetration, a Considerable stress increment was displayed for the dry sample, then the stress increment of optimum moisture sample for the same displacement.

Consecutively at 6.0mm, 7.6mm, and 8.25mm penetrations, the river sand samples were considered to fail. It was because the same weight remained for a significant type of penetration after the mentioned penetration.

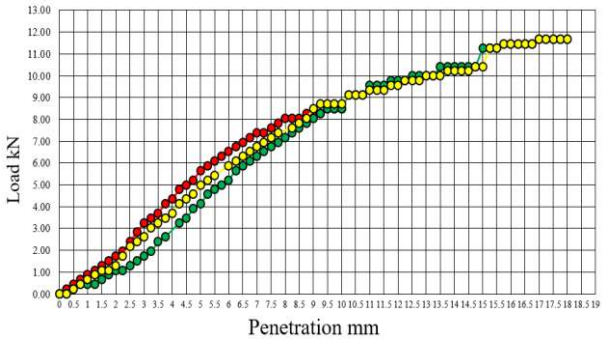

Fig. 5 CBR curve for river sand at optimum moisture condition

According to the preceding observations, the failure stresses for particular samples, was calculated as 3.813Mpa, 4.374Mpa, and 4.486Mpa stress.
An accelerated soil settlement was observed when soil fails under loading. Further, an increment of the shear strain was spotted while the shear stress remained at a very low increment. In general, the behavior of the sand is identified as elastoplastic before it fails. That is the reason which the load increased continuously with the penetration until the soil failure. After the failure, the sand was turned in to yield, and deformations were identified as plastic. Hence, it is hard to recover after a failure development. The position of the curve where the accelerated settlement of river sand begin, was considered as the failure load. Further, the Sea sand also was failed early before applying considerable load on it.

Table 3. Summary of specific gravities

Sample no	CBR values at 2.5 mm	CBR values at 5.0 mm
1	25.38%	34.38%
2	25.00%	34.18%
3	24.24%	32.14%

4.2.3 *Strength property tests*

Direct shear test:
The Friction angle and Cohesion values were recorded from the direct shear test graph for River sand.

Table 4. Friction angle and cohesion

Soil property	Value
Friction angle	28º5 ´ 36"
Cohesion	17.072 KN/m^2

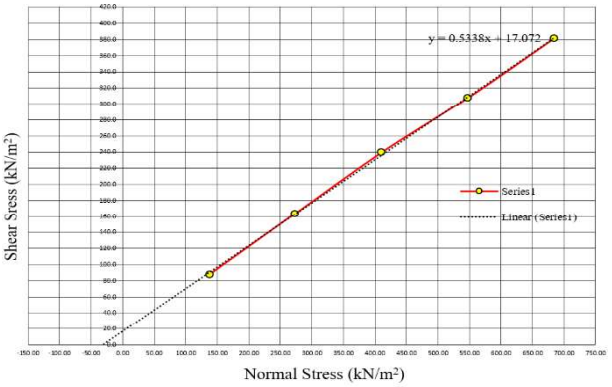

Fig. 6 Direct shear test for river sand sample

4.3 *Numerical analysis*

A numerical model was developed, and tested using Plaxis Connect Edition V20. It is a finite element program that is capable of simulating soil behavior. To simulate the effect of CBR mold and surcharge rings, the boundary conditions of the model were defined accordingly. Boundaries can be defined as completely free, fully fixed, or fixed for a specific direction. The Plaxis model dimensions were defined to tally the CBR laboratory test conditions.

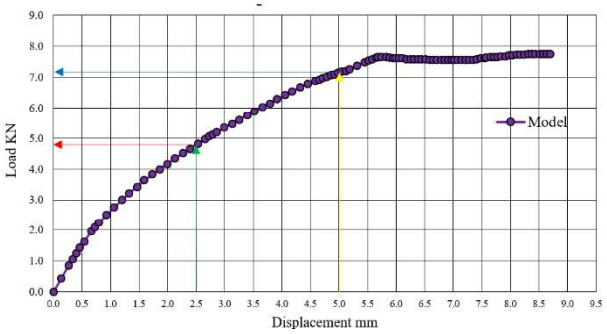

Fig. 7 Numerically developed load vs. displacement

To generate the model, the axisymmetric physique was chosen by considering the shape characteristics of the tests. The axisymmetric model is utilized in modeling circular structures consisting of a radial cross-section and loading focused around the central axis. Correspondingly, 15 nodes element distribution was followed rather than six node system to increase the accuracy.
A fourth-order displacement interpolation involving twelve Gauss points or stress points analysis is conducted rather than a three-point six node system in a 15 node triangle system generally. The Mohr-Coulomb method was considered to model development. Only half of the CBR test mold was created by Considering the symmetry. Model dimensions were included as 127 mm height and 76 mm width to match the CBR test apparatus.
In the initial step of the modeling process, a borehole was created in the desired location for interpreting the soil characteristics. To model the displacements that occurred by the load, the prescribed displacements method was utilized by giving uniform displacements along Y-axis

starting from 0 mm to the desired value and free displacement in X-axis. This was performed in the structures tab in Plaxis 2D, and endpoints were selected as (0 mm, 127 mm) and (25 mm, 127 mm) by matching half of the CBR plunger diameter.
To simulate the effect of CBR mold and surcharge rings, the boundary conditions of the model were defined accordingly. Boundaries can be defined as completely free, fully fixed, or fixed for a specific direction. The Plaxis model dimensions were defined to tally the CBR laboratory test conditions.

Numerically developed CBR curves and physically observed CBR curves were compared later.

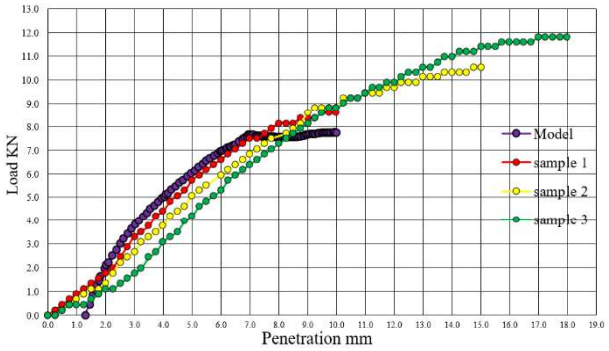

Fig. 8 Laboratory CBR vs. numerically developed curve

The comparison was executed to observe collations for the model and laboratory results. The calculated stress for the Plaxis model was comparatively within the range of laboratory results.

5 CONCLUSION AND RECOMMENDATION

As the Plaxis model and CBR test provide similar results, the Model can be used as an approximated substitute to the CBR testing. The CBR model is effective when it is difficult to continue laboratory CBR curves up to soil failure or up to a CBR value. The Gal Oya River Sand and Sea Sand in the South Eastern University of Sri Lanka are poorly graded sand according to the USCS soil classification.
CBR plunger was considered as a circular footing when calculating the failure loads. Finally, it is concluded that the calculation is not eligible because the failure curves of soils are restricted due to the confinement effect imparted by boundary walls of CBR mould.
It is recommended that further research be carried out on soil samples covering the Eastern Province region and that the research be continued, giving the reliability of the numerical model to the entire Eastern Province region. In particular, the geological boundaries of the Eastern Province and the Central Highlands can be introduced.

Laboratory CBR testing for river sand was performed in un-soaked conditions. Therefore, research recommends that the CBR tests also should be performed under the soak condition.
It is recommended to obtain Triaxial and Odometer test data from the Plaxis model and validate for direct usage afterward.

ACKNOWLEDGMENTS

Tests were performed at the Civil Engineering Department at the South Eastern University of Sri Lanka. The authors are thankful to the technicians of the laboratory for their valuable contribution to the execution of this experimental program. The authors are also grateful to the reviewers for their constructive comments which helped the cause of the manuscript.

REFERENCES

Abuildersengineer.com. 2012. TYPES OF FAILURE IN SOIL. [Online] Available at http://www.abuildersengineer.com/2012/11/types-of-failure-in-soil.html [Accessed 16 February 2020].

Catanzarity, F., 2016. BEARING CAPACITY FOR SHALLOW FOUNDATIONS. [Online] Geostru. Available at: https://www.geostru.eu/bearing-capacity-for-shallow-foundations/ [Accessed 20 May 2020].

Piyadasa, A., 2017. Prehistory of Sri Lanka 2: The Geographical and Geological Background of Sri Lanka | Sri Lanka Archaeology. [Online] Sri Lanka Archaeology. Available at: https://www.archaeology.lk/5186 [Accessed 30 January 2020].

P. Rahardjo, P., 2014. Geotechnical Failures Case Histories of Construction on Soft Soils, Forensic Investigations, and Counter Measures in Indonesia. Integrated Engineering, [online] 6(2), pp.11-23. Available at: https://pdfs.semanticscholar.org/7575/32923ff6652f7009344d0de40b48e993502f.pdf [Accessed 31 January 2020].

Rahardjo, P. P., 2014. Geotechnical Failures Case Histories of Construction on Soft. International Journal of Integrated Engineering, 6(2), pp. 11-23

Roys, S., and Bhalla, S., 2017. Role of Geotechnical Properties of Soil on Civil Engineering Structures. Research gate, [online] Available at: https://www.researchgate.net/publication/331920626_Role_of_Geotechnical_Properties_of_Soil_on_Civil_Engineering_Structures [Accessed 2 February 2020].

Trishna, B., 2018. Shear Failure of Soil: 3 Modes | Soil Engineering. [Online] Soil Management India. Available at:http://www.soilmanagementindia.com/shallow-foundation/shear-failure-of-soil/shear-failure-of-soil-3-modes-soil-engineering/14451 [Accessed 2 February 2020].

Vanapalli, S. K., 2009. Shear strength of unsaturated soils and its applications in geotechnical engineering practice. Newcastle, Australia, s.n.

Prediction of post- construction settlement of road embankment

G.A.N Jayaratne and H.S Thilakasiri
Department of Civil Engineering, Sri Lanka Institute of Information Technology, Sri Lanka

ABSTRACT: Ground improvement is mainly done to the subsurface that lack strength and stability to bear the structure to be constructed, and undergo large settlement during operation. Based on the soil properties and the layering, different soft ground treatment methods have to be applied. In this context, it is important to know the behaviour of the subsurface after ground improvement process. This study is mainly focused on the investigation of the accuracy of the settlement prediction methods during the post-construction stage of the Colombo-Katunayake Expressway (CKE) Project in Sri Lanka. Settlement prediction was done for the Defect Liability Period using the hyperbolic method, the Mesri method and Ladd method. A comparison of the predicted settlement with the actual measured settlement was done to assess the accuracy of the settlement prediction methods. From the comparison, it was evident that the hyperbolic method was more accurate and convenient to use in prediction of the settlement of the embankment.

KEY WORDS: Soft ground treatment methods; preloading; consolidation settlement; Asaoka method; hyperbolic method

1 INTRODUCTION

Ground improvement is done to strengthen and stabilize and reduce the post construction settlement. Such ground improvement will minimize the unfavourable settlements in the ground that could lead to the serviceability failure of the structure or sometimes, ultimate collapse. Fine-grained soils with particularly high degree of saturation and high organic content such as peat could be problematic for both stability of the embankments and settlement of embankments. In the Colombo-Katunayake Expressway project, from the chainage K0+000 to K25+800 starting from Colombo, the initial borehole profiles indicate the presence of peat layers, throughout the length of the section with a thickness varying from 0.5m to 14.2m. Mainly, the organic soil is concentrated in the first 8km from the Colombo side of the expressway. Depending on the thickness of the peat layers and the proposed structures, different ground improvement techniques such as; preloading, preloading with Prefabricated Vertical Drains (PVD), Crushed Stone Piles, Sand Compaction Piles, and Driven Piles have been used to minimize the settlement of the subsurface. Settlement monitoring was conducted during ground improvement at all sections and at some sections, for a defect liability period of three years, to assess the effectiveness of the soft ground improvement due to the application of the above-mentioned techniques.

2 RESEARCH METHODOLOGY

2.1 *Test Variables*

The study is primarily focused on preloading technique presented in Table 1 and then six locations were selected for the analysis of the preloading technique.

Table 1. Selected sections with Preloading

Chainage	Thickness of peat layer (m)	Depth to peat layer (m)
K3+400	1.4	3.5
K7+800	2.2	5.8
K12+150	12.1	4.4
K13+050	1.4	4
K18+800	1.2	2.8
K19+600	1.9	0.6

Figure 1 presents the variation of settlement with embankment height for selected K7+800 chainage which consists of an organic layer of thickness 5.8m.

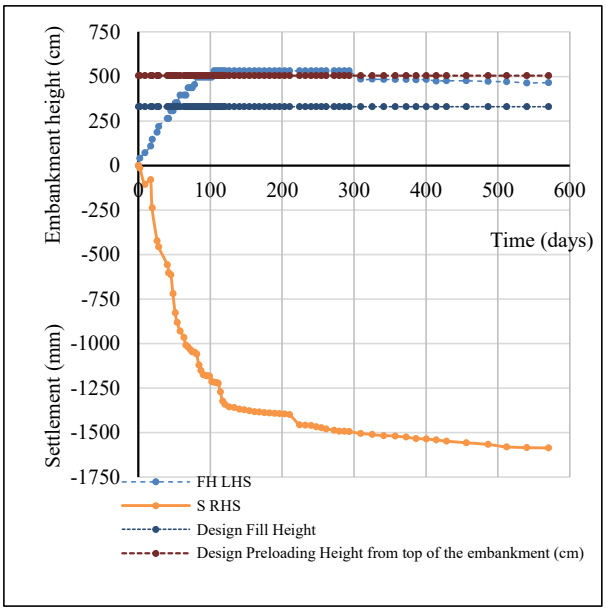

Fig. 1 Variation of settlement with embankment height for K7+800

2.2 *Applicability of Asaoka method to field settlement data*

The Asaoka method is one of the widely practiced settlement prediction methods, due to its ability to determine the end of primary consolidation settlement and its simplicity. (Asaoka, 1978).

Asaoka method was applied for the settlement data, where the surcharge loading remained a constant value, and the end of primary consolidation was obtained. The degree of consolidation attained in the soft soil by the time of removal of surcharge can be found out by determining the end of primary consolidation settlement.

2.3 *Applicability of hyperbolic method to field settlement data*

The hyperbolic method can be used to predict the settlement in the soil during the improvement (Tan, et al., 1991).

The hyperbolic plot of *t/s* vs *t* for the settlement monitoring data during the construction of the embankment was plotted and the parameters α and β according to hyperbolic equation was obtained. The settlement was then predicted using the hyperbolic relationship.

The hyperbolic equation given in Equation 1 was used for the prediction of settlement at a required time during preloading.

$$\frac{t}{s} = \alpha + \beta t \quad (1)$$

Where t is the time of the settlement s is observed and, α and β are constants obtained from the hyperbolic plot of the respective test location.

2.4 *Secondary compression based on Mesri method*

Mesri (2001) developed a relationship between C'_α/C_α for determination of the secondary compression settlement after surcharge removal. Using the Mesri method, the secondary compression index after surcharge removal and secondary settlement can be determined. (Mesri, et al., 2001)

The Mesri method was applied to determine secondary settlement after the removal of the surcharge. C'_α/C_α values cannot be obtained for R values less than 0.2 from Mesri's method, which is the limitation of this method.

Figure 2 presents the Mesri curves which are used to determine the C'_α/C_α ratio and thereby $\mathbf{C'_\alpha}$, the modified secondary compression index.

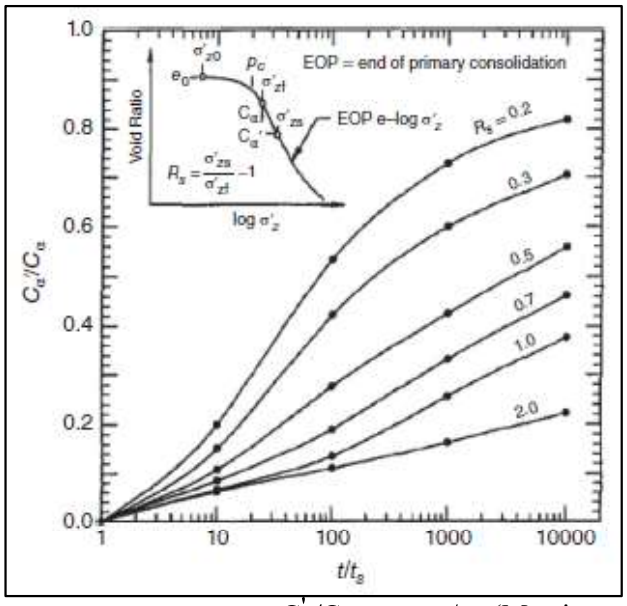

Fig. 2 Mesri graphs for C'_α/C_α versus t/t_s (Mesri, et al., 1997)

2.5 *Secondary compression based on the Ladd method*

Ladd uses a relationship between Adjusted Amount of Surcharge (AAOS) to C'_α/C_α to determine the modified secondary compression index (Han, 2015).

Figure 3 presents the Ladd graphs which were used to determine the C'_α/C_α ratio and thereby $\mathbf{C'_\alpha}$, the modified secondary compression index.

The C_α value for the analysis was obtained from the study done on peaty soil by Ariyarathna & Thilakasiri (2011), as shown in Equation 2.

$$C_\alpha = 0.033 C_C \quad (2)$$

Where C_α is the secondary compression index before surcharge removal and C_c is the compression index.

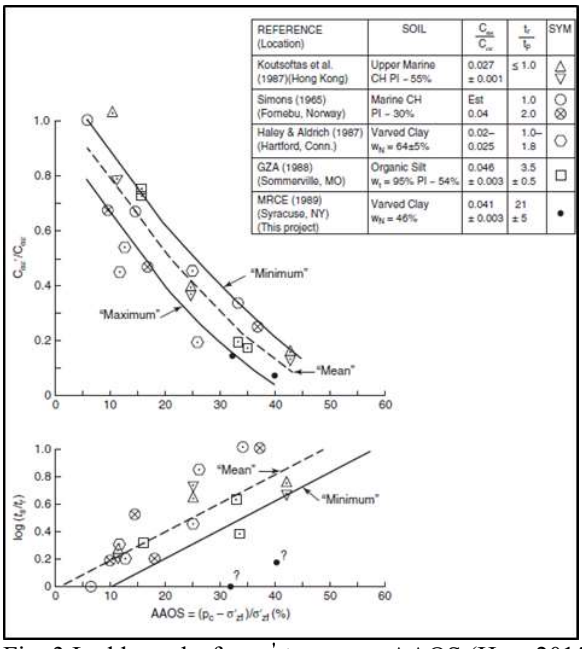

Fig. 3 Ladd graphs for $C_{\alpha}^{'}/C_{\alpha}$versus AAOS (Han, 2015)

All the above-stated methods were applied in the determination of the secondary settlement during the construction and the service phases.

3 RESULTS

From the application of the Asaoka method on the preloading locations, it was determined that primary consolidation had been completed by the time of removal of surcharge. For the Asaoka method application, the time which the embankment load was constant, was taken into consideration.

Figure 4 shows the Asaoka plot for Left Hand Side of K12+150 chainage embankment.

The primary settlement obtained by the application of the Asaoka method is presented in Table 2.

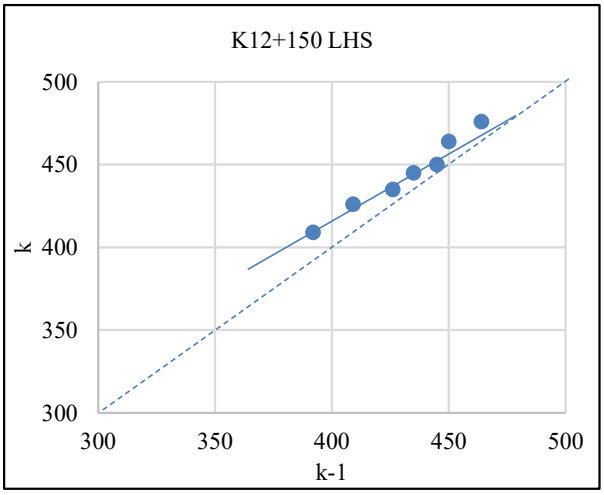

Fig. 4 Asaoka plot for K12+150 LHS

Table 2. Primary settlement comparison for preloading locations

Location	Peat layer thickness (m)	Primary settlement (using Asaoka method)		Settlement at removal of surcharge (mm)		Degree of consolidation achieved (%)	
		LH	RH	LH	RH	LH	RH
K3+400	1.4	419	460	423	464	100	100
K7+800	2.2	943	1461	978	1494	100	100
K12+150	12.1	474	475	484	473	100	99.6
K13+050	1.4	407	678	412	686	100	100
K18+800	1.2	320	317	312	313	97.5	98.7
K19+600	1.9	164	143	162*	140*	98.7	97.9

*Last settlement reading available. No surcharge removal done until last date of settlement monitoring

The end of primary consolidations was obtained using the Asaoka method and it was found that the soft soil layer had reached 100% of its primary consolidation by the time of removal of the surcharge.

The hyperbolic plot of *t*/*s* vs *t* for the settlement monitoring data during the construction of the embankment was plotted. The predicted settlement was then calculated using the hyperbolic equation and plotted against the actual settlement.

Figure 5 shows the application of the hyperbolic plot for K3+400 chainage.

Fig. 5 Hyperbolic settlement prediction for K3+400 RHS

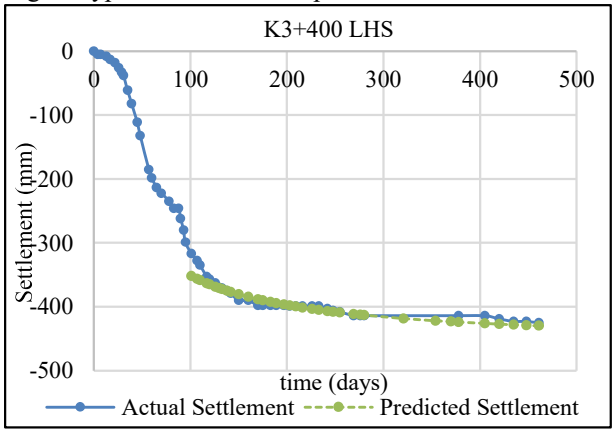

The actual settlement during the pre-construction stage will follow the hyperbolic variation, complying with the hyperbolic equation. The hyperbolic parameters obtained from the measured settlement satisfies the hyperbolic equation, thereby the predicted settlement follows the hyperbolic variation as well.

By the determination of the end of primary consolidation, the secondary consolidation settlement

was calculated using the Ladd and the Mesri methods.

The hyperbolic method, the Ladd method and the Mesri method were applied for the determination of secondary settlement during the service period.

Figure 6, 7 and 8 presents the settlement comparison done for K7+800 LHS during the service period using the Mesri method, the Ladd method and the hyperbolic method respectively.

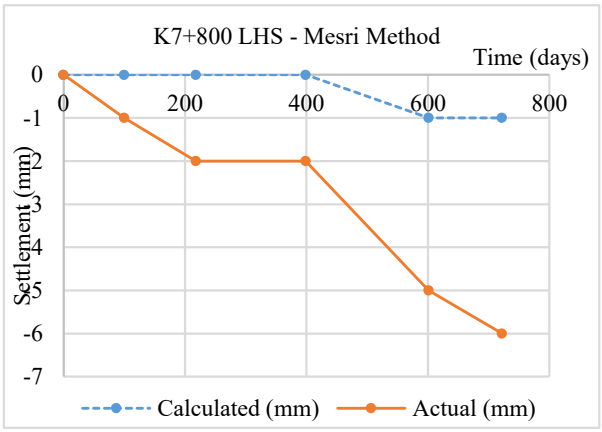

Fig. 6 Settlement during DLP using the Mesri method for K7+800 LHS

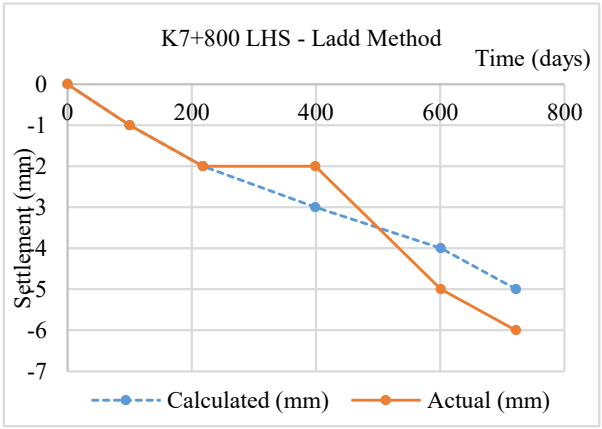

Fig. 7 Settlement during DLP using the Ladd method for K7+800 LHS

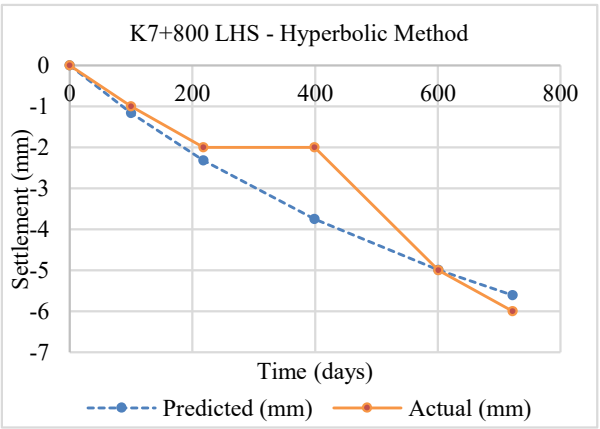

Fig. 8 Settlement during DLP using the hyperbolic method for K7+800 LHS

4 DISCUSSION

For the settlement prediction after the removal of the surcharge load, the Hyperbolic settlement prediction was satisfactory than the other three methods; the Ladd method and the Mesri method.

The hyperbolic method was applied to the settlement data for which the embankment loading was constant and the hyperbolic equations were obtained. From the above settlement prediction patterns, the hyperbolic prediction gives a much closer approach to the field settlement values.

Figure 9 shows the hyperbolic settlement prediction for K12+150 chainage.

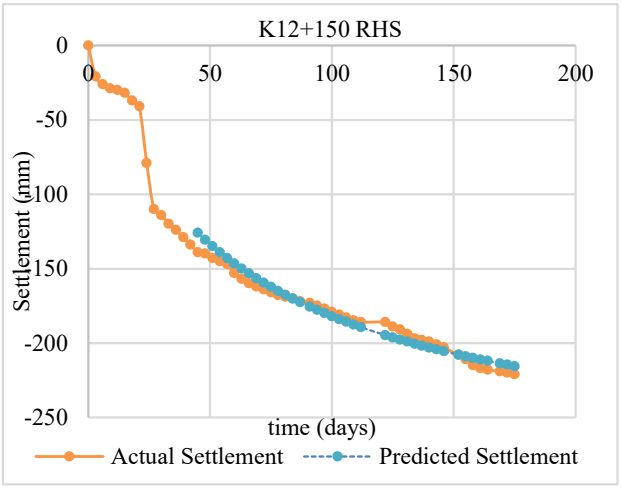

Fig. 9 Hyperbolic settlement prediction for K12+150 RHS

As shown in Figure 9, the variation of the predicted settlement shows a similar behaviour with the actual field settlement. Since critical consolidation takes place at the latter stage, at around a degree of consolidation of 40% to 90%, the hyperbolic method can be successfully used for the settlement prediction during the embankment construction period.

The hyperbolic method requires actual settlement data for the settlement prediction whereas the Ladd and the Mesri methods does not require settlement data and involves series of calculations to predict the settlement.

Figures 10 to 15 shows the settlement comparison for the Defect Liability Period using the three settlement prediction methods where applicable; hyperbolic, Mesri and Ladd methods, against the observed field settlement data for K3+400, K7+800, K12+150, K13+050, K18+800 and K19+600 chainages respectively.

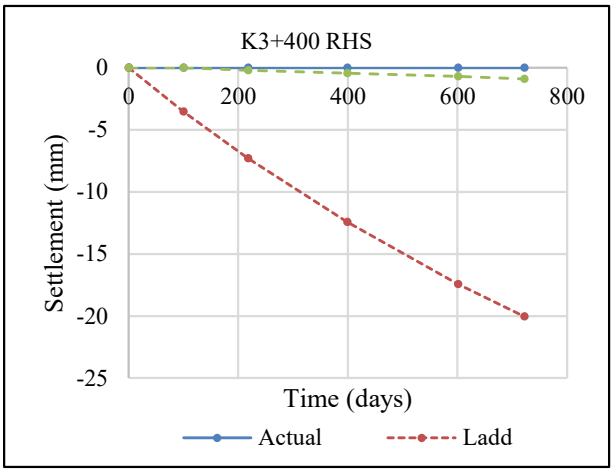

Fig. 10 Comparison of Observed settlement values with Predicted settlement values for K3+400

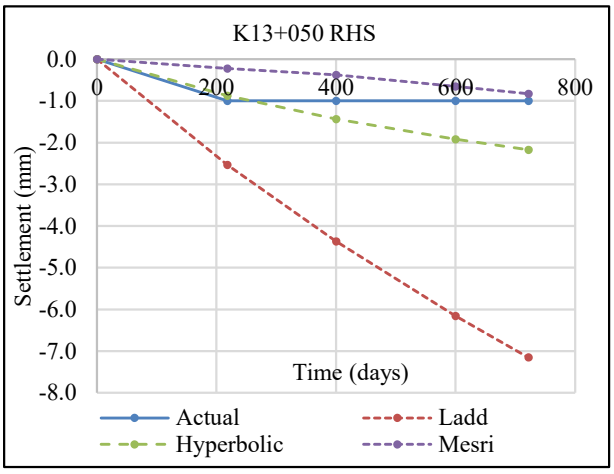

Fig. 13 Comparison of Observed settlement values with Predicted settlement values for K13+050

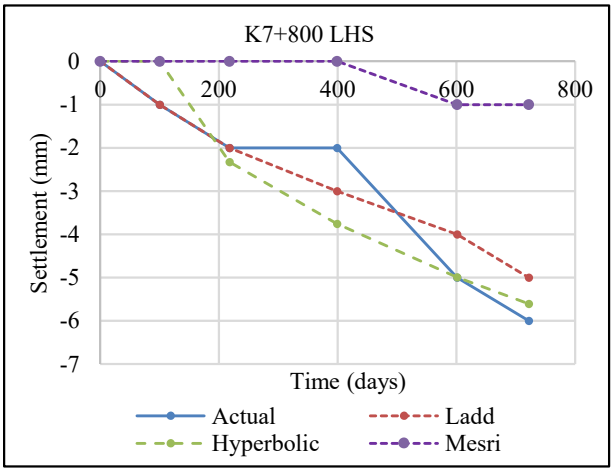

Fig. 11 Comparison of Observed settlement values with Predicted settlement values for K7+800

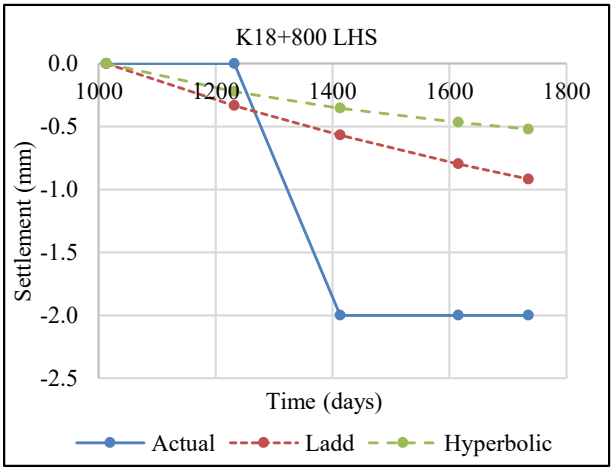

Fig. 14 Comparison of Observed settlement values with Predicted settlement values for K18+800

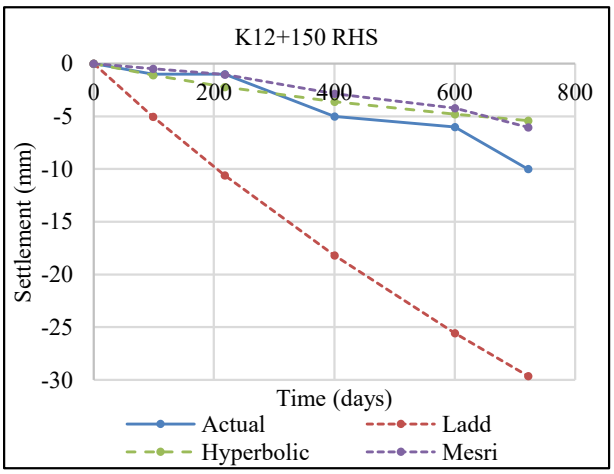

Fig. 12 Comparison of Observed settlement values with Predicted settlement values for K12+150

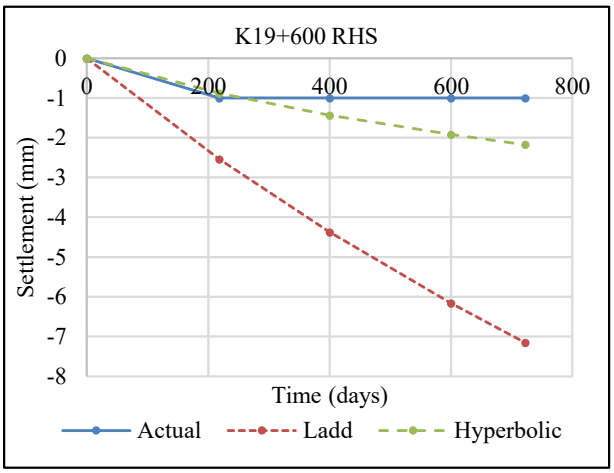

Fig. 15 Comparison of Observed settlement values with Predicted settlement values for K19+600

The Mesri method was not applicable for the following locations; K3+400, K18+800 and K19+600, where the R values were less than 0.2, as the Mesri graphs does not provide the necessary curves as per the curves given in Figure 2.

Considering the settlement prediction variations for the Defect Liability Period, it can be said that the hyperbolic method provides a better settlement prediction than the Ladd method, provided that the settlement measurements during the construction stage are available.

5 CONCLUSION

By determining the end of primary consolidation from the Asaoka method, all six sections considered in this study showed that the primary consolidation had been completed and the degree of consolidation was nearly 100%.

The hyperbolic method was applied for the settlement prediction during the construction of the embankment and the field parameters α and β in Equation 1 was obtained.

Both the Ladd and the Mesri methods are used to determine the secondary settlement after the removal of surcharge. However, the hyperbolic method, with α and β determined from the loading stage, were used to predict the post construction settlement. This prediction gave better settlement prediction results than that the other two methods; the Ladd method and the Mesri method, after the removal of surcharge.

By using the hyperbolic parameters obtained during the embankment construction stage, the settlement for the Defect Liability Period can be accurately predicted. This is an added advantage of using the hyperbolic method over the other two methods; the Ladd method and the Mesri method.

Based on this study it is concluded that the hyperbolic settlement prediction method can be successfully applied to determine the future settlement and check whether the actual post construction settlement is within the allowable construction limits.

ACKNOWLEDGMENTS

The authors appreciate the provision of field data of the CKE project from Metallurgical Corporation of China (MCC). The author is grateful for the consistent assistance given by Mr. Dinitha Vidurapriya.

REFERENCES

Ariyarathne, P. R. C. & Thilakasiri, H. S., 2011. Improvement of Sri Lankan Peaty Soil By Vacuum Consolidation. Hong Kong, UoM.

Asaoka, A., 1978. Observational Procedure of Settlement Prediction. Soils and Foundations, Volume 18, pp. 87-101.

Han, J., 2015. Principles and Practices of Ground Improvement. 1st ed. New Jersey: John Wiley & Sons Inc..

Mesri, G., Ajlouni, M. A., Feng, T. W. & Lo, D. O. K., 2001. Surcharging of Soft Ground to Reduce Secondary Settlement. In: C. Press, ed. Soft Soil Engineering. Illinois: CRC Press, pp. 55 - 65.

Mesri, G., Stark, T. D., Ajlouni, M. A. & Chen, C. S., 1997. Secondary Compression of Peat with or without surcharging. Journal of Geotechnical and Geoenvironmental Engineering, 123(5), pp. 411-421.

Pantazidou, M., 2000. On practical matters of calculating secondary compression & reduction of secondary compression by surcharging. Zografou, National Technical University of Athens.

Tan, T. S., Inoue, T. & Lee, S. L., 1991. Hyperbolic Method for Consolidation Analysis. Journal of Geotechnical Engineering, 117(11), pp. 1729-1737.